Journal of Medicinal Chemistry

Article

1,4-Oxazine #-secretase (BACE1) inhibitors: from hit generation to orally bioavailable brain penetrant leads.

Frederik J.R. Rombouts, Gary Tresadern, Óscar Delgado, Carolina Martinez Lamenca, Michiel Van Gool, Aránzazu García-Molina, Sergio A. Alonso De Diego, Daniel Oehlrich, Hana Prokopcova, Jose Manuel Alonso, Nigel Austin, Herman Borghys, Sven Van Brandt, Michel Surkyn, Michel De Cleyn, Ann Vos, Richard Alexander, Gregor J. Macdonald, Dieder Moechars, Harrie J.M. Gijsen, and Andrés A. Trabanco

J. Med. Chem., **Just Accepted Manuscript** • DOI: 10.1021/acs.jmedchem.5b01101 • Publication Date (Web): 17 Sep 2015

Just Accepted

ACS Publications

Journal of Medicinal Chemistry is published by the American Chemical Society. 1155 Sixteenth Street N.W., Washington, DC 20036

1,4-Oxazine β-secretase 1 (BACE1) inhibitors: from hit generation to orally bioavailable brain penetrant leads.

Frederik J. R. Rombouts,[a,] Gary Tresadern,[f] Oscar Delgado,[b] Carolina Martínez-Lamenca,[a] Michiel Van Gool,[b] Aránzazu García-Molina,[b] Sergio A. Alonso de Diego,[b] Daniel Oehlrich,[a] Hana Prokopcova,[a] José Manuel Alonso,[f] Nigel Austin,[d] Herman Borghys,[d] Sven Van Brandt,[a] Michel Surkyn,[a] Michel De Cleyn,[a] Ann Vos,[d] Richard Alexander,[e] Gregor Macdonald,[a] Dieder Moechars,[c] Harrie Gijsen,[a] Andrés A. Trabanco[b,]**

[a]Neuroscience Medicinal Chemistry, Janssen Research & Development, Janssen Pharmaceutica N. V., Turnhoutseweg 30, B-2340 Beerse, Belgium. [b]Neuroscience Medicinal Chemistry, Janssen Research & Development, Janssen-Cilag S. A., C/ Jarama 75A, 45007 Toledo, Spain. [c]Neuroscience-Biology, Janssen Research & Development, Janssen Pharmaceutica N. V., Turnhoutseweg 30, B-2340 Beerse, Belgium. [d]Discovery Sciences, Janssen Research & Development, Janssen Pharmaceutica N. V., Turnhoutseweg 30, B-2340 Beerse, Belgium. [e]Biologics Research, Janssen Research & Development, 1400 McKean Rd, Spring House, PA 19002. [f]Discovery Sciences, Janssen Research & Development, Janssen-Cilag S. A., C/ Jarama 75A, 45007 Toledo, Spain.

BACE1 inhibitor, Morpholine, 1,4-Oxazine, Amidine, Alzheimer's disease

ABSTRACT: 1,4-Oxazines are presented, which show good *in vitro* inhibition in enzymatic and cellular BACE1 assays. We describe lead optimization focused on reducing the amidine pK_a whilst optimizing interactions in the BACE1 active site. Our strategy permitted modulation of properties such as permeation and especially P-glycoprotein efflux. This led to compounds which were orally bioavailable, centrally active and which demonstrated robust lowering of brain and CSF Aβ levels respectively in mouse and dog models. The amyloid lowering potential of these molecules makes them valuable leads in the search for new BACE inhibitors for the treatment of Alzheimer's Disease.

INTRODUCTION

Alzheimer´s disease (AD) is a progressive neurodegenerative disorder and the major cause of dementia in the elderly. According to the World Health Organization (WHO) dementia affects 47.5 million people worldwide, a number that is projected to triple by 2050 with the aging population.[1,2] AD is characterized by progressive deposition of amyloid and misfolded Tau, followed by neurodegeneration and loss of function, leading ultimately to death.[3] Of the many attempts to target the underlying pathogenesis, amyloid lowering approaches have made the most progress so far, albeit without delivering a therapy to date.[4] Amyloid oligomer and plaque formation is thought to occur when the balance between non-amyloidogenic (α-secretase mediated) and the amyloidogenic processing of amyloid precursor protein (APP) is shifted (familial AD) or clearance of amyloid is impaired (sporadic AD).[5,6] In the amyloidogenic pathway, β-secretase 1 (BACE1) cleaves APP producing a 99 amino acid length soluble peptide fragment called C99, which is the rate-limiting step in Aβ formation. This peptide is further processed by γ-secretase to 36-43 amino acid length Aβ species, of which the longer isoforms,

especially Aβ42, are the most fibrillogenic and neurotoxic.[7] Consequently both β-secretase and γ-secretase are being pursued as targets to modulate Aβ production.[8] Since its discovery in 1999,[9] BACE1 has been a highly challenging target for drug discovery, and only after years of research medicinal chemists have managed progressing small molecule BACE1 inhibitors in clinical trials.[10] A breakthrough in the development of non-peptidomimetic BACE1 inhibitors was the identification of amidine- and guanidine-containing small molecules. Compared to previous peptidomimetic and amino-alcohol derived inhibitors, these molecules form a salt bridge and hydrogen bond interactions with Asp32 and Asp228 in the catalytic site of BACE1 in an optimal way (see schematic in Chart 1).[11] The use of a quaternary center alpha to the amidine or guanidine function permits substituents to enter adjacent binding pockets such as S2', S1 and S3.[12] The S3 pocket can be efficiently targeted via amide-tethered biaryl systems (Chart 1). In these amidine prototypes, the central aromatic ring (A) is a direct substituent on the quaternary center. The A-ring and amide nitrogen occupy the S1 pocket, whereas the distal aromatic ring (B) extends into the S3 pocket. The B-ring is generally a 2-pyridyl or 2-pyrazinyl ring, allowing for a quasi-coplanar orientation with the A-ring. The amide NH establishes an interaction with the backbone carbonyl oxygen of Gly230. The fourth substituent on the quaternary center (methyl as shown in the examples in Chart 1) is directed towards the S2' pocket. As such, the field has progressed towards potent inhibitors with low molecular weight and good ligand efficiency.

A challenge in the development of amidine and guanidine-based BACE1 inhibitors has been to modulate the intrinsic high basicity of the amidine function. In our previously reported benzoguanidine series,[13] we found this to be a key factor for obtaining compounds with favorable pharmacokinetic (PK) properties, as high basicity (pK_a ~ 10-11) has been associated

with unfavorable tissue distribution and P-glycoprotein (P-gp) mediated efflux.[14] Amidine-based warheads with pK_a below 9 have been reported by a number of companies[15] in the form of acyl- and sulfonylguanidines,[16] isoureas[17] and isothioureas[18] for which representative examples **1** and **2** are shown in Chart 1.[19,20] We have previously reported on the *de novo* design and synthesis of piperazinones **3** and **4** as BACE1 inhibitors with moderate enzymatic and cellular activity.[21] Interestingly, the amide function embedded in the 'warhead' of **3** and **4** helped to decrease the basicity of the amidine leading to compounds with *in vivo* activity. However, the blood brain barrier crossing with this piperazinone series was found to be sub-optimal, and concomitantly subcutaneous administration of high doses was needed to achieve significant *in vivo* reduction of Aβ peptides in mice.

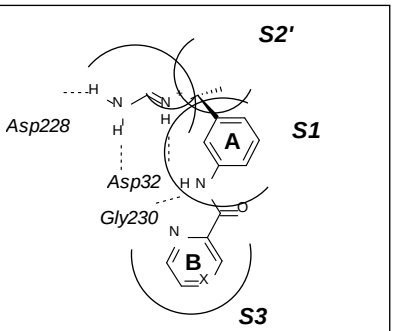

Pharmacophore of BACE1 inhibitors targeting the S3 pocket (X= CH, N)

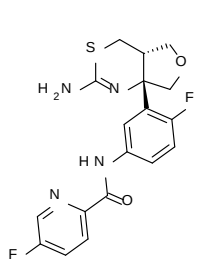

1 (LY-2886721, Eli Lilly)
BACE1 IC_{50} 15.5 nM
hAβ42 cell IC_{50} 6.6 nM

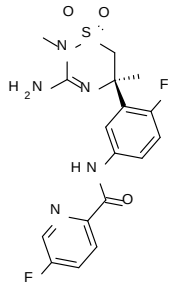

2 (MK-8931, Merck)
BACE1 IC_{50} 3.2 nM
hAβ42 cell IC_{50} 1.3 nM

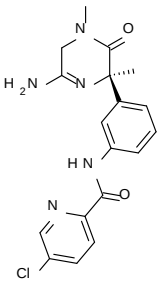

3 (Janssen)
BACE1 IC_{50} 324 nM
hAβ42 cell IC_{50} 36 nM

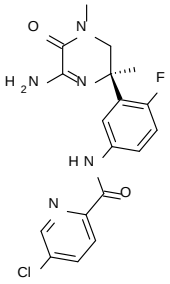

4 (Janssen)
BACE1 IC_{50} 23 nM
hAβ42 cell IC_{50} 28 nM

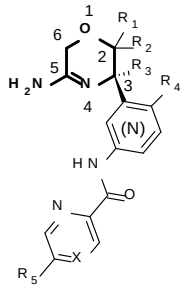

5, *This paper*

Chart 1. Representative overview of reported amidine containing BACE1 inhibitors targeting the S3 pocket. Internally generated enzymatic and cellular data are shown.

Herein we report the design and synthesis of novel 1,4-oxazines (**5**) as alternative warheads to the previously described piperazinones **3** and **4**. Lead optimization strategies to modify the pK_a of the amidine function resulted compounds (2*R*,3*R*)-**7a** and (2*R*,3*R*)-**7d** with a robust oral effect in lowering of Aβ peptides in mouse and dog models.

CHEMISTRY

In order to access 1,4-oxazines 3*R*-**6a-c**, acetophenones **13a**,**b** were converted to the corresponding amino nitriles *rac*-**14a**,**b** via a Strecker reaction (Scheme 1). Acidic hydrolysis of the cyano group and subsequent esterification of the resulting carboxylic acids *rac*-**15a**,**b** led to the aminoesters *rac*-**16a**,**b**. Reduction of *rac*-**16a**,**b** with lithium aluminium hydride (LAH) provided the racemic amino alcohols *rac*-**17a**,**b**. Separation of enantiomers via chiral supercritical fluid chromatography (SFC) followed by determination of the absolute stereochemistry by vibrational circular dichroism (VCD) provided the desired enantiomers 2*R*-**17a**,**b**.[22] The lactam rings 5*R*-**18a**,**b** were constructed next via a one-pot two step procedure involving amide formation at -15 °C in the presence of DIPEA, followed by Williamson etherification with *t*-BuOK. Subsequently, the corresponding amidine derivatives 5*R*-**20a**,**b** were obtained by sequential thionation of 5*R*-**18a**,**b** with P_2S_5, followed by aminolysis of the resulting thioamides 5*R*-**19a**,**b** with aqueous ammonia. Amination reaction on the bromoarene under Buchwald-type conditions using benzophenone imine as the nitrogen source led to 5*R*-**21a**,**b**. Finally, the target compounds 3*R*-**6a-c** were obtained via HATU or DMTMM mediated coupling of 5*R*-**21a**,**b** with the corresponding carboxylic acids.

Scheme 1. Synthesis route towards 1,4-oxazines 3*R*-**6a-c**.[a]

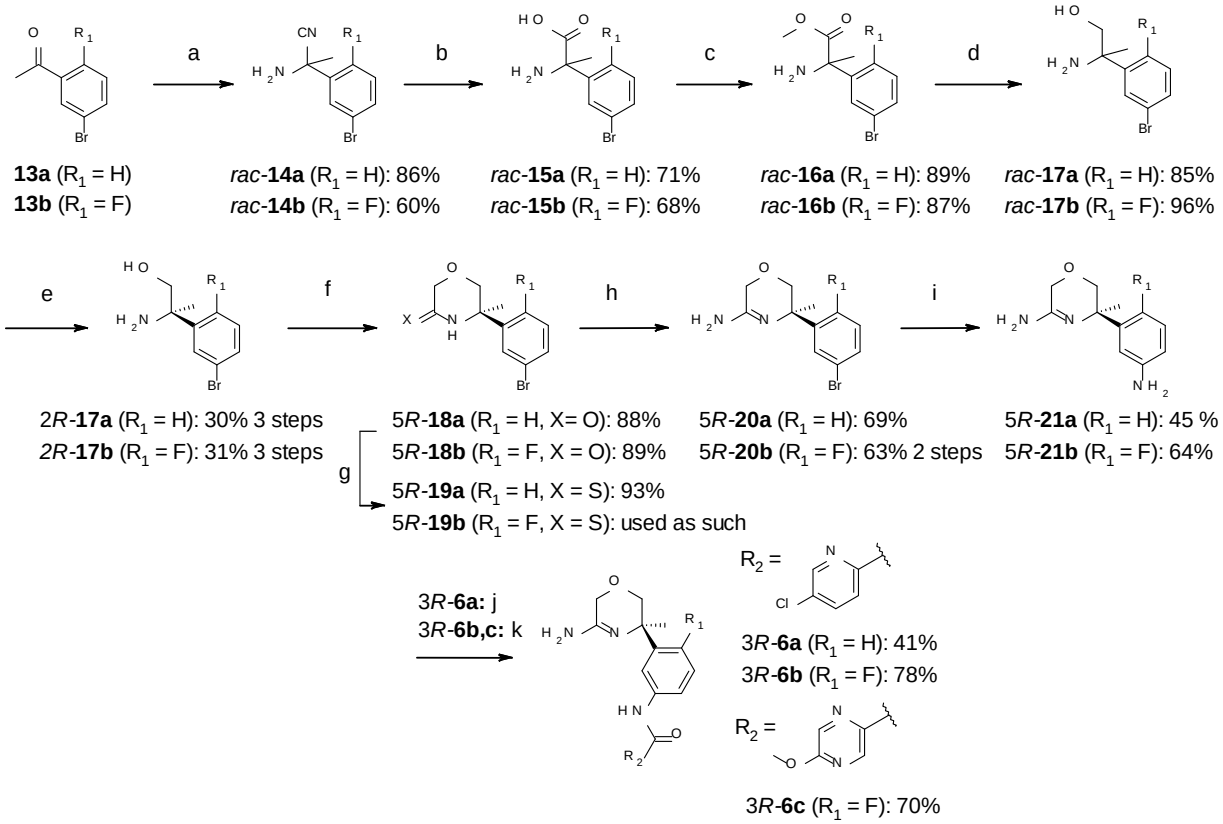

[a]Reagents and conditions: (a) TMSCN, NH_4Cl, 7 N NH_3/MeOH, rt, 4 d; (b) 6 N HCl, reflux, 16 h; (c) H_2SO_4, MeOH, reflux, 16 h; (d) $LiAlH_4$, THF, 0 °C, 1 h; (e) Chiral SFC separation; (f) i. chloroacetyl chloride, DIPEA, THF, -78 °C, 30 min, ii. *t*-BuOK, 0 °C, 90 min; (g) P_2S_5, THF, 50 °C, 50 min; (h) 33% NH_3 (aq), 60 °C, 4 h; (i) i. benzophenone imine, $Pd_2(dba)_3$, *rac*-BINAP, *t*-BuONa, toluene, 80 °C, 7 h, ii. 1 N HCl, rt, 16 h (j) 5-chloropyridine-2-carboxylic acid, HATU, *N*,*N*-dimethylaniline, DCM, rt, 5 h; (k) 5-methoxypyrazine-2-carboxylic acid, DMTMM, MeOH, rt, 3 h.

The synthesis routes for target molecules (2*S*,3*R*)-**7a**, (2*R*,3*R*)-**7a**, (2*S*,3*R*)-**8**, (2*R*,3*R*)-**8**, (2*R*,3*R*)-**9** and (2*S*,3*R*)-**9** bearing electron withdrawing groups (EWG) at the C-2 position start from the common intermediate 2*R*-**15b** (Scheme 2),which was obtained after chiral SFC separation of the racemate **15b** and VCD characterization. Thus, 2*R*-**15b** was cyclized to the morpholinedione 3*R*-**22** upon reaction with chloroacetyl chloride in a two-step procedure: first the amide bond was formed by treatment with NaOH in 1,4-dioxane, followed by aqueous work-up and subsequent lactonization by addition of $NaHCO_3$ in DMF. Compound 3*R*-**22** proved to be

a valuable precursor to access all envisioned modifications (**I**-**III**, Chart 2). Reduction of the lactone carbonyl with DIBAL-H to the corresponding hemi-acetal, followed by fluorination with DAST provided 5*R*-**23** as an inseparable 60:40 mixture of 6*R* and 6*S* diastereomer. Addition of Ruppert-Prakesh reagent (TMS-CF_3) to 3*R*-**22** provided hemi-ketal 5*R*-**24** as an unassigned 3:1 mixture of 6*S*/6*R* diastereomers. Interestingly 5*R*-**24** also reacted smoothly with DAST providing the 6-fluoro-6-trifluoromethyl-1,4-oxazine derivatives (5*R*,6*R*)-**25** and (5*R*,6*S*)-**25** as inseparable mixture in a 25:75 diastereomeric ratio. Hemi-ketal 5*R*-**24** was also chlorinated by reaction with $SOCl_2$ leading to 5*R*-**26**. Treatment of 5*R*-**26** with metallic zinc in acetic acid at 100 °C provided the CF_3 derivative 5*R*-**27**, as a 80:20 mixture of 6*R* and 6*S* diastereomer respectively.

Scheme 2. Synthesis of 1,4-oxazine-3-one precursors for BACE1 targeting amidines.[a]

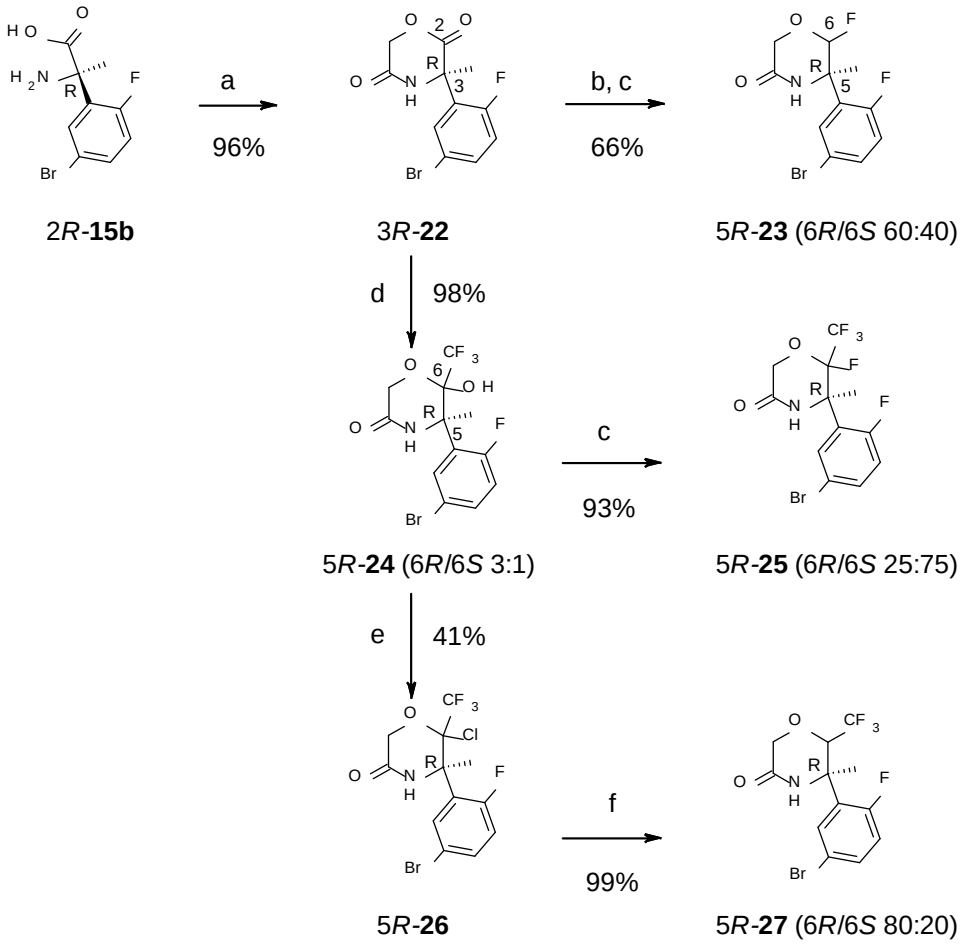

[a]Reagents and conditions: (a) i. Chloroacetyl chloride, 1 M NaOH , 1,4-dioxane, 2 h, ii. DMF, $NaHCO_3$, 80 °C, 3 h; (b) DIBAL-H, THF, -78 °C, 2 h; (c) DAST, DCM, 0 °C, 40 min (5*R*-**23**) to 2 h (5*R*-**25**); (d) $TMSCF_3$, TBAT, THF, 0 °C to rt, 20 min; (e) $SOCl_2$, DCM, 0 °C, 30 min, then add pyridine, 0 °C, 30 min; (f) Zn, AcOH, 80 °C, 3 h.

As shown in Scheme 3, 6*R*/6*S* diasteromeric mixtures 5*R*-**23**, 5*R*-**25** and 5*R*-**27** were converted to the target amidines (5*R*,6*S*)-**31,** (5*R*,6*R*)-**31,** (5*R*,6*S*)-**32,** (5*R*,6*R*)-**32,** (5*R*,6*R*)-**33** and (5*R*,6*S*)-**33** following a similar reaction sequence to that previously described for 3*R*-**6a-c** in Scheme 1. The only modification in the synthesis route was the conversion of the bromoarene to the aniline, for which we found a copper-catalyzed reaction with sodium azide to provide superior yields to the Buchwald-Hartwig protocol.[23] For occupying the S3 pocket the 5-methoxypyrazin-2-yl group was consistently used to allow for a comparison of properties between the different warheads in final compounds (2*S*,3*R*)-**7a,** (2*R*,3*R*)-**7a,** (2*S*,3*R*)-**8,** (2*R*,3*R*)-**8,** (2*R*,3*R*)-**9** and (2*S*,3*R*)-**9**.

Scheme 3. Preparation of 1,4-oxazine-based amidines C-2 substituted with different EWG.[a]

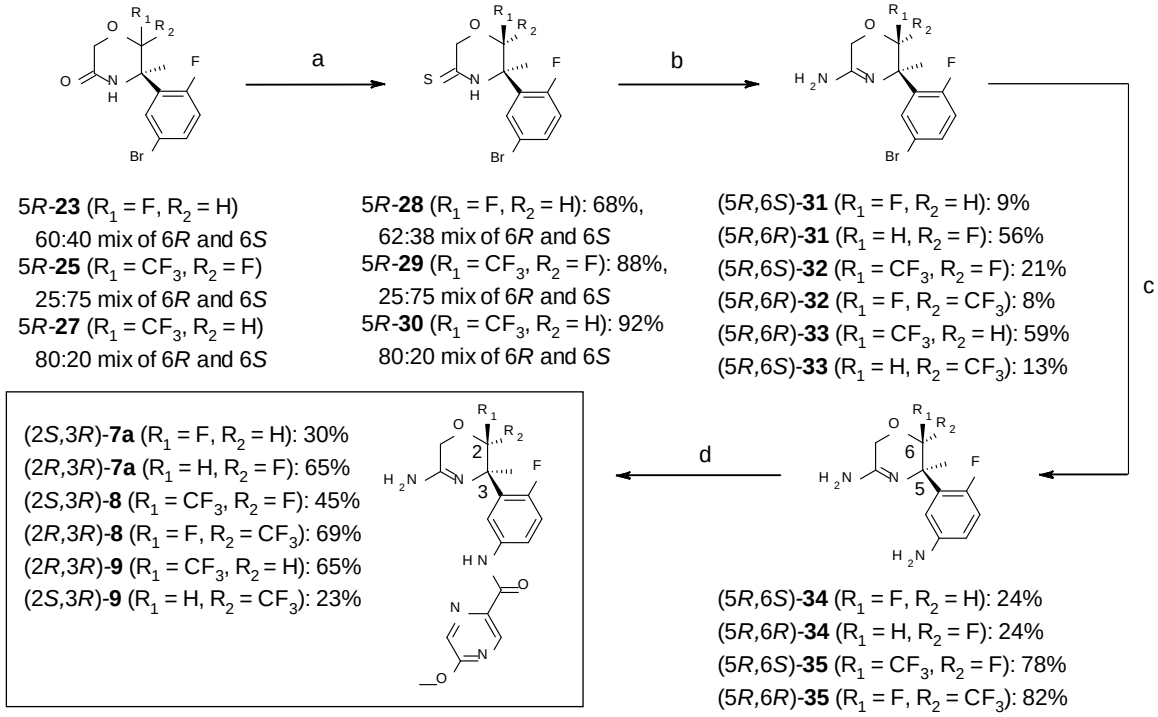

[a]Reagents and conditions: (a) P_2S_5, THF, 70 °C, 2-4 h; (b) 33 % NH_3 (aq), 60-80 °C, 24-48 h; (c) NaN_3, CuI, DMEDA, Na_2CO_3, DMSO, 110 °C, 1-4 h; (d) 5-methoxypyrazine-2-carboxylic acid, DMTMM, MeOH, 0 °C, 2-6 h.

A novel stereoselective route using Ellmann's sulfonamide was developed for the synthesis of compound (2*R*,3*R*)-**10** (Scheme 4). Condensation of *S*-Ellmann's sulfonamide with phenylglyoxylic ester (**37**) in the presence of Ti(O*i*Pr)$_4$ yielded the *S*-sulfoximine *S*-**38**. Conveniently, complete transesterification of the methyl ester with isopropanol occurred during the condensation step generating the isopropyl ester, which would be less reactive to the addition of cyclopropyl magnesium bromide in the subsequent reaction step. Similar to the protocol described in ref. 22, treatment of *S*-**38** with cyclopropylmagnesium bromide led exclusively to the imine addition product 2*R*-**39** with *R*-configuration at the quaternary center. Ester hydrolysis followed by the cleavage of the sulfoxamide S-N bond led to amino acid 3*R*-**40**, which was next cyclized to the lactone 3*R*-**41** following a similar route to the one previously described for 3*R*-**22**. Reduction of 3*R*-**41** with DIBAL-H followed by reaction with DAST provided 5*R*-**42** as a 3:2 mixture of 6*R*:6*S* diastereomers. Next, thionation with P_2S_5 to 5*R*-**43** and subsequent aminolysis, yielded the expected (5*R*,6*R*)-**44** after separation of the minor (5*R*,6*S*)-diastereoisomer by column chromatography. Finally, copper-catalyzed coupling of (5*R*,6*R*)-**44** with sodium azide to give aniline (5*R*,6*R*)-**45**, followed by amide formation with 5-methoxypyrazine-2-carboxylate yielded compound (2*R*,3*R*)-**10**.

Scheme 4. Enantioselective synthesis of C-3 cyclopropyl substituted 1,4-oxazine **9**.[a]

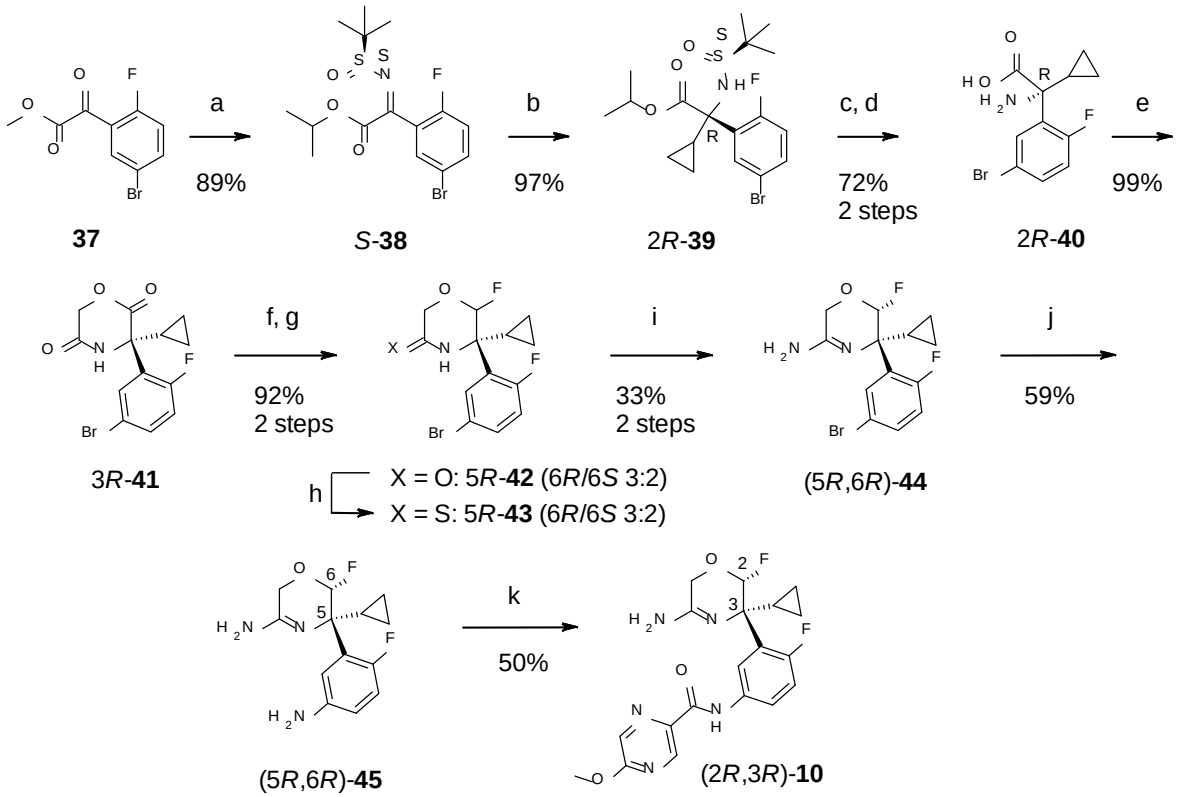

[a]Reagents and conditions: (a) *S*-*t*BuSONH$_2$, Ti(O*i*Pr)$_4$, heptane, 80 °C, 24 h; (b) *c*PrMgBr, DCM, -78 °C, 30 min; (c) 1 M NaOH, MeOH, reflux, 4 h; (d) 4 N HCl in 1,4-dioxane, rt, 1 h; (e) i. chloroacetyl chloride, 1 M NaOH, 1,4-dioxane, 1 h, ii. NaHCO$_3$, DMF, 80 °C, 2 h; (f) DIBAL-H, THF, -78 °C to rt, 2 h; (g) DAST, DCM, 0 °C, 40 min; (h) P_2S_5, THF, 70 °C, 4 h; (i) 33 % NH_3 (aq), 60 °C, 21 h; (j) NaN_3, CuI, DMEDA, Na_2CO_3, DMSO, 110 °C, 1 h; (k) 5-methoxypyrazine-2-carboxylic acid, DMTMM, MeOH, 0 °C, 6 h.

Racemic compounds (2*R**,3*R**)-**10** and (2*R**,3*R**)-**11** were prepared as shown in Scheme 5. First, ketones **46a,b** were converted to the α-aminonitriles *rac*-**47a,b** via a Strecker reaction. Direct acidic hydrolysis of the nitrile group in *rac*-**47a,b** to the carboxylic acids *rac*-**49a,b** was not successful in refluxing HCl (aq) due to rapid decarboxylation under the reaction conditions. This could be circumvented by the hydrolysis of the nitriles in *rac*-**47a,b** to the corresponding amides *rac*-**48a,b** with HBr in acetic acid, followed by basic hydrolysis with NaOH to *rac*-**49a,b**. The standard lactonization procedure involving initial *N*-acylation of *rac*-**49a,b** with chloroacetyl

chloride led also to decarboxylation. Fortunately, *O*-alkylation of *rac*-**49a,b** with *tert*-butyl chloroacetate to *rac*-**50a,b** followed by selective TFA-mediated hydrolysis of the *tert*-butyl ester yielded the amino acid derivatives *rac*-**51a,b**. Intramolecular cyclization of *rac*-**51a,b** with Mukaiyama reagent provided 1,4-oxazine-2,5-diones *rac*-**52a,b**. A similar reaction sequence to those previously described was used for the transformation of *rac*-**52a,b** into the target molecules *rac*-(2*R**,3*R**)-**11** and *rac*-(2*R**,3*R**)-**12**. However, since the amidine function in *rac*-(5*R**,6*R**)-**56a,b** was found to be more reactive towards a peptidic coupling than the aminopyridine fragment using DMTMM, the former needed to be selectively protected with a Boc group giving *rac*-(2*R**,3*R**)-**57a,b** prior to coupling reaction with the 5-methoxypyrazine-2-carboxylic acid. Subsequent cleavage of the Boc protecting group in *rac*-(5*R**,6*R**)-**58a,b** provided *rac*-(2*R**,3*R**)-**11** and *rac*-(2*R**,3*R**)-**12**, respectively.

Scheme 5. Synthesis of 1,4-oxazines *rac*-(2*R**,3*R**)-**11** and *rac*-(2*R**,3*R**)-**12** containing a pyridyl as A-ring.[a]

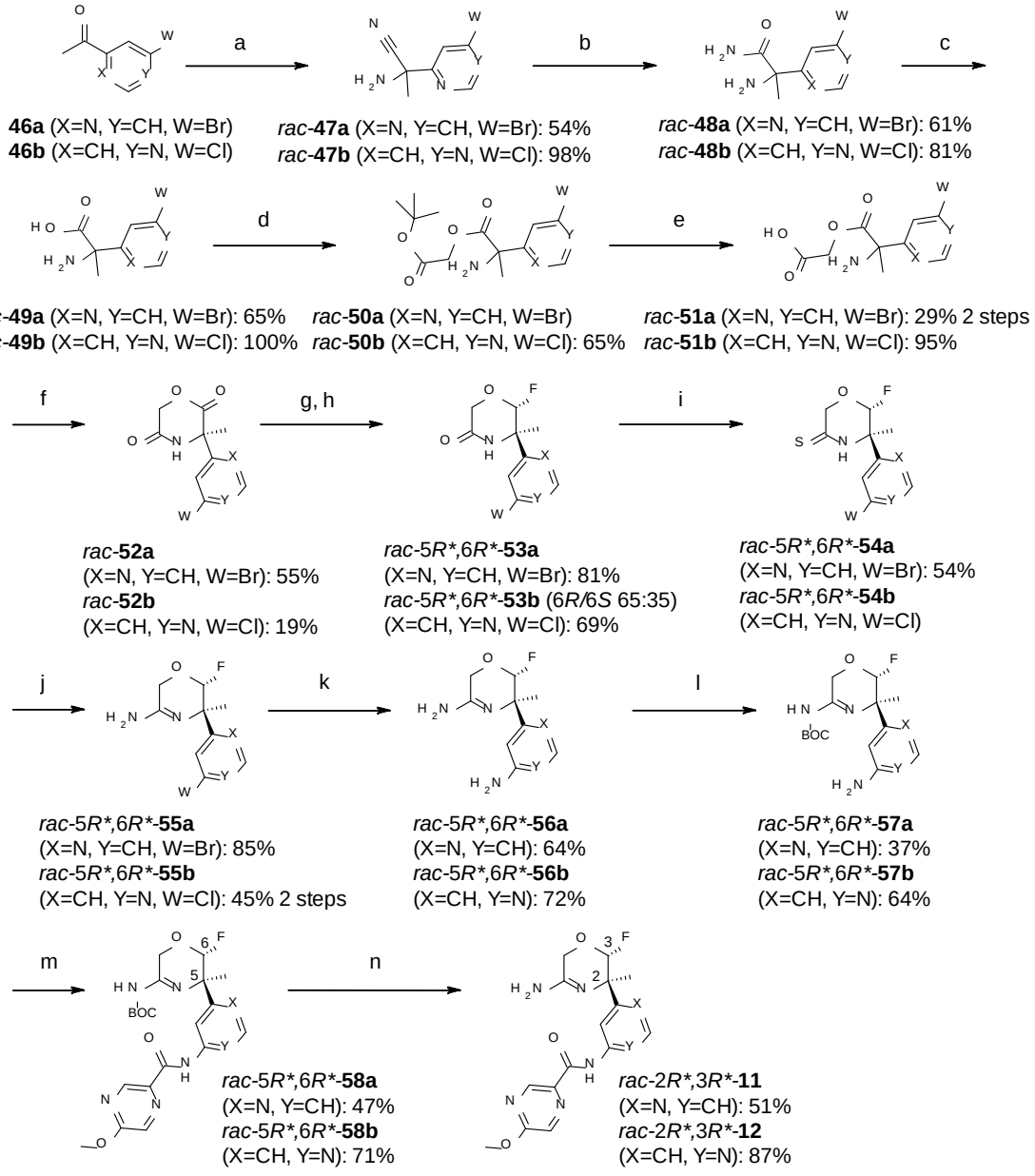

[a]Reagents and conditions: (a) TMSCN, NH_4Cl, NH_3/MeOH, 12 °C, 4 d; (b) 33 % HBr/AcOH, reflux, 12 h; (c) 1 M NaOH, 65 °C, 16 h; (d) $ClCH_2CO_2tBu$, Cs_2CO_3, DMF, rt, 3 h; (e) TFA, rt, 15 min; (f) 2-chloro-1-methylpyridinium iodide, DIPEA, DCM, reflux, 4 h; (g) DIBAL-H, THF, -78 °C to rt, 90 min; (h) DAST, DCM, 0 °C to rt; (i) P_2S_5, THF, 70 °C, 3 h; (j) 33 % NH_3 (aq), 80 °C, 2 h; (k) NaN_3, CuI, DMEDA, Na_2CO_3, DMSO, 110 °C, 24 h; (l) Boc_2O, DCM/ACN 1:1, rt, 22 h; (m) 5-methoxypyrazine-2-carboxylic acid, HATU, DIPEA, DMF, 50 °C, 3 h; (n) TFA, rt, 15 min.

RESULTS AND DISCUSSION

Our early benzoguanidine series provided us with an understanding of the optimal binding arrangement of the amidine motifs at the catalytic aspartates.[13] This series suffered from high basicity, examples having measured pK_a's in range of 11 and 12, which we associated with issues of poor permeation, brain penetration and P-gp efflux. We therefore emphasized the need to find similar amidine and guanidine binding motifs but with reduced basicity, assessed using calculated pK_a values. To implicitly capture elements of protein flexibility proposals were docked into multiple BACE1 crystal structures. At this preliminary stage we were using an entirely *in silico* approach as previously described.[21] A similar rational design concept but with different method of execution has been reported by others.[24] Alongside the previously reported piperazinones **3** and **4**,[21] the morpholine series **5** was prioritized highly by our approach. The docking of sample 1,4-oxazine molecules showed them to score particularly well, in fact, they were the best of all ideas profiled and docked optimally into the protein structure PDB 2VA7.[12] With regards to the basicity, the 1,4-oxazine was predicted to be in an ideal range.[25] For instance, whilst our previous benzoguanidines had a calculated basic pK_a of 11.1, an oxazine example such as 5-methyl-5-phenyl-5,6-dihydro-2*H*-1,4-oxazin-3-amine had a calculated basic pK_a of 6.4 (Scheme 6).[25] This apparently placed the 1,4-oxazines in a good range of basicity, being protonated in the acidic endosome environment in which BACE1 is active and therefore binding at the catalytic aspartates. Such a pK_a would be expected to provide a balanced degree of protonation at higher physiological pH, beneficial for CNS drugs.[26] However, comparison with the experimental pK_a reveals inaccuracy in the calculated value. Deeper analysis of this was performed once more examples were synthesised, and as the later discussion reveals, we may have been fortunate to have prioritised the oxazines via this in silico approach.

The morpholine derivatives 3*R*-**6a-c** were synthesized as early prototypes to set the baseline for potency and physicochemical properties of this class (Table 1). During the course of our research these molecules also got reported in an extensive warhead exploration published by Hoffmann-La Roche and Siena Biotech.[19,27] Based on previous SAR derived from the exploration of the piperazinone series **4**, 5-chloropyridine-2-carboxamide and 5-methoxy-2-pyrazinecarboxamide were chosen as B-rings to target the S3 pocket in the morpholine probe compounds 3*R*-**6a-c**. In addition, A-ring variations without (3*R*-**6a**) and with (3*R*-**6b**) a fluorine atom in *para*-position to the aniline on the A ring (see pharmacophore, Chart 1) were synthesized to assess its influence on pK_a and potency. Compounds 3*R*-**6a-c** had satisfactory inhibitory activity in the BACE1 enzymatic assay, with IC_{50}'s of 44, 22 and 44 nM respectively. This potency nicely translated into an inhibition of Aβ42 production of 9.1 nM (3*R*-**6a**), 4.1 nM (3*R*-**6b**) and 5.4 nM (3*R*-**6c**) in a human neuroblastoma cell line. *In vivo* reduction in Aβ peptides is assessed in mouse, hence determination of the cellular activity of 3*R*-**6a-c** in a mouse neuroblastoma cell line was also done and found to correlate well with the values obtained with the human cell line.

Table 1. *In vitro* profile of morpholines 3*R*-**6a-c**.[a]

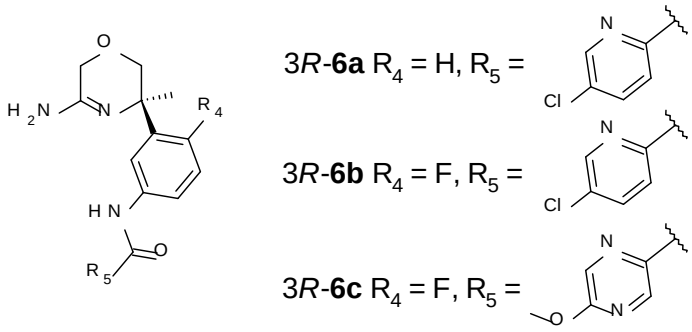

	3*R*-**6a**	3*R*-**6b**	3*R*-**6c**
BACE1 IC_{50} (nM)	44	22	44
hAβ42 cell IC_{50} (nM)	9.1	4.1	5.4
mAβ42 cell IC_{50} (nM)	7.4	4.5	4.3
hLM (% met. @ 15 min)	0	0	1
mLM (% met. @ 15 min)	6	10	6
f_u (brain, r, %)	2.9	3.1	10.1
f_u (plasma, h, %)	43	34	56
f_u, (plasma, m, %)	28	21	32
P_{app} A>B (nm/s)	n. d.	38	37
P_{app} A>B +elacridar (nm/s)	n. d.	231	154
P_{app} ratio	n. d.	6.0	4.2
pK_a	9.6	9.2	9.0

[a]See SI for assay details.

Further profiling of 3*R*-**6a-c** revealed that they had good metabolic stability in human (hLM) and mouse (mLM) liver microsomes, low binding to human and mouse plasma proteins and moderate non-specific binding to rat brain homogenate (f_u in plasma or brain). The experimental pK_a values were determined for 3*R*-**6a-c** and were found to be higher than predicted (3*R*-**6a** 9.6; 3*R*-**6b** 9.2; 3*R*-**6c** 9.0). The effect of a fluorine substituent in the A-ring was modest as seen for compound 3*R*-**6b** which showed only 0.4 Log unit (2.5 fold) reduction in pK_a when compared with the non-fluorine substituted analogue 3*R*-**6a**. In line with previous observations that high pK_a is associated with increased P-gp efflux,[20] high ratios of apparent permeability (P_{app}) in presence or absence of the P-gp inhibitor elacridar were measured for 3*R*-**6b** and 3*R*-**6c**: 6.0 and

4.2 respectively. Subcutaneous (s. c.) administration of a 30 mg/kg dose of 3*R*-**6b** to mouse (Table 2, A) showed modest brain levels (315 ng/g) at 2 h compared to plasma concentration (2397 ng/mL), resulting in a low brain/plasma ratio (K_p) of 0.13. These low concentrations in the brain translated into a marginal *in vivo* reduction of Aβ peptides in the brain of wild type (WT) CF-1 mice (Table 2, B) 2 h after dosing. When the same experiment was repeated using P-gp deficient CF-1 mice a more favorable brain/plasma ratio (K_p) of 1.1 was observed, which resulted into a much more pronounced reduction of Aβ peptides in brain compared to the one observed in WT animals. This experiment confirmed the detrimental role of P-gp efflux in the brain penetration of 3*R*-**6b**.

Table 2. Brain levels (A) and brain Aβ reduction (B) of 3*R*-**6b** in WT and P-gp deficient CF-1 mice.[a]

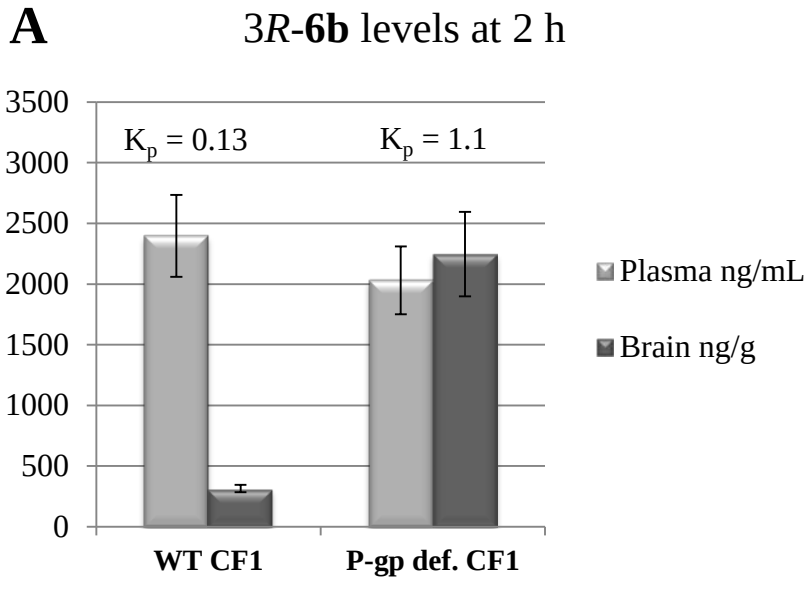

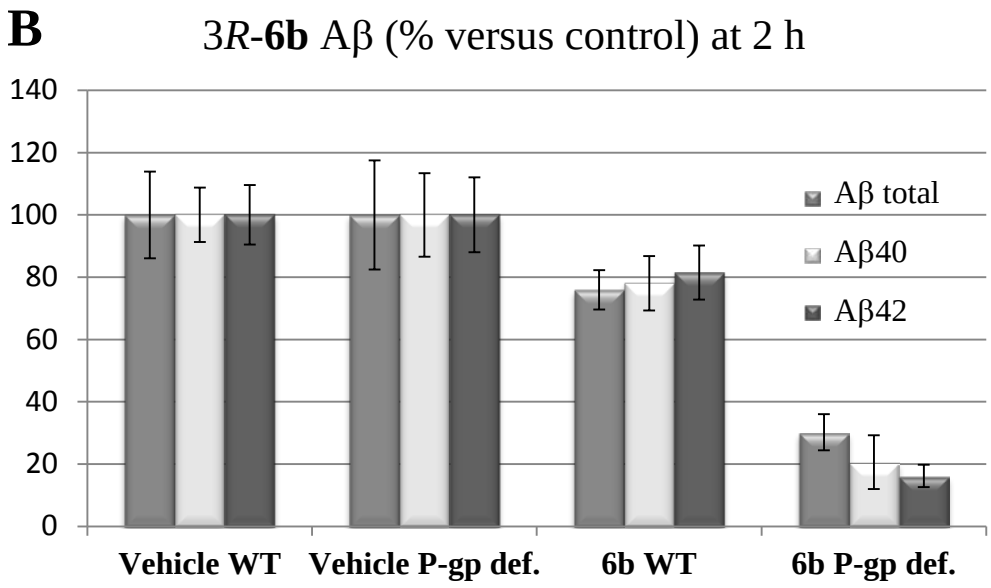

[a]30 mg/kg, s. c. (n=8); 3*R*-**6b** was formulated with 20 % SBEβCD at pH 3.5.

Whilst lower than our old benzoguanidine series the measured pK_a values were higher than expected from the initial calculations mentioned above.[13] This prompted a deeper inspection of the accuracy of the calculated pK_a's on these unusual amidine containing ring systems. A selection of 42 compounds containing a cyclic amidine substructure from our compound collection was subjected to experimental pK_a measurement (data in SI). The selection set encompassed multiple heterocyclic chemotypes and covering approximately a 10 log unit range in calculated pK_a. Molecules with multiple ionizable centers were in general avoided. The pK_a's were calculated with a variety of methods, and the correlation with experiment is shown in SI. In contrast to previous studies comparing performance across global datasets,[28] ADMET predictor performed better than ACD for these amidine ring systems (R^2 = 0.88 compared to R^2 = 0.75 for best ACD case). This was especially true in the relevant pK_a range of 6 to 10. These results prompted us to reassess our 1,4-oxazine series with calculations on specific prototypes (Scheme

6) confirming improved performance when using AP.[29] This reiterates the need to calibrate the performance of pK_a calculations for novel chemical systems.

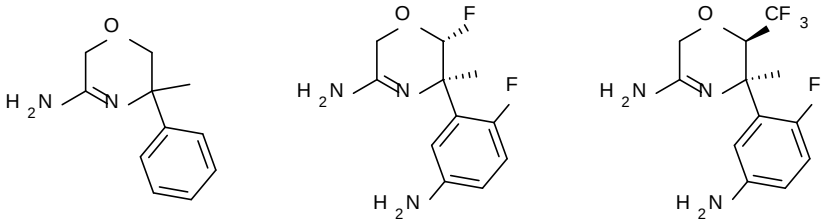

pKa Experiment	**9.8**	**8.1**	**8.0**
pKa calculated ACD[a]	**6.4**	**3.8**	**4.6**
pKa calculated ACD[b]	**10.4**	**9.7**	**9.9**
pKa calculated with AP	**9.6**	**7.3**	**6.7**

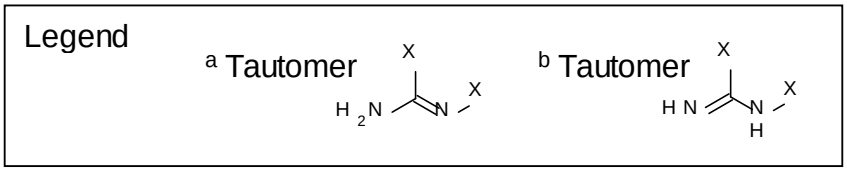

Scheme 6. Comparison of the calculated pK_a to experiment for prototype 1,4-oxazines using ACD v2014 and AP.

The crystal structure of 3*R*-**6a** with BACE1 was solved at 2.6 Å resolution (PDB code 5CLM, Figure 1). The result confirmed a binding mode similar to that seen for other bisarylamide substituted amidine BACE1 inhibitors.[17] Namely, the amidine group makes the key and strong network of interactions with the catalytic aspartate dyad (Asp32 and Asp228) involving several hydrogen bonds and a charge-charge interaction between the protonated amidine and anionic acid groups. The A-ring (phenyl) occupies the S1 pocket, and the B-ring (5-chloro-2-pyridyl) enters the S3 pocket. The S1 pocket is formed by amino acids including Phe108 whereas the S3 is bordered by the presence of Thr232 and amino acids from the 10s loop such as Gly11, Gln12

and Gly13 (10s loop, blue in Figure 1). Para substituents on the B-ring approach the salt bridge formed by Arg307 and Glu339. Between the A- and B-ring, the amide N-H forms an H-bond to the backbone carbonyl of Gly230. This bisarylamide has become a widely used group in substituted amidine BACE1 inhibitors, likely because of the optimal shape complementarity with the S1 and S3 pockets.[15]

Based on the finding that P-gp efflux was influenced by the basicity of the amidine containing warhead, several options for chemical modification of the 1,4-oxazine ring by the introduction of electron withdrawing substituents were possible to reduce its high pK_a. Close inspection of the 1,4-oxazine cycle reveals that the two possible sp^3 carbon substitution points have different environments. The carbon which is between the oxygen and the amidine (C-6) is more exposed towards solvent. On the other hand, the carbon between the oxygen and the quaternary carbon, (C-2), would direct its substituents towards the active site flap (green in Figure 1). The flap is a well-known feature of the BACE1 binding site, it is flexible and more open at lower pH, correlating with higher enzyme activity.[30] It is known to adopt different conformations dependent on the bound inhibitor. Molecules are reported which interact with amino acids such as Tyr71,[13] (Figure 1) and the adjacent Thr72 for example.[30] Therefore, given that the amidine warhead was satisfying the interactions at the catalytic aspartates, we set out to target alternative contacts with the flap. Specifically, C-2 position provided an ideal vector to interact with the aromatic ring of Tyr71, whilst steric factors would limit the size of the proposed substituents.

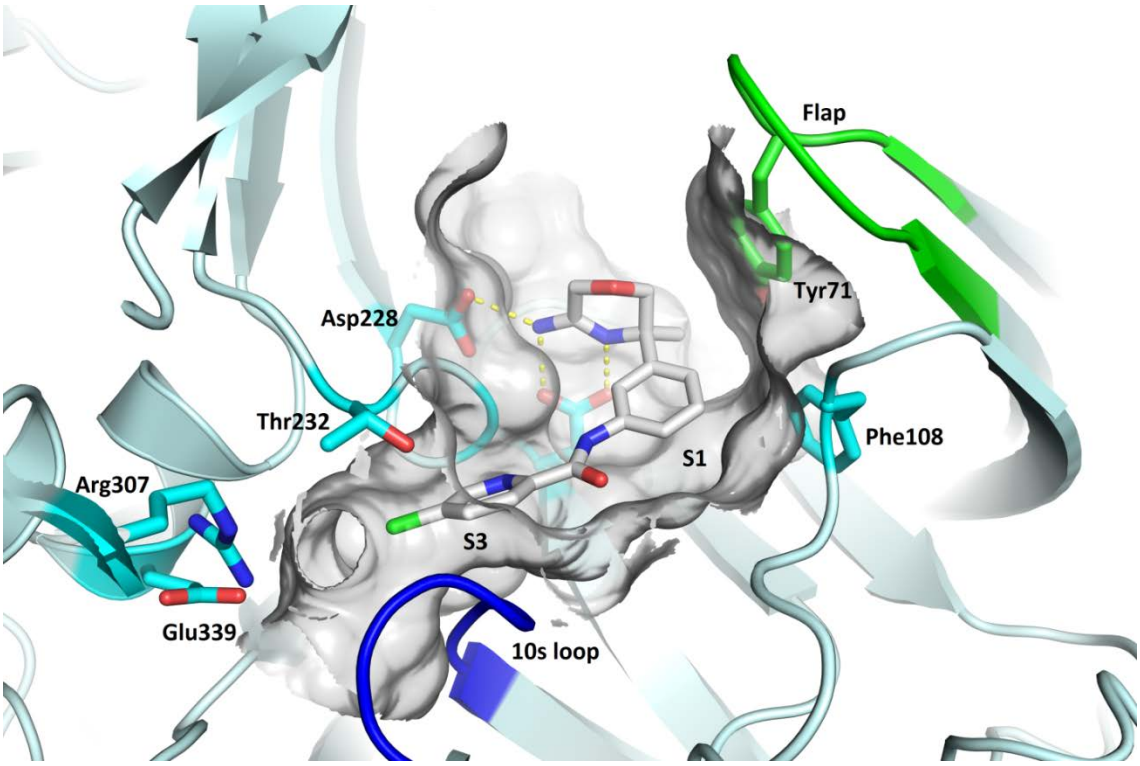

Figure 1. Crystal structure of 3*R*-**6a** in BACE1 (1-454). Amino acids as labelled. Active site flap highlighted in green and 10s loop in blue.

An overview of the different modifications explored at C-2 position of the 1,4-oxazine warhead is shown in Chart 2. A fluorine (**I**), CF_3 (**II**) and a combination of both groups (**III**) were selected as optimal C-2 substituents to further modulate pK_a of 3*R*-**6c** whilst interacting with the active site flap.

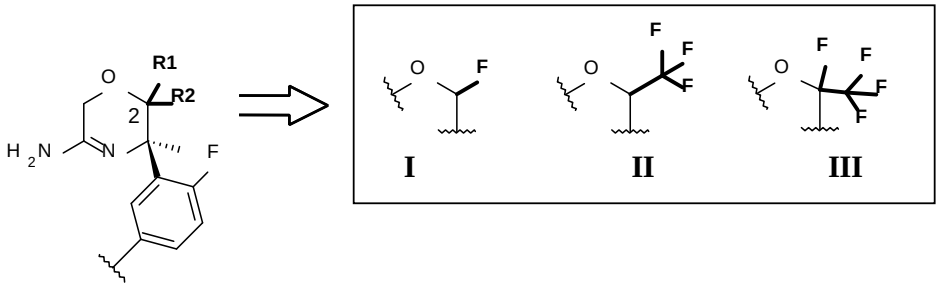

Chart 2. Scope of exploration at C-2 position to modulate pK_a.

BACE1 enzymatic and cellular activity, experimental pK_a values, P_{app} ratios and Log D values for 3*R*-**6c** and fluorinated 1,4-oxazines (2*S*,3*R*)-**7a**, (2*R*,3*R*)-**7a**, (2*S*,3*R*)-**8**, (2*R*,3*R*)-**8**, (2*R*,3*R*)-**9** and (2*S*,3*R*)-**9** are provided in Table 3.[31] Interestingly, the 2*R*-fluoro substituent in (2*R*,3*R*)-**7a** was found to be highly effective in reducing the basicity of the amidine: a pK_a of 7.8 was measured, which is a decrease by 1.2 log units when compared with the C-2 non-substituted oxazine 3*R*-**6c**. This was aligned with our expectations based on the AP calculated values for this substitution (Scheme 6). The reduction in pK_a was not detrimental for the primary enzymatic and cellular activity, with the discrepancy between both assays decreased when compared to 3*R*-**6c**. This is a general trend observed for our amidine-based BACE1 inhibitors: the lower the pK_a, the smaller the discrepancy becomes between enzymatic and cellular activity. A possible explanation is that highly basic inhibitors accumulate in the acidic endosomes where BACE1 is most active. As such they display apparently higher activity in cellular than biochemical assays, whereas lower pK_a results in cellular activity in closer accordance with the one in the biochemical assay due to a more uniform distribution of the compound in cellular compartments. Furthermore, compound (2*R*,3*R*)-**7a** showed good permeability in a LLC-MDR cell line (P_{app} 201 nm/s with elacridar) and a low P_{app} ratio of 1.1 providing additional support to the hypothesis that lowering the amidine pK_a would have beneficial effects in P_{app} ratios. Interestingly, while in the same pK_a range, the diastereomeric (2*S*,3*R*)-**7a** had a much reduced BACE1 IC_{50} of 102 nM, which translated in an equally reduced cellular activity of 93 nM. We hypothesized that this potency difference could be attributed to the anomeric effect, which favors the 2-fluoro substituent in the axial position. QM calculations indeed confirmed this effect stabilizes the bioactive conformation for (2*R*,3*R*)-**7a** (see SI). However in the case of (2*S*,3*R*)-**7a** the conformation with the 2-fluorine in axial position places the phenyl in the unfavorable equatorial position for

binding to BACE1.[32] An additional CF_3 group at C-2 position such as 2*S*-C(F)CF_3 disubstitution in (2*S*,3*R*)-**8** reduces pK_a by another log unit ((2*S*,3*R*)-**8**, pK_a = 6.8), while maintaining a potency of 20 nM in the BACE1 enzymatic assay. Unfortunately, the 2*S*-C(F)CF_3 disubstitution had a detrimental effect on the cellular activity and compound (2*S*,3*R*)-**8** was ~ 6-fold less potent than 3*R*-**6c**. Interestingly, the diastereoisomeric 2*R*-C(F)CF_3 1,4-oxazine (2*R*,3*R*)-**8** displayed poor inhibitory activity in both enzymatic and cellular assays. This drop in potency could be rationalized after a close inspection of the crystal structure (Figure 1) of 3*R*-**6c**, which suggests that the CF_3 group in (2*R*,3*R*)-**8** would be directed into the face of Tyr71, producing an unfavorable interaction between the negative electrostatic properties of both the CF_3 and the π cloud of Tyr71. A similar but less pronounced trend in enzymatic activity was also observed for the 2-C(H)CF_3 diastereoisomeric pair (2*R*,3*R*)-**9** (IC_{50} = 29 nM) and (2*S*,3*R*)-**9** (IC_{50} = 110 nM), although in this case it did not translate in a difference in cellular activity: (2*R*,3*R*)-**9** IC_{50} = 13 nM *vs* (2*S*,3*R*)-**9** IC_{50} = 14 nM. Compound (2*R*,3*R*)-**9**, with a pK_a of 7.8, illustrated again the ability of the electron withdrawing ability of the CF_3 group to reduce the amidine pK_a and its beneficial contribution to a lower P_{app} ratio of 1.2. Similarly, while the permeability for (2S,3R)-**8** was not determined, close analogues with different B-rings showed low P_{app} ratios in the 1.2 (5-chloropyridine-2-carboxamide) to 1.6 (4-cyanopyridyl-2-carboxamide) range.

Table 3. Comparison of BACE1 enzymatic and cellular activities, pK_a's and P_{app} ratios for different C-2 substituted 1,4-oxazine warheads.[a,b]

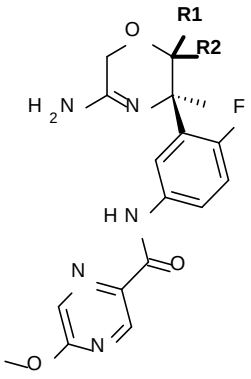

	3*R*-**6c**	(2*S*,3*R*)-**7a**	(2*R*,3*R*)-**7a**	(2*S*,3*R*)-**8**	(2*R*,3*R*)-**8**	(2*R*,3*R*)-**9**	(2*S*,3*R*)-**9**
				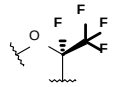	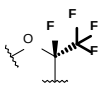	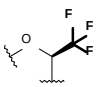	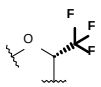
BACE1 IC_{50} (nM)	44	102	12	20	316	29	110
hAβ42 cell IC_{50} (nM)	5.4	93	9.1	34	324	13	14
P_{app} A>B (nm/s)	37	n. d.	176	n. d.	n. d.	137	n. d.
P_{app} A>B +elacridar (nm/s)	154	n. d.	201	n. d.	n. d.	160	n. d.
P_{app} ratio	4.2	n. d.	1.1	n. d.	n. d.	1.2	n. d.
LogD (pH 7.4)	n. d.	n. d.	2.04	3.43	n. d.	2.52	n. d.
pK_a	9.0	7.6	7.8	6.8	6.9	7.8	8.0

[a]See SI for assay details. [b]n. d.: not determined

LogD was also measured for the most promising leads (2*R*,3*R*)-**7a**, (2*S*,3*R*)-**8** and (2*R*,3*R*)-**9**, with (2*R*,3*R*)-**7a** showing the lowest value (LogD = 2.04). From the data obtained compound (2*R*,3*R*)-**7a** showed the most balanced profile with good enzymatic and cellular activity, low pK_a and LogD values, and good permeability and P_{app} ratio. Since sugars with anomeric fluorines are known to be hydrolytically unstable,[33] the chemical stability of (2*R*,3*R*)-**7a** was assessed by

LCMS-based experiments under a variety of conditions ranging from acidic to basic media and different temperatures after seven days (see SI). In these experiments, (2*R*,3*R*)-**7a** was found to be sufficiently stable at room temperature up to one week in buffer at pH 7.4 (92% remaining) and DMSO (100% remaining) to warrant further exploration.

Analysis of the crystal structure of 3*R*-**6a** suggested that space is available around the methyl substituent at the quaternary center in the S2' pocket, hence a limited synthetic effort was devoted to better fill this pocket. Compound (2*R*,3*R*)-**10** bearing a C-2 fluoro substituent and a cyclopropyl group at position C-3 was selected as a potential target. BACE1 enzymatic and cellular activity, metabolic stability data and pK_a values are given for compounds (2*R*,3*R*)-**10** and (2*R*,3*R*)-**7a** in Table 4. An approximately 5-fold decrease in enzymatic activity was measured for (2*R*,3*R*)-**10** (IC_{50} = 66 nM) compared to (2*R*,3*R*)-**7a** (IC_{50} = 12 nM), however, a much more significant 66-fold drop in cellular activity was also observed (2*R*,3*R*)-**10**: IC_{50} = 603 nM *vs* (2*R*,3*R*)-**7a**: IC_{50} = 9.1 nM). Compared to (2*R*,3*R*)-**7a**, (2*R*,3*R*)-**10** showed increased metabolic stability in hLM, but a slightly higher turnover in mLM. Finally, no difference in pK_a between (2*R*,3*R*)-**7a** and (2*R*,3*R*)-**10** was measured. We hence decided to maintain the methyl group at the quaternary center for further optimization of (2*R*,3*R*)-**7a**.

Table 4. Modification on the quaternary methyl group.[a]

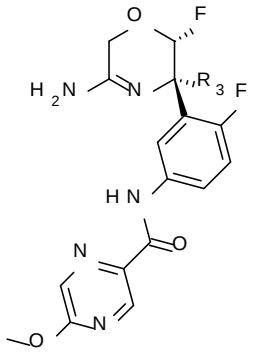

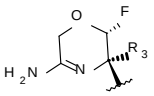	(2*R*,3*R*)-**7a** 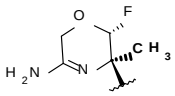	(2*R*,3*R*)-**10** 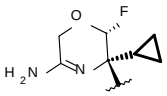
BACE1 IC_{50} nM	12	66
hAβ42 cell IC_{50} nM	9.1	603
pK_a	7.8	7.8

[a]See Experimental Section for assay details.

To generate additional SAR on potency and pK_a variation of the A-ring was studied next. Analogues *rac*-(2*R**,3*R**)-**11** and *rac*-(2*R**,3*R**)-**12** in which the A-phenyl ring is replaced by a 2- or 4-pyridyl ring were synthesized. BACE1 enzymatic and cellular activity, metabolic stability data and pK_a values are given for compounds (2*R*,3*R*)-**7a**, *rac*-(2*R**,3*R**)-**11**, *rac*-(2*R**,3*R**)-**12** in Table 5. Interestingly the reduced basicity of the amidines was maintained when replacing the phenyl A-ring in (2*R*,3*R*)-**7a** by a 2-pyridyl as in *rac*-(2*R**,3*R**)-**11** (pK_a = 7.8) and the regioisomeric 4-pyridyl analogue *rac*-(2*R**,3*R**)-**12** (pK_a = 7.6). In addition, the pK_a value of the pyridyl nitrogen in *rac*-(2*R**,3*R**)-**11** and *rac*-(2*R**,3*R**)-**12** was measured to be 2.6 and 2.8 respectively and hence no protonation of this ring is expected to occur under physiological conditions. Unfortunately, while the pK_a of *rac*-(2*R**,3*R**)-**11** and *rac*-(2*R**,3*R**)-**12** was in the desired range, the presence of the pyridyl ring was found to be detrimental for BACE1 activity,

with the 2-pyridyl isomer *rac*-(2*R**,3*R**)-**11** significantly less potent than (2*R*,3*R*)-**7a** and *rac*-(2*R**,3*R**)-**12** only active in the μM range.

Table 5. Overview of A-ring modifications.[a]

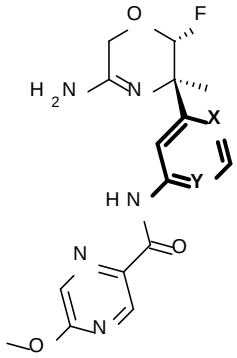

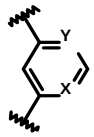	(2*R*,3*R*)-**7a** 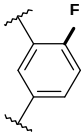	*rac*-(2*R**,3*R**)-**11** 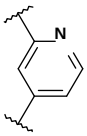	*rac*-(2*R**,3*R**)-**12** 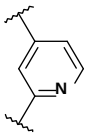
BACE1 IC_{50} nM	12	74	3467
hAβ42 cell IC_{50} nM	9.1	257	1445
pK_a	7.8	7.8; 2.6	7.6; 2.8

[a]See Experimental Section for assay details.

Finally, a limited SAR exploration of the B-ring in (2*R*,3*R*)-**7a** using different pyridine-2-yl carboxylic acids was performed following a similar synthetic route. A set of representative compounds (2*R*,3*R*)-**7a-d** along with BACE1 primary activity, data from broader profiling in ADME-tox assays and physicochemical properties, are given in Table 6. Although in general excellent enzymatic and cellular activity data were obtained for all compounds having a pyridyl B-ring ((2*R*,3*R*)-**7b-d**) subtle differences were observed regarding their *in vitro* ADME properties. For instance, while (2*R*,3*R*)-**7b** and (2*R*,3*R*)-**7d** retained excellent metabolic stability

across tested species, the trisubstituted pyridine (2*R*,3*R*)-**7c** was notably unstable in mLM. All compounds showed a low potential to inhibit CYP450 isoforms 1A2, 3A4, 2C9 and 2C19 compared to their IC_{50}'s. The strongest inhibition of the 2D6 isoform was observed for compound (2*R*,3*R*)-**7a** with an IC_{50} of 600 nM, still leading to a 50-fold margin when compared with the enzymatic BACE1 activity (IC_{50} = 12 nM). In addition, all compounds displayed high free fractions in plasma across species (5.0-60 % free) and a reasonable free fraction in rat brain tissue (1.0-4.4 % free). Cardiovascular safety of the compounds was first assessed using a hERG channel patch-clamp assay indicating that the B-ring has a strong effect on hERG inhibition. For instance, while the 5-methoxypyrazine (2*R*,3*R*)-**7a** showed a relatively weak inhibition of the hERG channel at 3 μM (33%), the pyridyl derivative (2*R*,3*R*)-**7b** showed a much stronger hERG inhibition (78%) at the same concentration. This strong interaction could be mitigated by installing a methyl group on the pyridine as in (2*R*,3*R*)-**7c** (52 % inhibition). Finally the 4-cyanopyridyl derivative (2*R*,3*R*)-**7d** showed 56 % hERG inhibition at 3 μM. As could be expected for this 2*R*-F substituted warhead, P_{app} ratios for analogues (2*R*,3*R*)-**7b-d** were generally acceptable, with (2*R*,3*R*)-**7d** being a notable exception with an P_{app} ratio of 3.6.

Table 6. Overview of B-ring modifications.[a, b]

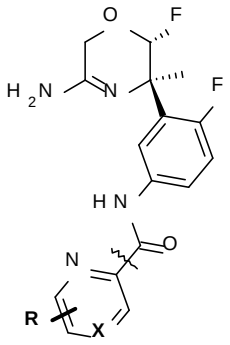

	(5*2*,6*3*)-**7a**	(2*R*,3*R*)-**7b**	(2*R*,3*R*)-**7c**	(2*R*,3*R*)-**7d**
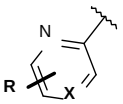	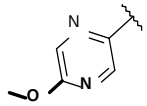	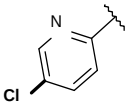	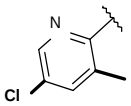	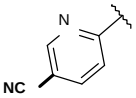
BACE1 IC_{50} nM	12	7.4	6.9	7.6
hAβ42 cell IC_{50} nM	9.1	5.2	3.3	8.1
hLM (% met. @ 15 min)	31	0	16	0
mLM (% met. @ 15 min)	3	17	98	2
dLM (% met. @ 15 min)	70	7	21	0
CYP450 inh. <10 μM	2D6 (0.6)	none	none	2D6 (4.3)
f_u (brain, r, %)	4.4	1.9	1.0	3.9
f_u (plasma, h, %)	60	18	11	41
f_u (plasma, m, %)	28	14	5.0	30
f_u (plasma, d, %)	34	n. d.	n. d.	42
hERG PX (% inh. @ 3 μM)	33	78	52	56
P_{app} A>B (nm/s)	176	85	93	51
P_{app} A>B +elacridar (nm/s)	201	167	142	183
P_{app} ratio	1.1	2.0	1.5	3.6
pK_a	7.8	7.9	7.4	7.9

[a]See Experimental Section for assay details. [b]n. d.: not determined

From the exploration of the B-ring, compounds (2*R*,3*R*)-**7a** and (2*R*,3*R*)-**7d** showed the best balance between potency, hERG liability, and *in vitro* P-gp efflux liability, and therefore were progressed to *in vivo* PK/PD evaluation. The results obtained are summarized in Table 7. In these experiments, compounds were dosed orally (p. o.) to male Swiss mice at 10 mg/kg. Plasma

levels are shown for three time points. For each time point, one hemisphere of the brain was used to conduct bioanalysis, and the other hemisphere for AlphaLisa quantification of Aβ. In line with the measured P_{app} ratios of 1.1 and 3.6, a higher brain uptake relative to plasma was observed for compound (2*R*,3*R*)-**7a** (K_p = 0.65) compared to (2*R*,3*R*)-**7d** (K_p = 0.33). Gratifyingly, a robust Aβ42 reduction of 62 % for (2*R*,3*R*)-**7a** and 57 % for (2*R*,3*R*)-**7d** was observed in brain homogenate at 4 h after administration, corresponding to brain levels of 195 ng/g for (2*R*,3*R*)-**7a** and 98 ng/g for (2*R*,3*R*)-**7d**. This substantial reduction in Aβ42 is in line with their high *in vitro* potency (resp. 12 and 7.6 nM) and good free fraction in brain. Moreover, this significant reduction of Aβ42 in brain is maintained up to 7-8 h.

Table 7. Mouse pharmacokinetic profile of (2*R*,3*R*)-**7a** and (2*R*,3*R*)-**7d** with associated Aβ levels in brain.[a]

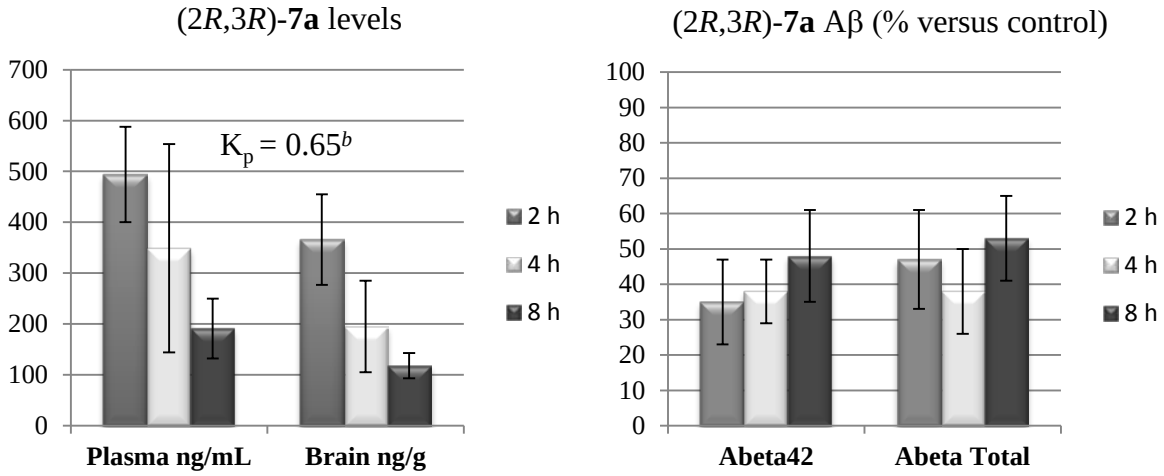

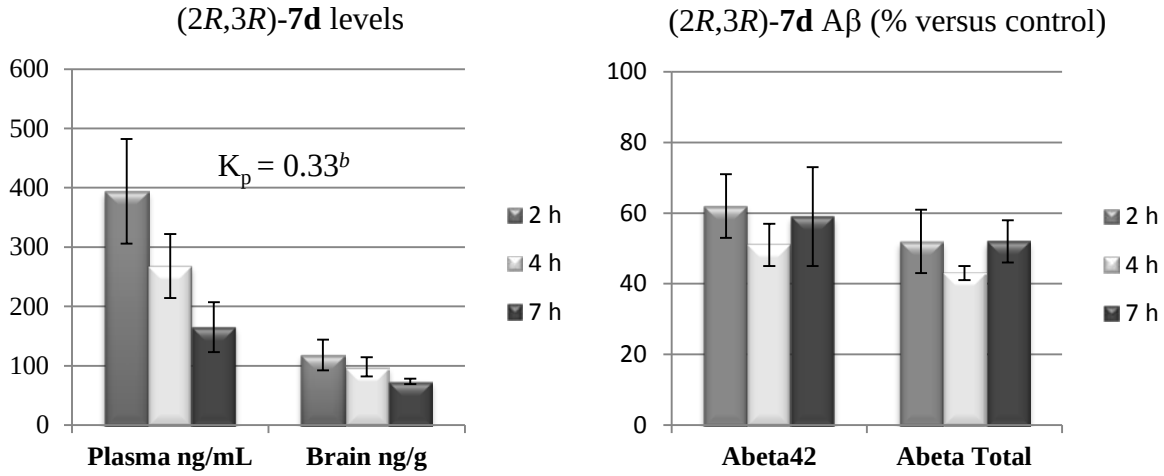

[a]10 mg/kg p. o. Male Swiss SPF mouse fasted (n=6); (2*R*,3*R*)-**7a** formulated with 20 % HPβCD at pH 3.9; (2*R*,3*R*)-**7d** formulated with 20 % SBEβCD at pH 3.5. [b]Calculated with $AUC_{0\text{-last}}$, see SI.

Since (2*R*,3*R*)-**7a** suffers from a high metabolic turnover in dog liver microsomes (dLM,70 % metabolized after 15 min), the more metabolically stable (2*R*,3*R*)-**7d** was selected for subsequent dog efficacy studies. Dog *in vivo* plasma concentrations and measured Aβ levels in cerebrospinal fluid (CSF) after administration of increasing doses from 0.08 to 10 mg/kg are given in Table 8.[34] From this study it can be seen that there is a linear relation between dose and plasma levels with an exceptionally long half-life of about 25 h, which underscores the chemical stability of these fluoromorpholines under physiological conditions. In agreement with this, a dose dependent reduction of Aβ42 was observed in CSF, with the 2.5 mg/kg dose showing over 90 % reduction of CSF Aβ42 up to 50 h post dosing.

Table 8. Dog *in vivo* plasma levels and CSF Aβ42 levels of (2*R*,3*R*)-**7d**.[a]

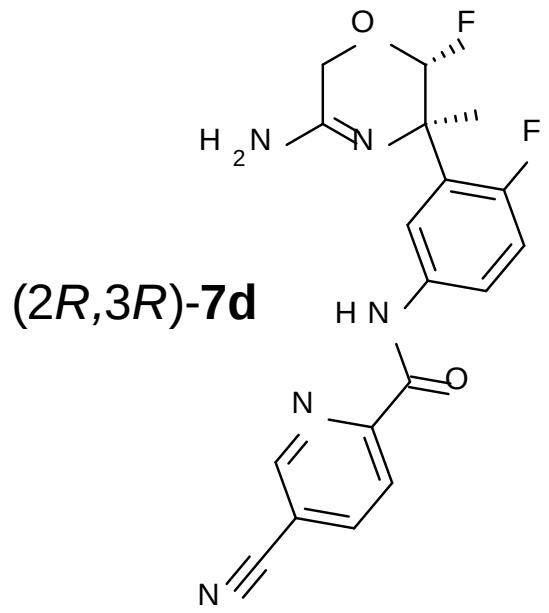

BACE1 IC_{50} nM	7.6
hAβ42 cell IC_{50} nM	8.1
dLM (% met. after 15 min)	0
C_{max} (2.5 mg/kg, ng/mL)	571 ± 131
$T_{½}$ (2.5 mg/kg, h)	25 ± 4
T_{max} (2.5 mg/kg, h)	2.5 ± 1.0
CSF Aβ42 dog EC_{50} (ng/mL)[34]	~ 20

Compound levels in plasma

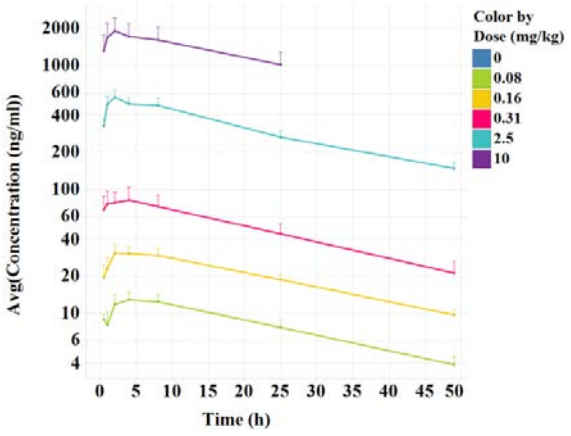

Aβ42 levels in CSF

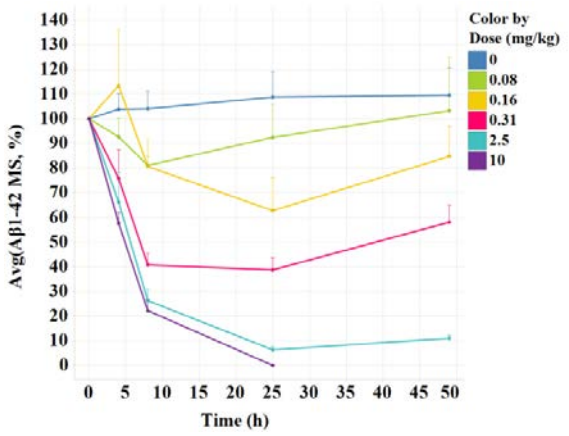

[a]Male (n=2/dose group) and female (n=2/dose group) Beagle dog fasted; (2*R*,3*R*)-**7d** formulated with 20 % HPβCD at pH 3.5.

CONCLUSIONS

In summary, a novel class of 1,4-oxazine-based BACE1 inhibitors has been identified through rational design. The medicinal chemistry optimization effort through careful structural warhead modification to fine tune the amidine pK_a along with BACE1 primary activity, has resulted in the identification of 2-fluoro-1,4-oxazines (**I**, Chart 2). Lead optimization efforts identified (2*R*,3*R*)-**7a** and (2*R*,3*R*)-**7d** as potent orally bio-available BACE1 inhibitors displaying a robust reduction of Aβ peptides in mice. This amyloid reduction was also confirmed for (2*R*,3*R*)-**7d** in dog, where this compound was able to dose dependently decrease Aβ levels in CSF up to 50 h post dosing. Challenges remain to navigate the narrow physical chemical property space, especially balancing brain penetration with other critical parameters like metabolic stability and cardiovascular safety (hERG inhibition). Further optimization studies using fluoromorpholines and the other fluorinated warheads described above are under way and will be disclosed in due time.

EXPERIMENTAL SECTION

Enzymatic BACE1 assay. Primary BACE1 enzymatic activity was assessed by a FRET assay using an amyloid precursor protein (APP) derived 13 amino acids peptide that contains the 'Swedish' Lys-Met/Asn-Leu mutation of the APP beta-secretase cleavage site as a substrate (Bachem cat No. M-2465) and soluble BACE1(1-454) (Aurigene, Custom made). This substrate contains two fluorophores, (7-methoxycoumarin-4-yl) acetic acid (Mca) is a fluorescent donor with excitation wavelength at 320 nm and emission at 405 nm and 2,4-dinitrophenyl (Dnp) is a proprietary quencher acceptor. The increase in fluorescence is linearly related to the rate of proteolysis. In a 384-well format, BACE1 is incubated with the substrate and the inhibitor. The amount of proteolysis is directly measured by fluorescence measurement in the Fluoroskan

microplate fluorometer (Thermo scientific). For the low control no enzyme was added to the reaction mixture.

Cellular Aβ assay. Cellular activity was assessed using a SKNBE2 (human) or Neuro-2a (mouse) neuroblastoma cell line expressing the wild type Amyloid precursor protein (hAPP695). The compounds are diluted and added to these cells, incubated for 18 hours and then measurements of Aβ42 and Aβtotal are taken. Aβ42 and Aβtotal are measured by a sandwich αlisa assay using biotinylated antibody (AbN/25) attached to streptavidin-coated beads and antibody (cAb42/26) conjugated acceptor beads. In the presence of Aβ42, the beads come into close proximity. The excitation of the donor beads provokes the release of singlet oxygen molecules that triggers a cascade of energy transfer in the acceptor beads, resulting in light emission.

Metabolic stability assay. To test for metabolic stability, compounds (1 μM) were incubated at 37 °C with mouse, rat and human liver microsomes at a protein concentration of 1 mg protein/mL microsomal protein, 1 mM NADPH, 1 mM $MgCl_2$, and 0.1 M phosphate buffer, pH 7.4. DMSO Stock solutions (5 mM) of each compound were diluted with acetonitrile:water (1:1) to provide a working stock solution at 0.1 mM. The total incubation volume was 0.5 mL with a final total solvent content of 0.01% (v/v) DMSO and 0.5% (v/v) acetonitrile. The reaction was initiated by the addition of 100 μL pre-warmed NADPH solution. The incubation mixture was sampled at 15 min, and the sample quenched with 200 μL acetonitrile, centrifuged and analyzed using a specific HPLC-MS/MS technique. The percentage metabolized was taken as the disappearance of test compound at 15 min.

CYP450 inhibition assay. The potential to reversibly inhibit the major human P450 isoforms (CYPs 1A2, 2C9, 2C19, 2D6, and 3A4 was determined using recombinantly expressed human

CYPs. Specific probe substrates were used for each CYP isoform which were known to be selectively metabolized to defined fluorescent metabolites. Each test compound was incubated with individual CYPs over a concentration range up to 10 μM. At the end of the incubation, the level of fluorescence was measured on a plate reader. The level of fluorescence in the presence and absence of test compound was used to determine the IC_{50} against each CYP isoform.

Plasma protein binding assay. The binding to mouse, dog and human plasma proteins was determined by Rapid Equilibrium Dialysis (RED Device, Thermo Fisher Scientific, Geel, Belgium). The RED device consists of a 48 well plate containing disposable inserts bisected by a semi-permeable membrane creating two chambers. A 300 μL aliquot of plasma containing test compound at 5 μM was placed one side and 500 μL of phosphate buffered saline (PBS) the other. The plate was sealed and incubated at approximately 37 °C for 4.5 h. After 4.5 h samples were removed and both the plasma and buffer compartment and analyzed for test compound using a specific HPLC-MS/MS method to estimate free and bound concentrations.

Non-specific binding to brain tissue assay. The *in vitro* non-specific binding of compounds to rat brain homogenate was determined using the RED Device (see above). Each test compound was diluted with rat brain homogenate, prepared following a 1:10 dilution with PBS, to achieve a final concentration of 5 μM. The plate was incubated at approximately 37 °C for 5 h. After 5 h samples were removed from both the brain homogenate and buffer compartment and analyzed for test compound using a specific HPLC-MS/MS method to estimate free and bound concentrations.

***In vitro* permeability/P-gp efflux assay.** The *in vitro* permeability and potential to be transported by P-glycoprotein (P-gp) was determined using an LLC cell line transfected with human MDR1 (P-glycoprotein). Each test compound (5 μM) was added to either the apical (A)

side of a confluent monolayer of LLC-MDR1 cells and permeability towards the basolateral (B) direction measured by monitoring the appearance of the test compound on the opposite side of the membrane using a specific LC-MS/MS method. Permeability was assessed in with and without elacridar (GF 120918, CAS 143851-98-3), a well-known P-gp inhibitor. The A>B+elacridar/A>B ratio (P_{app} ratio) was calculated and used to determine if the test compound was subject to efflux by P-gp.

Mouse *in vivo* PK and Aβ quantification. Male CD1 Swiss Specific Pathogen Free (SPF) mice (Charles River company, Germany) were dosed p. o. or s. c. with the formulated (20% HPβCD) compound. After the indicated time of treatment, the animals were sacrificed and Aβ levels were analyzed. Blood was collected by decapitation and exsanguinations in EDTA-treated collection tubes. Blood was centrifuged at 1900 g for 10 min at 4 °C and the plasma recovered and flash frozen for later analysis. The brain was removed from the cranium and hindbrain. The cerebellum was removed, and the left and right hemisphere were separated. The left hemisphere was stored at -18 °C for quantitative analysis of test compound levels. The right hemisphere was rinsed with phosphate buffered saline (PBS) buffer and immediately frozen on dry ice and stored at -80 °C until homogenization for biochemical assays. The other hemisphere is homogenized and centrifuged and processed for the quantification of Aβ total and Aβ42 via ELISA as described previously.[35] Briefly for the quantification of Aβtotal Aβ42 the antibody pair JRF/rAb/2 and 4G8 or JRF/cAb42/26 and JRF/rAb/2 antibody was used for capturing and detection respectively.

Dog *in vivo* PK and Aβ quantification. Female beagle dogs were dosed p. o. with the formulated (20% HPβCD) compound or vehicle. At the indicated time points CSF was sampled in conscious dogs from the lateral ventricle. Quantification of Aβ42 in dog CSF was performed

using MesoScale Discovery (MSD)'s electrochemiluminescence detection technology as described previously.[34]

pK_a assay. Dissociation constants were determined at 25 °C by potentiometric titration of a solution of the compound of interest using a Sirius GlpKa apparatus, and values were calculated using the Henderson-Hasselbach equation. For poorly soluble compounds, titrations were performed with MeOH as co-solvent. In this case pK_a was calculated via Yasuda-Shedlovsky extrapolation.

LogD assay. The LogD of compounds was determined chromatographically at Sirius Analytical Ltd.[36]

Analytical methods. All final compounds were characterized by ^{1}H NMR and LC/MS. ^{1}H Nuclear Magnetic Resonance spectra were recorded on Bruker spectrometers: 360 MHz, DPX-400 MHz and AV-500 MHz. Purity of all final compounds was ≥95% by NMR. For the ^{1}H spectra, all chemical shifts are reported in part per million (δ) units, and are relative to the residual signal at 7.26 and 2.50 ppm for $CDCl_3$ and DMSO, respectively. All the LC/MS analyses were performed using an Agilent G1956A LC/MS quadrupole coupled to an Agilent 1100 series liquid chromatography (LC) system consisting of a binary pump with degasser, autosampler, thermostated column compartment and diode array detector. The mass spectrometer (MS) was operated with an atmospheric pressure electro-spray ionization (API-ES) source in positive ion mode. The capillary voltage was set to 3000 V, the fragmentor voltage to 70 V and the quadrupole temperature was maintained at 100°C. The drying gas flow and temperature values were 12.0 L/min and 350 °C, respectively. Nitrogen was used as the nebuliser gas, at a pressure of 35 psig. Data acquisition was performed with Agilent Chemstation software. Analyses were carried out on a YMC pack ODS-AQ C18 column (50 mm long x 4.6 mm I.D.; 3

μm particle size) at 35 °C, with a flow rate of 2.6 mL/min. A gradient elution was performed from 95% (Water + 0.1% Formic acid)/5% Acetonitrile to 5% (Water + 0.1% Formic acid)/95% Acetonitrile in 4.8 min; the resulting composition was held for 1.0 min; from 5% (Water + 0.1% formic acid)/95% Acetonitrile to 95% (Water + 0.1% formic acid)/5% Acetonitrile in 0.2 min. The standard injection volume was 2 μL. Acquisition ranges were set to 190-400 nm for the UV-PDA detector and 100-1400 m/z for the MS detector. Optical rotations measurements were carried out on a 341 Perkin Elmer polarimeter in the indicated solvents.

Synthetic protocols.

***N*-{3-[(3*R*)-5-Amino-3-methyl-3,6-dihydro-2*H*-1,4-oxazin-3-yl]phenyl}-5-chloropyridine-2-carboxamide (3*R*-6a).** 5-Chloro-2-pyridinecarboxylic acid (0.27 g, 1.72 mmol) was added to a stirred solution of intermediate 5*R*-**21a** (0.235 g, 1.145 mmol) in DCM (10 mL) at rt. Then, *N*,*N*-dimethylaniline (0.218 mL, 1.72 mmol) was added and after stirring for 5 min at rt HATU (0.500 g, 1.32 mmol) was added. The mixture was stirred at rt for 5 h. The mixture was diluted with water and sat. aq. aqueous Na_2CO_3 and extracted with DCM. The organic layer was separated, dried (Na_2SO_4), filtered and the solvents evaporated *in vacuo*. The crude product was purified by flash column chromatography (silica; 7 N solution of ammonia in MeOH/DCM 0/100 to 4/96). The desired fractions were collected and concentrated *in vacuo*. The resulting product was triturated with diisopropyl ether, filtered and dried. The product was purified again by flash column chromatography (silica; 7 N solution of ammonia in MeOH/EtOAc 0/100 to 4/96). The desired fractions were collected and concentrated *in vacuo* to yield 3*R*-**6a** (0.16 g, 41% yield). ^{1}H NMR (500 MHz, $CDCl_3$) δ 9.85 (br s, 1H), 8.56 (d, *J*=2.0 Hz, 1H), 8.25 (d, *J*=8.4 Hz, 1H), 7.88 (dd, *J*=2.3, 8.4 Hz, 1H), 7.77 (br d, *J*=8.1 Hz, 1H), 7.71-7.74 (m, 1H), 7.37 (t, *J*=7.9 Hz, 1H), 7.20 (d, *J*=7.8 Hz, 1H), 4.25 (br s, 2H), 4.16 (d, *J*=15.5 Hz, 1H), 4.09 (d, *J*=15.5 Hz, 1H), 3.74

(d, *J*=11.4 Hz, 1H), 3.62 (d, *J*=11.4 Hz, 1H), 1.56 (s, 3H); LC-MS m/z 345 $[M+H]^+$; $[\alpha]^{20}_D$ = – 88.8 (*c* = 0.68 in DMF).

***N*-{3-[(3*R*)-5-Amino-3-methyl-3,6-dihydro-2*H*-1,4-oxazin-3-yl]-4-fluorophenyl}-5-chloropyridine-2-carboxamide (3*R*-6b).** 5-Chloro-2-pyridinecarboxylic acid (155 mg, 0.99 mmol) was added to a mixture of 4-(4,6-dimethoxy-1,3,5-triazin-2-yl)-4-methyl morpholinium chloride (297 mg, 1.08 mmol) in MeOH (4 mL). The mixture was stirred for 5 min at rt, after which it was cooled to 0 ºC and a solution of aniline 5*R*-**21b** in MeOH (4 mL) was added. Then the mixture was stirred at rt for 3 h. The reaction was quenched with half-saturated aq Na_2CO_3 solution and extracted with DCM. The organic layer was separated, dried (Na_2SO_4), filtered and concentrated *in vacuo*. The crude product was purified by flash column chromatography (silica; 7 N solution of ammonia in MeOH/DCM 0/100 to 3/97). The desired fractions were collected and the solvents evaporated *in vacuo* and subsequently triturated with heptane, sonicated, filtered and dried *in vacuo* at 50 ºC to yield 3*R*-**6b** as a white solid (253 mg, 78% yield). ^{1}H NMR (400 MHz, $CDCl_3$) δ 9.82 (br s, 1H), 8.54 (d, *J*=2.3 Hz, 1H), 8.23 (d, *J*=8.3 Hz, 1H), 7.93 (td, *J*=3.6, 8.3 Hz, 1H), 7.87 (dd, *J*=2.3, 8.5 Hz, 1H), 7.67 (dd, *J*=2.8, 6.9 Hz, 1H), 7.05 (dd, *J*=8.9, 11.4 Hz, 1H), 4.14 (d, *J*=15.3 Hz, 1H), 4.06 (d, *J*=15.3 Hz, 1H), 3.92 (dd, *J*=0.9, 11.4 Hz, 1H), 3.82 (d, *J*=11.4 Hz, 1H), 1.58 (s, 3H) (2H exchanged); ^{13}C NMR (101 MHz, DMSO-d_6) δ 161.45, 156.16, 156.36 (d, *J*=242.0 Hz, 1C), 148.49, 147.02, 137.80, 134.18, 134.11 (d, *J*=14.6 Hz, 1C), 133.80 (br d, *J*=2.3 Hz, 1C), 123.80, 122.63 (d, *J*=4.6 Hz, 1C), 120.67 (d, *J*=8.5 Hz, 1C), 115.70 (d, *J*=25.4 Hz, 1C), 70.74 (d, *J*=5.8 Hz, 1C), 62.32, 54.70 (d, *J*=4.2 Hz, 1C), 26.30 (d, *J*=4.2 Hz, 1C); LC-MS m/z 363 $[M+H]^+$; $[\alpha]^{20}_D$ = +31.9 (*c* = 0.69 in DMF); m. p. = 146.7 ºC.

***N*-{3-[(3*R*)-5-Amino-3-methyl-3,6-dihydro-2H-1,4-oxazin-3-yl]-4-fluorophenyl}-5-methoxypyrazine-2-carboxamide (3*R*-6c).** Starting from 5*R*-**19b** (100 mg, 0.448 mmol) and

following the same procedure as for 3*R*-**6b** the corresponding oxazinamine 3*R*-**6c** was obtained (112 mg, 70% yield). ^{1}H NMR (500 MHz, $CDCl_3$) δ 9.49 (br s, 1H), 9.00 (d, *J*=1.2 Hz, 1H), 8.13 (d, *J*=1.2 Hz, 1H), 7.91 (ddd, *J*=2.9, 4.0, 8.7 Hz, 1H), 7.64 (dd, *J*=2.6, 6.9 Hz, 1H), 7.05 (dd, *J*=8.7, 11.6 Hz, 1H), 4.21 (br s, 2H), 4.13 (d, *J*=15.5 Hz, 1H), 4.06 (s, 3H), 4.05 (d, *J*=15.5 Hz, 1H), 3.92 (dd, *J*=1.2, 11.5 Hz, 1H), 3.81 (d, *J*=11.5 Hz, 1H), 1.58 (s, 3H); ^{13}C NMR (101 MHz, DMSO-d_6) δ 161.61, 161.28, 156.18, 156.30 (d, *J*=242.0 Hz, 1C), 142.10, 141.39, 137.95, 133.93 (d, *J*=2.7 Hz, 1C), 133.55, 122.69, 120.72 (d, *J*=8.1 Hz, 1C), 115.66 (d, *J*=25.0 Hz, 1C), 70.76 (d, *J*=6.9 Hz, 1C), 62.32, 54.70 (d, *J*=3.9 Hz, 1C), 54.26, 26.29 (d, *J*=4.2 Hz, 1C); LC-MS m/z 360 $[M+H]^+$; $[\alpha]^{20}_D$ = +32.2 (*c* = 0.61 in DMF); m. p. = 178.8 ºC.

***N*-{3-[(2*R*,3*R*)-5-Amino-2-fluoro-3-methyl-3,6-dihydro-2*H*-1,4-oxazin-3-yl]-4-fluorophenyl}-5-methoxypyrazine-2-carboxamide ((2*R*,3*R*)-7a)**. Starting from (5*R*,6*R*)-**34** (2.42 g, 6.1 mmol) and following the same procedure as for 3*R*-**6b** the corresponding (2*R*,3*R*)-**7a** was obtained as a white solid (1.5 g, 65% yield). ^{1}H NMR (360 MHz, $CDCl_3$) δ 9.46 (s, 1H), 8.98 (d, *J*=1.5 Hz, 1H), 8.11 (d, *J*=1.5 Hz, 1H), 7.83 (ddd, *J*=2.7, 4.1, 8.9 Hz, 1H), 7.52 (dd, *J*=2.7, 6.8 Hz, 1H), 7.07 (dd, *J*=8.8, 11.3 Hz, 1H), 6.04 (d, *J*=52.3 Hz, 1H), 4.59 (br s, 2H), 4.26 (d, *J*=15.7 Hz, 1H), 4.06 (s, 3H), 4.03 (d, *J*=15.7 Hz, 1H), 1.65 (t, *J*=2.0 Hz, 3H); ^{13}C NMR (101 MHz, DMSO-d_6) δ 161.60, 161.38, 156.16, 155.67 (d, *J*=241.4 Hz, 1C), 141.46, 137.91, 134.37 (d, *J*=2.2 Hz, 1C), 133.50, 131.61 (dd, *J*=5.5, 13.6 Hz, 1C), 121.89 (br d, *J*=2.9 Hz, 1C), 121.55 (d, *J*=8.8 Hz, 1C), 115.97 (d, *J*=25.7 Hz, 1C), 105.00 (dd, *J*=7.3, 225.9 Hz, 1C), 57.83 (dd, *J*=4.8, 26.8 Hz, 1C), 56.37 (d, *J*=2.9 Hz, 1C), 54.24, 25.11 (br d, *J*=2.9 Hz, 1C); LC-MS m/z 378 $[M+H]^+$; $[a]^{20}_D$ = +117.3 (*c* = 0.69 in DMF); m. p. = 212.4 ºC.

***N*-[3-[(2*S*,3*R*)-5-Amino-2-fluoro-3-methyl-morpholin-3-yl]-4-fluoro-phenyl]-5-methoxy-pyrazine-2-carboxamide ((2*S*,3*R*)-7a).** Starting from (5*R*,6*S*)-**34** (0.040 g, 0.166 mmol) and

following the same procedure as for 3*R*-**6b** the corresponding (2*S*,3*R*)-**7a** was obtained (0.019 g, 30%). ^{1}H NMR (400 MHz, $CDCl_3$) δ 9.52 (br s, 1H), 9.01 (d, *J*=1.3 Hz, 1H), 8.13 (d, *J*=1.3 Hz, 1H), 8.03 (ddd, *J*=2.9, 4.2, 8.8 Hz, 1H), 7.86 (dd, *J*=2.7, 6.7 Hz, 1H), 7.07 (dd, *J*=8.8, 11.4 Hz, 1H), 6.09 (dd, *J*=1.5, 51.5 Hz, 1H), 4.29 (d, *J*=15.6 Hz, 1H), 4.16 (d, *J*=15.6 Hz, 1H), 4.06 (s, 3H), 1.55 (s, 3H) (2H exchanged); ^{13}C NMR (101 MHz, $CDCl_3$) δ 162.25, 160.97, 156.59 (d, *J*=242.8 Hz, 1C), 153.97, 141.89, 137.35, 133.78 (d, *J*=2.2 Hz, 1C), 133.35, 131.25 (d, *J*=13.9 Hz, 1C), 120.65 (d, *J*=5.1 Hz, 1C), 120.06 (d, *J*=8.8 Hz, 1C), 116.28 (d, *J*=25.7 Hz, 1C), 105.12 (dd, *J*=9.2, 226.3 Hz, 1C), 57.89 (dd, *J*=4.4, 25.7 Hz, 1C), 56.18 (d, *J*=5.1 Hz, 1C), 54.38, 26.35 (t, *J*=4.0 Hz, 1C); LC-MS m/z 378 $[M+H]^+$; m. p. = 211.8 ºC.

***N*-{3-[(2*R*,3*R*)-5-Amino-2-fluoro-3-methyl-3,6-dihydro-2H-1,4-oxazin-3-yl]-4-fluorophenyl}-5-chloropyridine-2-carboxamide ((2*R*,3*R*)-7b).** Starting from (5*R*,6*R*)-**34** (500 mg, 2.07 mmol) and following the same procedure as for 3*R*-**6b** the corresponding amide (2*R*,3*R*)-**7b** was obtained as a white solid (600 mg, 76%). ^{1}H NMR (360 MHz, DMSO-d_6) δ 10.74 (s, 1H), 8.78 (d, *J*=2.2 Hz, 1H), 8.19 (dd, *J*=2.2, 8.8 Hz, 1H), 8.14 (d, *J*=8.8 Hz, 1H), 7.76-7.84 (m, 1H), 7.74 (dd, *J*=2.6, 7.3 Hz, 1H), 7.18 (dd, *J*=8.8, 11.7 Hz, 1H), 6.07 (br s, 2H), 5.87 (d, *J*=53.8 Hz, 1H), 4.04 (d, *J*=16.1 Hz, 1H), 3.94 (d, *J*=16.1 Hz, 1H), 1.49 (s, 3H); ^{13}C NMR (91 MHz, DMSO-d_6) δ 161.61, 156.21, 155.75 (d, *J*=241.5 Hz, 1C), 148.51, 147.04, 137.83, 134.30 (d, *J*=2.1 Hz, 1C), 134.23, 131.67 (dd, *J*=5.5, 13.8 Hz, 1C), 123.93, 121.98, 121.60 (d, *J*=8.3 Hz, 1C), 116.05 (d, *J*=25.6 Hz, 1C), 105.01 (dd, *J*=6.9, 226.3 Hz, 1C), 57.85 (dd, *J*=4.5, 26.6 Hz, 1C), 56.39 (d, *J*=3.5 Hz, 1C), 25.15 (br d, *J*=5.5 Hz, 1C); LC-MS m/z 381 $[M+H]^+$; m. p. = 220.4 ºC.

***N*-{3-[(2*R*,3*R*)-5-Amino-2-fluoro-3-methyl-3,6-dihydro-2*H*-1,4-oxazin-3-yl]-4-fluorophenyl}-5-chloro-3-methylpyridine-2-carboxamide hydrochloride ((2*R*,3*R*)-7c).**

Starting from (5*R*,6*R*)-**34** (150 mg, 0.38 mmol) and following the same procedure as for 3*R*-**6b** the corresponding amide (2*R*,3*R*)-**7c** was obtained. The purified compound (2*R*,3*R*)-**7c** was dissolved in isopropanol/DIPE and a few drops of a 6 N HCl solution in isopropanol were added. The resulting precipitate was collected after evaporation of the solvents yielding (2*R*,3*R*)-**7c** as a white solid (77 mg, 47%, HCl salt). ^{1}H NMR (360 MHz, DMSO-d_6) δ 11.18 (s, 1H), 10.80 (s, 1H), 9.68 (s, 1H), 8.98 (s, 1H), 8.60 (d, *J*=2.6 Hz, 1H), 8.05-8.07 (m, 1H), 8.01 (ddd, *J*=2.6, 4.2, 9.0 Hz, 1H), 7.75 (dd, *J*=2.6, 7.3 Hz, 1H), 7.33 (dd, *J*=9.0, 11.9 Hz, 1H), 6.15 (d, *J*=50.5 Hz, 1H), 4.76 (d, *J*=17.9 Hz, 1H), 4.67 (d, *J*=17.9 Hz, 1H), 2.58 (s, 3H), 1.73 (s, 3H); ^{13}C NMR (101 MHz, DMSO-d_6) δ 163.98, 162.16, 154.88 (d, *J*=243.1 Hz, 1C), 147.75, 144.36, 139.66, 135.82, 135.45 (d, *J*=2.3 Hz, 1C), 132.70, 126.52 (dd, *J*=4.2, 12.3 Hz, 1C), 122.23 (d, *J*=8.5 Hz, 1C), 119.63, 117.12 (d, *J*=24.7 Hz, 1C), 104.28 (dd, *J*=5.8, 232.7 Hz, 1C), 58.19 (dd, *J*=4.2, 25.4 Hz, 1C), 56.99 (d, *J*=4.2 Hz, 1C), 21.71 (dd, *J*=2.5, 4.8 Hz, 1C), 18.88; LC-MS m/z 395 $[M+H]^+$; m. p. = 129.4 ºC.

***N*-{3-[(2*R*,3*R*)-5-Amino-2-fluoro-3-methyl-3,6-dihydro-2*H*-1,4-oxazin-3-yl]-4-fluorophenyl}-5-cyanopyridine-2-carboxamide ((2*R*,3*R*)-7d).** Starting from (5*R*,6*R*)-34 (834 mg, 3.46 mmol) and following the same procedure as for 3*R*-**6b** the corresponding amide (2*R*,3*R*)-**7d** was obtained as a white solid (615 mg, 48%). ^{1}H NMR (500 MHz, DMSO-d_6) δ 10.86 (s, 1H), 9.19 (d, *J*=2.0 Hz, 1H), 8.57 (dd, *J*=2.0, 8.1 Hz, 1H), 8.27 (d, *J*=8.1 Hz, 1H), 7.78-7.83 (m, 1H), 7.76 (dd, *J*=2.6, 7.2 Hz, 1H), 7.18 (dd, *J*=8.7, 11.8 Hz, 1H), 6.05 (br s, 2H), 5.87 (d, *J*=53.7 Hz, 1H), 4.04 (d, *J*=15.9 Hz, 1H), 3.94 (d, *J*=15.9 Hz, 1H), 1.49 (s, 3H); ^{13}C NMR (101 MHz, DMSO-d_6) δ 161.17, 156.21, 155.87 (d, *J*=242.1 Hz, 1C), 152.54, 151.42, 142.10, 134.08 (d, *J*=2.2 Hz, 1C), 131.70 (dd, *J*=5.9, 13.2 Hz, 1C), 122.34, 122.08 (br d, *J*=2.2 Hz, 1C), 121.74 (d, *J*=8.8 Hz, 1C), 116.55, 116.06 (d, *J*=25.7 Hz, 1C), 111.48, 104.98 (dd, *J*=7.3, 225.9

Hz, 1C), 57.84 (dd, *J*=4.8, 26.8 Hz, 1C), 56.38 (d, *J*=3.7 Hz, 1C), 25.09 (br d, *J*=3.7 Hz, 1C); LC-MS m/z 372 $[M+H]^+$; $[a]^{20}_D$ = +125.0 (*c* = 0.51 in DMF); m. p. = 223.4 ºC.

***N*-{3-[(2*S*,3*R*)-5-Amino-2-fluoro-3-methyl-2-(trifluoromethyl)-3,6-dihydro-2*H*-1,4-oxazin-3-yl]-4-fluorophenyl}-5-methoxypyrazine-2-carboxamide ((2*S*,3*R*)-8)**. Starting from (5*R*,6*S*)-**35** (0.20 g, 0.65 mmol) and following the same procedure as for 3*R*-**6b** the corresponding (2*S*,3*R*)-**8** was obtained (0.13 g, 45% yield). ^{1}H NMR (360 MHz, $CDCl_3$) δ 9.49 (br s, 1H), 9.02 (d, *J*=1.3 Hz, 1H), 8.16 (d, *J*=1.3 Hz, 1H), 7.84 (dd, *J*=2.9, 7.3 Hz, 1H), 7.64 (td, *J*=3.3, 8.8 Hz, 1H), 7.02 (dd, *J*=8.8, 12.4 Hz, 1H), 4.44-4.56 (m, 2H), 4.34 (br s, 2H), 4.07 (s, 3H), 1.87 (br s, 3H); ^{13}C NMR (101 MHz, DMSO-d_6) δ 161.62, 161.56, 157.33 (d, *J*=245.8 Hz, 1C), 154.03, 141.57, 137.96, 134.14 (d, *J*=2.2 Hz, 1C), 133.46, 127.24 (dd, *J*=4.8, 10.6 Hz, 1C), 122.75 (d, *J*=1.5 Hz, 1C), 121.92 (d, *J*=9.5 Hz, 1C), 120.65 (dq, *J*=35.2, 286.8 Hz, 1C), 116.16 (d, *J*=26.4 Hz, 1C), 106.52 (qd, *J*=32.3, 240.6 Hz, 1C), 59.02, 58.41 (br d, *J*=30.1 Hz, 1C), 54.26, 25.17; LC-MS m/z 444 $[M-H]^-$; $[a]^{20}_D$ = +75.6 (*c* = 0.17 in MeOH); m. p. = 80.0 ºC.

***N*-[3-[(2*R*,3*R*)-5-Amino-2-fluoro-3-methyl-2-(trifluoromethyl)-3,6-dihydro-2*H*-1,4-oxazin-3-yl]-4-fluorophenyl}-5-methoxypyrazine-2-carboxamide ((2*R*,3*R*)-8)**. Starting from (5*R*,6*R*)-**35** (0.2 g, 0.65 mmol) and following the same procedure as for 3*R*-**6b** the corresponding (2*R*,3*R*)-**8** was obtained (200 mg, 69% yield). ^{1}H NMR (360 MHz, $CDCl_3$) δ 9.49 (br s, 1H), 9.02 (d, *J*=1.5 Hz, 1H), 8.15 (d, *J*=1.5 Hz, 1H), 7.83-7.89 (m, 1H), 7.67 (td, *J*=2.4, 6.9 Hz, 1H), 7.04 (dd, *J*=8.8, 12.1 Hz, 1H), 4.53 (d, *J*=15.7 Hz, 1H), 4.46 (d, *J*=15.7 Hz, 1H), 4.38 (br s, 2H), 4.07 (s, 3H), 1.83 (s, 3H); ^{13}C NMR (101 MHz, DMSO-d_6) δ 161.60, 161.38, 157.26 (d, *J*=245.8 Hz, 1C), 153.70, 141.43, 137.97, 133.56 (d, *J*=2.2 Hz, 1C), 133.47, 128.28 (d, *J*=11.0 Hz, 1C), 125.27, 121.76 (d, *J*=8.8 Hz, 1C), 121.00 (dq, *J*=35.2, 289.8 Hz, 1C), 115.55 (d, *J*=27.1 Hz, 1C), 106.34 (qd, *J*=33.8, 204.7 Hz, 1C), 59.07 (d, *J*=2.9 Hz, 1C), 58.42 (dd, *J*=2.9, 25.7 Hz, 1C),

54.24, 24.13 (br d, *J*=6.6 Hz, 1C); LC-MS m/z 444 $[M-H]^-$; $[a]^{20}_D$ = -128.6 (*c* = 0.22 in MeOH); m. p. = 198.4 ºC.

***N*-{3-[(2*R*,3*R*)-5-Amino-3-methyl-2-(trifluoromethyl)-3,6-dihydro-2*H*-1,4-oxazin-3-yl]-4-fluorophenyl}-5-methoxypyrazine-2-carboxamide ((2*R*,3*R*)-9).** Starting from (5*R*,6*R*)-**36** (0.20 g, 0.69 mmol) and following the same procedure as for 3*R*-**6b** the corresponding (2*R*,3*R*)-**9** was obtained (0.19 g, 65% yield). ^{1}H NMR (360 MHz, $CDCl_3$) δ 9.55 (br s, 1H), 9.02 (d, *J*=1.5 Hz, 1H), 8.15 (d, *J*=1.5 Hz, 1H), 8.02 (ddd, *J*=2.9, 4.4, 8.8 Hz, 1H), 7.89 (dd, *J*=2.7, 6.8 Hz, 1H), 7.05 (dd, *J*=8.8, 11.7 Hz, 1H), 4.65 (q, *J*=8.2 Hz, 1H), 4.32 (br s, 2H), 4.23 (s, 2H), 4.07 (s, 3H), 1.68 (s, 3H); ^{13}C NMR (91 MHz, DMSO-d6) δ 161.66, 161.35, 156.95 (d, *J*=243.0 Hz, 1C), 155.06, 141.43, 137.97, 133.97 (d, *J*=2.1 Hz, 1C), 133.59, 130.44 (d, *J*=13.1 Hz, 1C), 122.70 (d, *J*=3.5 Hz, 1C), 121.22 (d, *J*=9.0 Hz, 1C), 124.33 (q, *J*=286.5 Hz, 1C), 115.39 (d, *J*=24.9 Hz, 1C), 73.25 (q, *J*=26.3 Hz, 1C), 59.45, 54.78 (d, *J*=3.5 Hz, 1C), 54.30, 28.57 (d, *J*=2.8 Hz, 1C); LC-MS m/z 428 $[M+H]^+$; $[a]^{20}_D$ = -42.4 (*c* = 0.18 in MeOH); m. p. = 252.5 ºC.

***N*-{3-[(2*S*,3*R*)-5-Amino-3-methyl-2-(trifluoromethyl)-3,6-dihydro-2*H*-1,4-oxazin-3-yl]-4-fluorophenyl}-5-methoxypyrazine-2-carboxamide ((2*S*,3*R*)-9).** Starting from (5*R*,6*S*)-**36** (0.10 g, 0.34 mmol) and following the same procedure as for 3*R*-**6b** the corresponding (2*S*,3*R*)-**9** was obtained (0.034 g, 23% yield). ^{1}H NMR (400 MHz, DMSO-d_6) δ 10.44 (br s, 1H), 8.88 (d, *J*=1.3 Hz, 1H), 8.38 (d, *J*=1.3 Hz, 1H), 7.94 (dd, *J*=2.6, 7.5 Hz, 1H), 7.84-7.91 (m, 1H), 7.11 (dd, *J*=8.8, 12.1 Hz, 1H), 5.76 (br s, 2H), 4.41 (q, *J*=7.6 Hz, 1H), 4.26 (d, *J*=15.5 Hz, 1H), 4.20 (d, *J*=15.5 Hz, 1H), 4.01 (s, 3H), 1.56 (s, 3H); ^{13}C NMR (101 MHz, DMSO-d_6) δ 161.63, 161.44, 156.66 (d, *J*=243.6 Hz, 1C), 154.73, 141.50, 137.91, 134.26 (d, *J*=2.2 Hz, 1C), 133.47, 132.04 (d, *J*=10.3 Hz, 1C), 121.29 (d, *J*=3.7 Hz, 1C), 120.82 (d, *J*=8.8 Hz, 1C), 124.16 (q, *J*=283.9 Hz,

1C), 115.99 (d, *J*=24.9 Hz, 1C), 74.63 (dq, *J*=5.1, 27.9 Hz, 1C), 62.50, 55.57 (d, *J*=3.7 Hz, 1C), 54.26, 22.23; LC-MS m/z 428 $[M+H]^+$; m. p. = 214.7 ºC.

***N*-[3-[(2*R*,3*R*)-5-Amino-3-cyclopropyl-2-fluoro-2,6-dihydro-1,4-oxazin-3-yl]-4-fluorophenyl]-5-methoxy-pyrazine-2-carboxamide ((2*R*,3*R*)-10).** Starting from (5*R*,6*R*)-**45** (0.20 g, 0.75 mmol) and following the same procedure as for 3*R*-**6b** the corresponding (2*R*,3*R*)-**10** was obtained (0.15 g, 50% yield). ^{1}H NMR (360 MHz, $CDCl_3$) δ 9.46 (s, 1H), 8.99 (d, *J*=1.5 Hz, 1H), 8.13 (d, *J*=1.46 Hz, 1H), 7.82 (ddd, *J*=2.93, 4.03, 8.78 Hz, 1H), 7.39 (dd, *J*=2.74, 6.77 Hz, 1H), 7.08 (dd, *J*=8.78, 11.71 Hz, 1H), 6.22 (d, *J*=52.33 Hz, 1H), 4.44 (br s, 2H), 4.22 (d, *J*=15.37 Hz, 1H), 4.06 (s, 3H), 3.99 (d, *J*=15.37 Hz, 1H), 1.65 (dt, *J*=3.29, 8.42 Hz, 1H), 0.50-0.60 (m, 1H), 0.47 (d, *J*=15.00 Hz, 1H), 0.38 (qd, *J*=4.88, 9.51 Hz, 1H), 0.17-0.26 (m, 1H); ^{13}C NMR (101 MHz, DMSO-d_6) δ 161.57 (br d, *J*=5.1 Hz, 1C), 161.35, 157.37, 155.70 (d, *J*=240.6 Hz, 1C), 141.45, 137.93, 134.24 (d, *J*=2.2 Hz, 1C), 133.50, 131.79 (br d, *J*=12.5 Hz, 1C), 121.92 (d, *J*=3.7 Hz, 1C), 121.36 (d, *J*=8.8 Hz, 1C), 115.90 (d, *J*=25.7 Hz, 1C), 105.37 (dd, *J*=8.4, 226.3 Hz, 1C), 58.75 (dd, *J*=5.1, 27.9 Hz, 1C), 56.95 (d, *J*=2.9 Hz, 1C), 54.24, 16.02 (d, *J*=6.6 Hz, 1C), 2.20, -1.60; LC-MS m/z 404 $[M+H]^+$.

***rac*-*N*-{2-[(2*R**,3*R**)-5-Amino-2-fluoro-3-methyl-3,6-dihydro-2*H*-1,4-oxazin-3-yl]pyridin-4-yl}-5-methoxypyrazine-2-carboxamide (*rac*-(2*R**,3*R**)-11).** Di-*tert*-butyldicarbonate (0.85 g, 3.88 mmol) was added to 0.54 g (2.43 mmol) aniline *rac*-(5*R**,6*R**)-**56a** in 100 mL DCM/ACN (1:1), and the resulting mixture was stirred 22 h at rt. Then, all volatiles were evaporated at rt and the crude was purified by flash column chromatography (silica; 7 N solution of NH_3 in MeOH/DCM 0/100 to 10/90). The product fractions were evaporated providing the Boc-amidine *rac*-(5*R**,6*R**)-**57a** as a yellow oil (0.29 mg, 37 % yield), and another fraction of starting material *rac*-(5*R**,6*R**)-**56a** was recovered (0.27 g, 49%).

HATU (0.18 g, 0.46 mg) was added to a solution of *rac*-(5*R**,6*R**)-**57a** (0.050 g, 0.154 mmol), 5-methoxypyrazine-2-carboxylic acid (0.071 g, 0.462 mmol) and DIPEA (0.16 mL, 0.925 mmol) in 2 mL dry DMF, and the resulting mixture was stirred 3 h at 50 °C. After cooling to rt, DCM and 2 N Na_2CO_3 were added to the mixture and it was stirred for 30 min at rt. The organic layer was separated and the aq layer was extracted with DCM. The combined organic layers were dried (Na_2SO_4), filtered and concentrated. The residue was purified by flash column chromatography (silica; 7 N solution of ammonia in MeOH/DCM 0/100 to 10/90). The desired fractions were collected and concentrated *in vacuo* yielding amide *rac*-(5*R**,6*R**)-**58** as a transparent oil (33.1 mg, 47%).

Rac-(5*R**,6*R**)-**58a** (33.1 mg, 0.0719 mmol) was dissolved in TFA (3 mL) and stirred for 15 min. Then, the mixture was evaporated to dryness and sat. aq. $NaHCO_3$ and DCM were added. The biphasic mixture was stirred until gas evolution ceased, and then the organic layer was separated. The aq layer was extracted twice with DCM. The combined organic layers were dried (Na_2SO_4), filtered and the solvent was evaporated. The residue was purified by flash column chromatography (silica; 7 N solution of ammonia in MeOH/DCM 0/100 to 10/90). The desired fractions were collected and concentrated *in vacuo* yielding *rac*-(2*R**,3*R**)-**11** as beige crystals, which were washed with diethyl ether and dried *in vacuo* at 50 °C (14.8 mg, 51%).^{1}H NMR (360 MHz, DMSO-d_6) δ 10.89 (br s, 1H), 8.92 (d, *J*=1.3 Hz, 1H), 8.44 (d, *J*=5.7 Hz, 1H), 8.43 (d, *J*=1.3 Hz, 1H), 7.96 (d, *J*=1.9 Hz, 1H), 7.75 (dd, *J*=1.9, 5.7 Hz, 1H), 6.02 (br s, 2H), 5.92 (d, *J*=54.5 Hz, 1H), 4.06 (d, *J*=16.1 Hz, 1H), 4.03 (s, 3H), 3.95 (d, *J*=16.1 Hz, 1H), 1.42 (d, *J*=0.7 Hz, 3H); ^{13}C NMR (101 MHz, DMSO-d_6) δ 164.99, 162.49, 161.81, 156.02, 149.08, 145.79, 142.01, 137.49, 133.63, 112.39, 111.55 (d, *J*=1.9 Hz, 1C), 107.06 (d, *J*=225.4 Hz, 1C), 60.40 (d,

J=25.4 Hz, 1C), 56.41 (d, *J*=3.9 Hz, 1C), 54.36, 26.02; LC-MS m/z 361 $[M+H]^+$. m. p.: decomposition around 230 ºC.

***rac*-*N*-{4-[(2*R**,3*R**)-5-Amino-2-fluoro-3-methyl-3,6-dihydro-2*H*-1,4-oxazin-3-yl]pyridin-2-yl}-5-methoxypyrazine-2-carboxamide (*rac*-(2*R**,3*R**)-12).** Di-*tert*-butyldicarbonate (0.234 g, 1.07 mmol) was added portionwise to a stirred solution of intermediate *rac*-(5*R**,6*R**)-**56b** (0.200 g, 0.892 mmol), triethylamine (1.00 mL, 19.1 mmol) and 4-dimethylaminopyridine (0.006 g, 0.05 mmol) in THF (1 mL) at rt for 3 h. The mixture was quenched with sat. aq. $NaHCO_3$ solution. The aqueous layer was extracted with EtOAc. The organic layer was dried ($MgSO_4$), filtered and the solvents evaporated *in vacuo* to yield the corresponding Boc-amidine *rac*-(5*R**,6*R**)-**57b** (0.185 g, 64% yield) which was used as such in the then reaction step.

HATU (70.3 mg, 0.185 mmol) was added to a solution of *rac*-(5*R**,6*R**)-**57b** (50.0 mg, 0.154 mmol), 5-methoxypyrazine-2-carboxylic acid (28.5 mg, 0.185 mmol) and DIPEA (79.7 mL, 0.462 mmol) in dry DMF (2 mL), and the resulting mixture was stirred overnight at rt. The solvent was evaporated and the residue was taken up in DCM and 2 N Na_2CO_3. The organic layer was separated and the aqueous layer was extracted with DCM. The combined organic layers were dried (Na_2SO_4), filtered and concentrated. The residue was purified by flash column chromatography (silica; 7 N solution of ammonia in MeOH/DCM 0/100 to 10/90). The desired fractions were collected and concentrated *in vacuo* yielding providing *rac*-(5*R**,6*R**)-**58b** as a transparent glass (50.5 mg, 71%).

Rac-(5*R**,6*R**)-**58b** (50 mg) was dissolved in TFA (5 mL) and the resulting mixture was stirred for 15 min before it was evaporated to dryness. Sat. aq. $NaHCO_3$ and DCM were added, the biphasic mixture was stirred gas evolution ceased, and then the organic layer was separated. The aqueous layer was extracted twice with DCM. The combined organic layers were separated,

dried ($MgSO_4$) and the solvent was evaporated providing *rac*-(2*R**,3*R**)-**12** as off-white crystals, which were triturated with diethyl ether, filtered and dried *in vacuo* at 50 °C (34.2 mg, 87%). ^{1}H NMR (360 MHz, DMSO-d_6) δ 10.06 (s, 1H), 8.95 (d, *J*=1.2 Hz, 1H), 8.45 (d, *J*=1.2 Hz, 1H), 8.32 (d, *J*=5.3 Hz, 1H), 8.28 (d, *J*=1.6 Hz, 1H), 7.24 (dd, *J*=1.6, 5.3 Hz, 1H), 6.13 (br s, 2H), 5.82 (br d, *J*=52.7 Hz, 1H), 4.10 (d, *J*=15.4 Hz, 1H), 4.03 (s, 3H), 4.00 (d, *J*=15.4 Hz, 1H), 1.45 (d, *J*=0.7 Hz, 3H); ^{13}C NMR (101 MHz, DMSO-d_6) δ 162.05, 161.06, 156.45 (br s, 2C), 150.88, 148.06, 141.55, 136.66, 134.04, 118.02, 111.18, 106.36 (d, *J*=227.3 Hz, 1C), 58.49 (d, *J*=25.8 Hz, 1C), 56.69 (d, *J*=3.9 Hz, 1C), 54.44, 25.69; LC-MS m/z 361 $[M+H]^+$.

***rac*-2-Amino-2-(3-bromophenyl)-propionitrile (*rac*-14a).** Trimethylsilylcyanide (20 g, 200 mmol) was added to a stirred solution of 3-bromoacetophenone **13a** (20 g, 100 mmol) and NH_4Cl (11 g, 200 mmol) in 7 N NH_3/MeOH (400 mL). The mixture was stirred at rt for 4 days. Then the solvent was evaporated *in vacuo* and the residue was taken up in EtOAc (100 mL). The solid was filtered and the filtrate was evaporated *in vacuo* to yield intermediate *rac*-**14a** (20 g, 86% yield) which was used in the then step without further purification. ^{1}H NMR (360 MHz, DMSO-d_6) δ 7.78 (t, *J*=1.8 Hz, 1H), 7.60 (ddd, *J*=0.9, 1.7, 7.9 Hz, 1H), 7.56 (ddd, *J*=1.1, 1.9, 7.9 Hz, 1H), 7.39 (t, *J*=8.0 Hz, 1H), 3.15 (br s, 2H), 1.64 (s, 3H); LC-MS m/z 225 $[M+H]^+$.

***rac*-2-Amino-2-(5-bromo-2-fluorophenyl)propanenitrile (*rac*-14b).** Starting from 1-(5-bromo-2-fluorophenyl)ethanone (46.3 g, 213 mmol) and following the same procedure as for *rac*-**14a** the corresponding aminonitrile *rac*-**14b** was obtained (30 g, 60% yield). ^{1}H NMR (360 MHz, $CDCl_3$) δ 7.80 (dd, *J*=2.2, 6.9 Hz, 1H), 7.48 (ddd, *J*=2.5, 4.2, 8.6 Hz, 1H), 7.03 (dd, *J*=8.6, 10.8 Hz, 1H), 2.18 (br s, 2H), 1.86 (s, 3H); LC-MS m/z 243 $[M+H]^+$.

***rac*-2-Amino-2-(3-bromophenyl)-propionic acid (*rac*-15a).** Intermediate *rac*-**14a** (47 g, 209 mmol) was dissolved in acetic acid (250 mL) and HCl (37% in water, 240 mL) was added. Then the mixture was refluxed for 16 h, after which the reaction mixture was concentrated in vacuo.

Water was added and the aqueous layer was washed with EtOAc. Then the aqueous layer was adjusted to pH 7 by slow addition of 25% aq. NaOH solution. The resulting solid was filtered, washed with water and diethyl ether, and dried under vacuum at 50 °C to yield intermediate *rac*-**15a** (36 g, 71% yield); LC-MS m/z 242 $[M-H]^-$. NMR shifts were in accordance to those reported previously.[37]

***rac*-2-Amino-2-(5-bromo-2-fluorophenyl)propanoic acid (*rac*-15b).** Starting from *rac*-**14b** (19.9 g, 81.9 mmol) and following the same procedure as for *rac*-**15a** the corresponding aminonitrile *rac*-**15b** was obtained (14.6 g, 68% yield). ^{1}H NMR (360 MHz, DMSO-d_6) δ 7.78 (br s, 1H), 7.64 (dd, *J*=2.6, 6.9 Hz, 1H), 7.55 (ddd, *J*=2.6, 4.2, 8.6 Hz, 1H), 7.18 (dd, *J*=8.6, 11.2 Hz, 1H), 1.64 (s, 3H) (2H exchanged); LC-MS m/z 260 $[M+H]^+$.

***rac*-Methyl 2-amino-2-(3-bromophenyl)propanoate (*rac*-16a).** Intermediate *rac*-**15a** (36 g, 147 mmol) was dissolved in MeOH (1 L). Then sulphuric acid (103 mL, 1.93 mol) was added and the reaction mixture was stirred at reflux temperature overnight. After cooling to rt, the solvent was evaporated *in vacuo*. The residue was dissolved in water, basified with aq. $NaHCO_3$ to pH 8 and extracted with EtOAc. The combined organic layers were dried ($MgSO_4$), filtered and evaporated to provide *rac*-**16a** (36 g, 89% yield). ^{1}H NMR (500 MHz, $CDCl_3$) δ 7.68 (t, *J*=1.7 Hz, 1H), 7.37-7.44 (m, 2H), 7.21 (t, *J*=7.8 Hz, 1H), 3.72 (s, 3H), 1.95 (br s, 2H), 1.68 (s, 3H); LC-MS m/z 258 $[M+H]^+$.

***rac*-Methyl 2-amino-2-(5-bromo-2-fluorophenyl)propanoate (*rac*-16b).** Starting from *rac*-**15b** (14.6 g, 55.5 mmol) and following the same procedure as for *rac*-**16a** the corresponding

amino ester *rac*-**16b** was obtained (13.9 g, 87%). ^{1}H NMR (400 MHz, DMSO-d_6) δ ppm 1.27 - 1.51 (m, 3 H), 2.51 (br s, 2 H), 3.55 - 3.71 (m, 3 H), 7.12 (dd, *J*=10.9, 8.7 Hz, 1 H), 7.49 (ddd, *J*=8.7, 4.4, 2.5 Hz, 1 H), 7.87 (dd, *J*=7.0, 2.5 Hz, 1 H); LC-MS m/z 276 $[M+H]^+$.

(2*R*)-2-Amino-2-(3-bromophenyl)-propan-1-ol (2*R*-17a). Ester *rac*-**16a** (7.5 g, 29.1 mmol) was dissolved THF (200 mL) and cooled to -15 ºC. Then, LAH (1 M in THF; 22 mL, 22 mmol) was added dropwise while stirring. The mixture was left warming up slowly to 0 ºC during 1 h. Then more THF (150 mL) was added and sat. aq. Na_2SO_4 was added dropwise until hydrogen evolution ceased. Then anhydrous Na_2SO_4 was added and the stirring was continued overnight at rt. The mixture was filtered over celite, rinsed with THF and the solvent evaporated *in vacuo*. The crude product was purified by flash column chromatography (silica; 7 N solution of ammonia in MeOH/DCM 0/100 to 3/97). The desired fractions were collected and concentrated *in vacuo* to yield *rac*-**17a** (5.70 g, 85% yield) as an oil. ^{1}H NMR (500 MHz, $CDCl_3$) δ 7.64 (t, *J*=1.9 Hz, 1H), 7.38-7.44 (m, 2H), 7.25 (t, *J*=7.8 Hz, 1H), 3.64 (d, *J*=10.7 Hz, 1H), 3.59 (d, *J*=10.7 Hz, 1H), 1.81 (br s, 3H), 1.46 (s, 3H); LC-MS m/z 230 $[M+H]^+$.

Intermediate *rac*-**17a** (18.0 g) was separated into the corresponding enantiomers by preparative SFC on a Chiralpak® Diacel AD x 250 mm column using CO_2 and MeOH with 0.2% $iPrNH_2$ as mobile phase to yield amino alcohol 2*R*-**17a** (7.21 g, 40% yield). ^{1}H NMR (400 MHz, $CDCl_3$) δ 7.63 (t, *J*=1.8 Hz, 1H), 7.38-7.43 (m, 2H), 7.25 (t, *J*=7.9 Hz, 1H), 3.64 (d, *J*=10.7 Hz, 1H), 3.58 (d, *J*=10.7 Hz, 1H), 1.78 (br s, 3H), 1.45 (s, 3H); LC-MS m/z 230 $[M+H]^+$; $[\alpha]^{20}_D$ = -14.9 (*c* = 0.29 in MeOH).

(2*R*)-2-Amino-2-(5-bromo-2-fluorophenyl)propan-1-ol (2*R*-17b). Starting from *rac*-**16b** (14.2 g, 48.4 mmol) and following the same procedure as for *rac*-**17a** the corresponding aminonitrile *rac*-**17b** was obtained (12.0 g, 96% yield). ^{1}H NMR (400 MHz, $CDCl_3$) δ 7.63 (dd,

J=2.5, 7.4 Hz, 1H), 7.36 (ddd, *J*=2.5, 4.2, 8.5 Hz, 1H), 6.93 (dd, *J*=8.5, 11.8 Hz, 1H), 3.82 (d, *J*=10.6 Hz, 1H), 3.64 (dd, *J*=1.2, 10.6 Hz, 1H), 1.89 (br s, 3H), 1.48 (d, *J*=0.9 Hz, 3H); LC-MS m/z 248 $[M+H]^+$.

rac-**17b** (16.6 g, 66.9 mmol) was purified by chiral SFC on (CHIRALPAK AD-H 5µm 250x20 mm). Mobile phase (0.3% isopropylamine, 80% CO_2, 20% MeOH) , yielding 5.3 g 2*R*-**17b** (32% yield). ^{1}H NMR (500 MHz, $CDCl_3$) δ 7.62 (dd, *J*=2.6, 7.2 Hz, 1H), 7.36 (ddd, *J*=2.5, 4.3, 8.6 Hz, 1H), 6.93 (dd, *J*=8.6, 11.8 Hz, 1H), 3.83 (d, *J*=10.7 Hz, 1H), 3.65 (br d, *J*=10.7 Hz, 1H), 2.61 (br s, 3H), 1.48 (s, 3H); LC-MS m/z 248 $[M+H]^+$; $[\alpha]^{20}_D$ = +2.0 (*c* = 0.61 in DMF).

(5*R*)-5-(3-Bromophenyl)-5-methyl-morpholin-3-one (5*R*-18a). Chloroacetyl chloride (0.55 mL, 6.95 mmol) was added dropwise to a stirred solution of intermediate 2*R*-**17a** (1.6 g, 6.95 mmol) in THF (60 mL) and diisopropylethyl amine (1.44 mL, 8.34 mmol) at -78 ºC. The mixture was stirred for 30 min at -78 ºC. Then potassium *tert*-butoxide (1.95 g, 17.38 mmol) was added and the mixture was stirred at -15ºC and left warming up to 0 ºC during 90 min. The mixture was diluted with sat. aq. NH_4Cl and extracted with DCM. The organic layer was separated, dried (Na_2SO_4), filtered and the solvents evaporated in vacuo. The crude product was triturated with Et_2O, filtered and dried to yield intermediate 5*R*-**18a** (1.65 g, 88% yield) as a white solid. 1H NMR (500 MHz, $CDCl_3$) δ 7.54 (t, J=1.9 Hz, 1H), 7.46 (td, J=1.3, 7.7 Hz, 1H), 7.31-7.35 (m, 1H), 7.28 (t, J=7.5 Hz, 1H), 6.41 (br s, 1H), 4.19-4.28 (m, 2H), 3.82 (d, J=11.8 Hz, 1H), 3.72 (d, J=11.8 Hz, 1H), 1.67 (s, 3H); LC-MS m/z 311 [M+H]+; $[\alpha]^{20}_D$ = – 71.6 (c = 0.62 in DMF); m. p. = 135.2 ºC.

(5*R*)-5-(5-Bromo-2-fluorophenyl)-5-methylmorpholin-3-one (5*R*-18b). Starting from 2*R*-**17b** (5.1 g, 20.6 mmol) and following the same procedure as for 5*R*-**18a** the corresponding morpholinone 5*R*-**18b** was obtained (5.9 g, 89%). ^{1}H NMR (500 MHz, $CDCl_3$) δ 7.51 (dd, *J*=2.6,

7.2 Hz, 1H), 7.43 (ddd, *J*=2.6, 4.3, 8.7 Hz, 1H), 6.98 (dd, *J*=8.7, 11.6 Hz, 1H), 6.60 (br s, 1H), 4.30 (d, *J*=11.8 Hz, 1H), 4.15-4.26 (m, 2H), 3.72 (d, *J*=11.8 Hz, 1H), 1.64 (s, 3H); LC-MS m/z 288 $[M+H]^+$; $[a]^{20}_D$ = -53.4 (*c* = 0.67 in DMF); m. p. = 161.9 ºC.

(5*R*)-5-(3-Bromophenyl)-5-methylmorpholine-3-thione (5*R*-19a). THF (40 mL) was added to a mixture of intermediate 5*R*-**18a** (1.14 g, 3.92 mmol) and phosphorus pentasulfide (0.704 g, 3.17 mmol) at rt. The mixture was stirred at 50 ºC for 50 min. Then the mixture was cooled to rt and filtered over cotton and evaporated *in vacuo*. The crude product was purified by flash column chromatography (silica; DCM). The desired fractions were collected and evaporated *in vacuo* to yield the thioamide 5*R*-**19a** (1.05 g, 93% yield) as a yellow solid. ^{1}H NMR (500 MHz, $CDCl_3$) δ 8.44 (br s, 1H), 7.45-7.52 (m, 2H), 7.26-7.33 (m, 2H), 4.56-4.65 (m, 2H), 3.86 (d, *J*=11.8 Hz, 1H), 3.77 (d, *J*=11.8 Hz, 1H), 1.71 (s, 3H); LC-MS m/z 286 $[M+H]^+$; $[\alpha]^{20}_D$ = –190.0 (*c* = 0.6 in DMF).

(5*R*)-5-(5-Bromo-2-fluorophenyl)-5-methylmorpholine-3-thione (5*R*-19b). Starting from 5*R*-**18b** (5.3 g, 18.4 mmol) and following the same procedure as for 5*R*-**19a** the corresponding thione 5*R*-**19b** was obtained (4.1 g, 72% yield). ^{1}H NMR (400 MHz, $CDCl_3$) δ 8.48 (br s, 1H), 7.46 (ddd, *J*=2.5, 4.4, 8.5 Hz, 1H), 7.41 (dd, *J*=2.4, 7.0 Hz, 1H), 7.01 (dd, *J*=8.5, 11.6 Hz, 1H), 4.62 (d, *J*=18.4 Hz, 1H), 4.54 (d, *J*=18.4 Hz, 1H), 4.33 (d, *J*=12.0 Hz, 1H), 3.74 (d, *J*=12.0 Hz, 1H), 1.69 (d, *J*=0.9 Hz, 3H); LC-MS m/z 304 $[M+H]^+$; $[\alpha]^{20}_D$ = –167.3 (*c* = 0.6 in DMF).

(5*R*)-5-(3-Bromophenyl)-5-methyl-5,6-dihydro-2*H*-1,4-oxazin-3-amine trifluoroacetate salt (5*R*-20a). The thioamide 5*R*-**19a** (0.205 g, 0.716 mmol) and 32% aqueous ammonia solution (12 mL) were stirred in a sealed tube at 60 ºC for 4 h. After cooling, the mixture was diluted with water and extracted with DCM. The organic layer was separated, dried (Na_2SO_4), filtered and the solvent evaporated *in vacuo*. DCM (15 mL) and TFA (0.25 mL) were added and the mixture was

concentrated *in vacuo*. To this residue, Et_2O and heptane were added and evaporated. Diisopropyl ether was added, and the suspension was sonicated for 20 min and then stirred overnight at rt. The white precipitate was filtered and washed with diisopropyl ether and dried *in vacuo* to yield intermediate 5*R*-**20a** (0.19 g, 69% yield) as a white solid. ^{1}H NMR (400 MHz, $CDCl_3$) δ 7.57 (t, *J*=1.7 Hz, 1H), 7.36 (td, *J*=0.9, 7.9 Hz, 1H), 7.32 (br d, *J*=7.90 Hz, 1H), 7.20 (t, *J*=7.90 Hz, 1H), 4.13 (d, *J*=15.5 Hz, 1H), 4.05 (d, *J*=15.5 Hz, 1H), 3.68 (d, *J*=11.3 Hz, 1H), 3.56 (d, *J*=11.3 Hz, 1H), 3.32 (br s, 2H), 1.50 (s, 3H); LC-MS m/z 269 $[M+H]^+$; $[\alpha]^{20}_D$ = –112.6 (*c* = 0.66 in DMF).

(5*R*)-5-(5-Bromo-2-fluorophenyl)-5-methyl-5,6-dihydro-2*H*-1,4-oxazin-3-amine (5*R*-20b). Starting from 5*R*-**19b** (4.1 g, 13.5 mmol) and following the same procedure as for 5*R*-**20a** the corresponding oxazinamine 5*R*-**20b** was obtained (4.1 g, 87% yield). ^{1}H NMR (500 MHz, $CDCl_3$) δ 7.70 (dd, *J*=2.6, 6.9 Hz, 1H), 7.32 (ddd, *J*=2.6, 4.1, 8.6 Hz, 1H), 6.90 (dd, *J*=8.5, 11.4 Hz, 1H), 4.21 (br s, 2H), 4.11 (d, *J*=15.6 Hz, 1H), 4.03 (d, *J*=15.6 Hz, 1H), 3.86 (dd, *J*=1.4, 11.3 Hz, 1H), 3.77 (d, *J*=11.5 Hz, 1H), 1.54 (d, *J*=0.9 Hz, 3H); LC-MS m/z 287 $[M+H]^+$.

(5*R*)-5-(3-Aminophenyl)-5-methyl-5,6-dihydro-2*H*-1,4-oxazin-3-amine (5*R*-21a). Toluene (1.5 mL) was added to a mixture of intermediate 5*R*-**20a** (0.05 g, 0.13 mmol), tris(dibenzylideneacetone)dipalladium(0) (0.012 g, 0.013 mmol), rac-2,2'-bis(diphenylphosphino)-1,1'-binaphthyl (0.024 g, 0.04 mmol) and sodium *tert*-butoxide (0.031 g, 0.326 mmol) in a sealed tube and under nitrogen at rt. The mixture was flushed with nitrogen for a few min and then benzophenone imine (0.028 mL, 0.17 mmol) was added and the mixture was stirred at 80 ºC for 7 h. After cooling, a mixture of 1 N HCl/THF (1/1.4 mL) was added and the mixture was stirred at rt overnight. The mixture was diluted with water and washed with EtOAc. The aqueous layer was basified with sat. aq. Na_2CO_3 and extracted with DCM/EtOH 9/1 (10

times). The combined organic layers were dried (Na_2SO_4), filtered and the solvents evaporated *in vacuo*. The crude product was purified by flash column chromatography (silica; 7 N solution of ammonia in MeOH/DCM 0/100 to 8/92). The desired fractions were collected and concentrated *in vacuo* to yield intermediate 5*R*-**21a** (0.012 g, 45% yield) as an oil. ^{1}H NMR (500 MHz, $CDCl_3$) δ 7.12 (t, *J*=7.9 Hz, 1H), 6.75-6.80 (m, 2H), 6.56 (br d, *J*=7.6 Hz, 1H), 4.13 (d, *J*=15.4 Hz, 1H), 4.06 (d, *J*=15.4 Hz, 1H), 3.68 (d, *J*=11.6 Hz, 1H), 3.60-3.75 (m, 2H), 3.57 (d, *J*=11.6 Hz, 1H), 3.09 (br s, 2H), 1.50 (s, 3H); LC-MS m/z 206 $[M+H]^+$.

(5*R*)-5-(5-Amino-2-fluorophenyl)-5-methyl-5,6-dihydro-2*H*-1,4-oxazin-3-amine (5*R*-21b). Toluene (1.5 mL) was added to a mixture of intermediate 5*R*-**20b** (3.2 g, 11.1 mmol), tris(dibenzylideneacetone)dipalladium(0) (1.02 g, 1.11 mmol), rac-2,2'-bis(diphenylphosphino)-1,1'-binaphthyl (2.08 g, 3.34 mmol) and sodium *tert*-butoxide (1.93 g, 20.1 mmol) in a sealed tube and under nitrogen at rt. The mixture was flushed with nitrogen for a few min and then benzophenone imine (3.74 mL, 22.3 mmol) was added and the mixture was stirred at 100 ºC for 2 h. After cooling the mixture was diluted with water and extracted with DCM. The organic layer was dried (Na_2SO_4), filtered and the solvents concentrated *in vacuo*. The crude product was purified by flash column chromatography (silica; 7 N solution of ammonia in MeOH/DCM 0/100 to 3/97). The desired fractions were collected and concentrated *in vacuo* to yield the intermediate benzophenone imine as a yellow foam (3.6 g, 83% yield). This imine (3.6 g, 9.29 mmol) was dissolved in HCl (0.6 M in 2-propanol, 66 mL) and the resulting mixture was stirred at rt for 30 min. Diethyl ether (400 mL) was added and the precipitated product (HCl salt of 5*R*-**21b**) was filtered and washed with ether. ^{1}H NMR (400 MHz, DMSO-d_6) δ ppm 1.61 (s, 3 H), 3.81 - 3.89 (m, 1 H), 4.08 (d, *J*=12.0 Hz, 1 H), 4.48 - 4.61 (m, 2 H), 6.63 - 6.88 (m, 3 H), 7.03 (br dd, *J*=12.1, 8.4 Hz, 2 H), 8.62 (s, 1 H), 9.26 (s, 1 H), 10.76 (s, 1 H). Since the HCl salt of 5*R*-**21b**

was hygroscopic, the base was liberated prior to the next step. Hence 5*R*-**21b** was dissolved in MeOH and excess 7 N solution of ammonia in MeOH was added. Then all volatiles were evaporated *in vacuo*. The residue was purified by flash column chromatography (silica; 7 N solution of ammonia in MeOH 1/99 to 12/88). The desired fractions were collected and concentrated *in vacuo* to yield 5*R*-**21b** as an off white solid (1.6 g, 77%). LC-MS m/z 224 $[M+H]^+$.

(3*R*)-3-(5-Bromo-2-fluorophenyl)-3-methylmorpholine-2,5-dione (3*R*-22). Enantiopure 5*R*-**15a** was obtained via preparative SFC of *rac*-**15a** on a Chiralpak® Diacel AD x 250 mm column using CO_2 and MeOH with 0.2% $iPrNH_2$ as mobile phase. To a cooled solution of intermediate 5*R*-**15b** (41.3 g, 145 mmol) in water (150 mL), a solution of chloroacetyl chloride (24 mL, 304.5 mmol) in 1,4-dioxane (75 mL) was added dropwise. Simultaneously, NaOH (5 M in water, 29 mL) was added to adjust the pH at 10-11. The reaction mixture was stirred at rt for 2 h. The organic layer was separated, and the aqueous layer extracted with Et_2O. Then the aqueous layer was acidified with HCl (6 M in water) until pH 2. The precipitated white solid was collected by filtration, washed with water and dried. The obtained intermediate (42 g, 124 mmol) and $NaHCO_3$ (20.8 g, 248 mmol) were dissolved in DMF (1000 mL), and the reaction mixture was stirred at 80 ºC for 3 h. The mixture was partially concentrated *in vacuo*, cooled to rt and then filtered over celite. The filtrate was concentrated *in vacuo*, and the residue was purified by flash column chromatography (silica; MeOH/DCM 0/100 to 5/95). The desired fractions were collected and concentrated *in vacuo* to yield intermediate 3*R*-**22** (36 g, 96% yield). ^{1}H NMR (400 MHz, DMSO-d_6) δ 9.12 (br s, 1H), 7.68 (ddd, *J*=2.5, 4.4, 8.7 Hz, 1H), 7.63 (dd, *J*=2.5, 6.9 Hz, 1H), 7.29 (dd, *J*=8.7, 11.2 Hz, 1H), 4.97 (d, *J*=16.4 Hz, 1H), 4.74 (d, *J*=16.4 Hz, 1H), 1.84 (s, 3H); LC-MS m/z 302 $[M+H]^+$; $[\alpha]^{20}_D$ = +31.6 (*c* = 0.53 in DMF); m. p. = 162.6 ºC.

(5*R*)-5-(5-Bromo-2-fluorophenyl)-6-fluoro-5-methylmorpholin-3-one (5*R*-23). A solution of intermediate 3*R*-**22** (10 g, 21.5 mmol) in THF (105 mL) was cooled to -78 °C under N_2 atmosphere. Then, diisobutylaluminium hydride (1 M in toluene, 43 mL, 43 mmol) was slowly added. The reaction mixture was allowed to reach rt over 2 h. The reaction mixture was cooled down to 0 °C and quenched by the slow addition of aq. 1 N HCl solution. The mixture was then extracted with EtOAc, the organic layers were separated, dried (Na_2SO_4), filtered and the solvent evaporated *in vacuo* to yield the hydroxymorpholinone (6.6 g, 100% yield) as a 80:20 mixture of diastereoisomers which was used as such in the following reaction. The crude hydroxymorpholinone (6.3 g, 20.7 mmol) was dissolved in DCM (84 mL) and the reaction was cooled down to 0 °C. Then DAST (3 mL, 24.9 mmol) was added dropwise. After 20 min at 0 °C the reaction mixture was quenched with sat. aq. $NaHCO_3$ and extracted with DCM. The combined organic layers were dried ($MgSO_4$), filtered, and the solvent evaporated *in vacuo.* The crude product was suspended in diisopropyl ether, filtered and dried *in vacuo* at 60°C to yield intermediate 5*R*-**23** (4.2 g, 66% yield) as an 80:20 mixture of 6*R* and 6*S* isomers. ^{1}H NMR (400 MHz, DMSO-d_6) δ 8.97 (s, 1H), 7.55-7.68 (m, 1.2H), 7.45 (dd, *J*=2.5, 7.3 Hz, 0.8H), 7.29 (dd, *J*=8.5, 11.8 Hz, 0.8H), 7.25 (dd, *J*=8.5, 12.00 Hz, 0.2H), 6.03 (d, *J*=50.9 Hz, 0.8H), 6.01 (d, *J*=50.7 Hz, 0.2H), 4.28 (d, *J*=16.3 Hz, 0.2H), 4.20 (d, *J*=16.4 Hz, 0.2H), 4.19 (d, *J*=16.6 Hz, 0.8H), 4.11 (d, *J*=16.6 Hz, 0.8H), 1.64 (s, 0.6H), 1.56 (s, 2.4H); LC-MS m/z 306 $[M+H]^+$.

(5*R*)-5-(5-Bromo-2-fluorophenyl)-6-hydroxy-5-methyl-6-(trifluoromethyl)morpholin-3-one (5*R*-24). To a solution of intermediate 3*R*-**22** (11.6 g, 38.5 mmol) in THF (117 mL) was added tetrabutylammonium difluorotriphenylsilicate (2.08 g, 3.85 mmol). Then (trifluoromethyl)trimethylsilane (12.5 mL, 84.6 mmol) was added dropwise, and the reaction mixture was stirred at rt for 20 min. The mixture was quenched with aqueous NaCl and extracted

with EtOAc. The combined organic layers were dried ($MgSO_4$), filtered and concentrated *in vacuo* to yield intermediate 5*R*-**24** (14 g, 98% yield) as a 3:1 6*R*/6*S* mixture, which was used as such in the following step. ^{1}H NMR (500 MHz, DMSO-d_6) δ 8.51 (s, 1H), 8.39 (br s, 1H), 7.57-7.64 (m, 1H), 7.46 (br d, *J*=5.5 Hz, 1H), 7.18 (dd, *J*=8.8, 12.9 Hz, 1H), 4.31 (d, *J*=16.5 Hz, 1H), 4.17 (d, *J*=16.5 Hz, 1H), 1.72 (s, 3H); LC-MS m/z 372 $[M+H]^+$; m. p. = 191.2 ºC.

(5*R*)-5-(5-Bromo-2-fluorophenyl)-6-fluoro-5-methyl-6-(trifluoromethyl)morpholin-3-one (5*R*-25). Intermediate 5*R*-**24** (3.35 g, 9.00 mmol) was suspended in DCM (25 mL) and after cooling the reaction mixture at 0 ºC, DAST (1.32 mL, 10.80 mmol) was added dropwise. The reaction mixture was stirred at 0 ºC for 2 h and then quenched with sat. aq. $NaHCO_3$. The organic layer was separated and the aqueous layer was extracted with DCM. The combined organic layers were dried ($MgSO_4$), filtered and the solvent evaporated *in vacuo*. The crude product was purified by flash column chromatography (silica; MeOH/DCM 0/100 to 1/99). The desired fractions were collected and concentrated *in vacuo* to yield intermediate 5*R*-**25** (3.15 g, 93% yield) as a 25:75 6*R*/6*S* mixture as an off white solid. ^{1}H NMR (500 MHz, $CDCl_3$) δ 7.61 (td, *J*=2.1, 7.1 Hz, 0.25H), 7.48-7.53 (m, 1H), 7.45 (dd, *J*=2.3, 7.2 Hz, 1H), 7.13 (br s, 1H), 7.00 (dd, *J*=8.7, 12.1 Hz, 0.25H), 6.99 (dd, *J*=8.7, 12.4 Hz, 0.75H), 4.52-4.59 (m, 1.25H), 4.48 (d, *J*=15.9 Hz, 0.75H), 2.00 (s, 0.75H), 1.96 (s, 2.25H); LC-MS m/z 374 $[M+H]^+$.

(5*R*)-5-(5-Bromo-2-fluorophenyl)-6-chloro-5-methyl-6-(trifluoromethyl)morpholin-3-one (5*R*-26). Intermediate 5*R*-**24** (14 g, 37.6 mmol) was dissolved in DCM (600 mL) and cooled to 0 °C and then thionyl chloride (11.2 mL, 150 mmol) was added dropwise. The reaction mixture was stirred for 30 min at 0 °C and then pyridine (18.2 mL, 225.7 mmol) was added. After 30 min the reaction was hydrolyzed with aq. 1 N HCl and then extracted with DCM. The organic layers were separated, dried ($MgSO_4$), filtered and evaporated *in vacuo*. The crude product was purified

by flash column chromatography (silica; 7 N solution of ammonia in MeOH/DCM 0/100 to 2/98). The desired fractions were collected and concentrated *in vacuo* to yield intermediate 5*R*-**26** (6 g, 41% yield) as a mixture of diastereoisomers. ^{1}H NMR (400 MHz, DMSO-d_6) δ 9.10 (br s, 1H), 7.69 (ddd, *J*=2.5, 3.9, 8.8 Hz, 1H), 7.48-7.62 (m, 1H), 7.27 (dd, *J*=8.8, 12.9 Hz, 1H), 4.76 (br d, *J*=16.2 Hz, 1H), 4.42 (dd, *J*=0.9, 16.8 Hz, 1H), 1.90 (s, 3H); LC-MS m/z 390 $[M+H]^+$; m. p. = 147.0 ºC.

(5*R*)-5-(5-Bromo-2-fluorophenyl)-5-methyl-6-(trifluoromethyl)morpholin-3-one (5*R*-27). To a solution of intermediate 5*R*-**26** (3 g, 7.68 mmol) in acetic acid (136 mL), zinc (1.26 g, 19.2 mmol) was added. The reaction mixture was then stirred at 80 °C for 3 h, after that the reaction was filtered hot and concentrated *in vacuo*. The residue was dissolved in DCM and washed with ammonium hydroxide solution. The organic phase was separated, dried ($MgSO_4$) and the solvent concentrated *in vacuo.* The crude product purified by column chromatography (silica; 7 N solution of ammonia in MeOH/DCM 0/100 to 3/97). The desired fractions were collected and concentrated *in vacuo* to yield intermediate 5*R*-**27** (2.7 g, 99% yield). ^{1}H NMR (400 MHz, $CDCl_3$) δ 7.42-7.52 (m, 2H), 7.16 (s, 1H), 6.99 (dd, *J*=9.1, 11.9 Hz, 1H), 4.48 (d, J=17.1 Hz, 1H), 4.34 (d, J=17.1 Hz, 1H), 1.92 (d, J=0.7 Hz, 3H); LC-MS m/z 356 $[M+H]^+$.

(5*R*)-5-(5-Bromo-2-fluorophenyl)-6-fluoro-5-methylmorpholine-3-thione (5*R*-28). THF (100 mL) was added to a mixture of intermediate 5*R*-**23** (4.20 g, 13.7 mmol) and phosphorus pentasulfide (3.66 g, 16.5 mmol) at rt. The mixture was stirred at 70 ºC for 3 h. Then the mixture was cooled to rt and filtered over cotton and evaporated *in vacuo*. The crude product was purified by flash column chromatography (silica; EtOAc/Heptane 0/1 to 1/0). The desired fractions were collected and evaporated *in vacuo* to yield the thioamide 5*R*-**28** as a yellow solid (3 g, 68% yield, as a 62:38 6*R*/6*S* mixture).

(5*R*)-5-(5-Bromo-2-fluorophenyl)-6-fluoro-5-methyl-6-(trifluoromethyl)morpholine-3-thione (5*R*-29). Starting from 5*R*-**25** (3.05 g, 8.15 mmol) and following the same procedure as for 5*R*-**28** the corresponding thione 5*R*-**29** was obtained (2.80 g, white foam, 88% yield) as a 25:75 6*R*/6*S* mixture. ^{1}H NMR (500 MHz, DMSO-d_6) δ 11.44 (br s, 0.25H), 11.30 (br s, 0.75H), 7.69-7.77 (m, 1H), 7.67 (br d, *J*=6.9 Hz, 0.25H), 7.60 (dd, *J*=2.3, 7.2 Hz, 0.75H), 7.30 (dd, *J*=8.8, 12.6 Hz, 0.75H), 7.27 (dd, *J*=8.9, 12.7 Hz, 0.25H), 5.07 (d, *J*=18.2 Hz, 0.25H), 5.05 (d, *J*=17.9 Hz, 0.75H), 4.78 (d, *J*=18.2 Hz, 0.25H), 4.74 (d, *J*=18.2 Hz, 0.75H), 1.92 (br s, 2.25H), 1.90 (br s, 0.75H); LC-MS m/z 390 $[M+H]^+$.

(5*R*)-5-(5-Bromo-2-fluoro-phenyl)-5-methyl-6-(trifluoromethyl)morpholine-3-thione (5*R*-30). Starting from 5*R*-**27** (9.8 g, 27.5 mmol) and following the same procedure as for 5*R*-**28** the corresponding thioamide 5*R*-**30** was obtained (9.4 g, white foam, 92% yield) as a 80:20 6*R*/6*S* mixture.

(5*R*, 6*S*)-5-(5-Bromo-2-fluorophenyl)-6-fluoro-5-methyl-2,6-dihydro-1,4-oxazin-3-amine ((5*R*,6*S*)-31) and (5*R*, 6*R*)-5-(5-bromo-2-fluorophenyl)-6-fluoro-5-methyl-2,6-dihydro-1,4-oxazin-3-amine ((5*R*,6*R*)-31). The crude thione 5*R*-**28** (3.0 g, 9.3 mmol) was dissolved in 7 N solution of ammonia in MeOH (150 mL) and the reaction mixture was stirred in a sealed tube at 60 ºC for 18 h. Next, the solvent was evaporated and the residue re-dissolved in 7 N solution of ammonia in MeOH (150 mL) and stirred in a sealed tube at 60 ºC for another 18 h. Then the solvent was evaporated and the crude product purified by column chromatography (silica; 7 N solution of ammonia in MeOH/DCM 0/1 to 1/9). The desired fractions were collected and concentrated *in vacuo* to yield the amidine (5*R*,6*R*)-**31** (1.6 g, 56%), ^{1}H NMR (360 MHz, $CDCl_3$) δ 8.00 (dd, *J*=2.6, 6.9 Hz, 1H), 7.35 (ddd, *J*=2.7, 4.3, 8.7 Hz, 1H), 6.91 (dd, *J*=8.6, 11.5 Hz, 1H), 6.04 (dd, *J*=1.8, 51.6 Hz, 1H), 4.34 (br s, 2H), 4.26 (d, *J*=15.3 Hz, 1H), 4.13 (d, *J*=15.3 Hz, 1H),

1.51 (t, *J*=1.5 Hz, 3H); LC-MS m/z 305 $[M+H]^+$; and (5*R*,6*S*)-**31** (0.27 g, 9%),^{1}H NMR (360 MHz, $CDCl_3$) δ 7.44 (dd, *J*=2.6, 6.9 Hz, 1H), 7.37 (ddd, *J*=2.7, 4.3, 8.7 Hz, 1H), 6.93 (dd, *J*=8.6, 11.5 Hz, 1H), 5.98 (d, *J*=51.9 Hz, 1H), 4.43 (br s, 2H), 4.25 (d, *J*=15.7 Hz, 1H), 3.99 (d, *J*=15.7 Hz, 1H), 1.61 (t, *J*=2.0 Hz, 3H); LC-MS m/z 305 $[M+H]^+$.

(5*R*,6*S*)-5-(5-Bromo-2-fluorophenyl)-6-fluoro-5-methyl-6-(trifluoromethyl)-5,6-dihydro-2*H*-1,4-oxazin-3-amine ((5*R*,6*S*)-32) and (5*R*,6*R*)-5-(5-bromo-2-fluorophenyl)-6-fluoro-5-methyl-6-(trifluoromethyl)-5,6-dihydro-2*H*-1,4-oxazin-3-amine ((5*R*,6*R*)-32). Starting from 5*R*-**27** (10 g, 25.6 mmol) and following the same procedure as for 5*R*-**28** both diastereomers of **32** were separately isolated: (5*R*,6*S*)-**32** (2.0 g, 21% yield), ^{1}H NMR (400 MHz, $CDCl_3$) δ 7.44 (dd, *J*=2.5, 7.3 Hz, 1H), 7.40 (ddd, *J*=2.5, 4.0, 8.5 Hz, 1H), 6.89 (dd, *J*=8.7, 12.4 Hz, 1H), 4.25-4.55 (m, 4H), 1.79 (s, 3H); LC-MS m/z 305 $[M+H]^+$, and (5*R*,6*R*)-**32** (0.75 g, 8% yield), ^{1}H NMR (400 MHz, $CDCl_3$) δ 7.58 (td, *J*=2.4, 7.0 Hz, 1H), 7.38 (ddd, *J*=2.6, 4.0, 8.7 Hz, 1H), 6.89 (dd, *J*=8.8, 12.0 Hz, 1H), 4.50 (d, *J*=15.4 Hz, 1H), 4.43 (d, *J*=15.3 Hz, 1H), 4.35 (br s, 2H), 1.74-1.81 (m, 3H); LC-MS m/z 373 $[M+H]^+$.

(5*R*,6*R*)-5-(5-Bromo-2-fluorophenyl)-5-methyl-6-(trifluoromethyl)-2,6-dihydro-1,4-oxazin-3-amine ((5*R*,6*R*)-33) and (5*R*,6*S*)-5-(5-Bromo-2-fluorophenyl)-5-methyl-6-(trifluoromethyl)-2,6-dihydro-1,4-oxazin-3-amine ((5*R*,6*S*)-33). Starting from *5R*-**30** (6 g, 16.1 mmol) and following the same procedure as for (5*R*,6*R*)-**31** the corresponding amidine diastereomers of **33** were separately isolated: (5*R*,6*R*)-**33** (3.4 g, 59% yield),^{1}H NMR (400 MHz, $CDCl_3$) δ 8.02 (dd, *J*=2.6, 7.1 Hz, 1H), 7.36 (ddd, *J*=2.4, 4.2, 8.7 Hz, 1H), 6.89 (dd, *J*=8.7, 11.5 Hz, 1H), 4.59 (dq, *J*=1.1, 8.3 Hz, 1H), 4.32 (br s, 2H), 4.20 (d, *J*=0.8 Hz, 2H), 1.64 (d, *J*=1.2 Hz, 3H); LC-MS m/z 355 $[M+H]^+$; $[a]^{20}_D$ = -66.5 (*c* = 1.23 in DMF), and (5*R*,6*S*)-**33** (0.75 g, 13% yield), which was isolated in impure form.

(5*R*,6*R*)-5-(5-Amino-2-fluorophenyl)-6-fluoro-5-methyl-5,6-dihydro-2*H*-1,4-oxazin-3-amine ((5*R*,6*R*)-34). Bromide (5*R*,6*R*)-**31** (1.6 g, 5.24 mmol) was combined with NaN_3 (0.85 g, 13 mmol), CuI (1.25 g, 6.5 mmol) and Na_2CO_3 (1.1 g, 10.5 mmol) in DMSO (75 mL) and the reaction was degassed. After that, *N*,*N'*-dimethylethylenediamine (1 mL, 9.1 mmol) was added and the mixture was heated at 110 °C for 4 h. The reaction mixture was poured into DCM. Ammonium hydroxide (28% in water) was added and the organic layer was separated and washed three times with ammonium hydroxide. Then the organic layer was dried ($MgSO_4$), filtered and concentrated *in vacuo.* The crude product was purified by column chromatography (silica; 7 N solution of ammonia in MeOH in DCM 0/100 to 10/90). The desired fractions were collected and concentrated *in vacuo* to yield the corresponding aniline (5*R*,6*R*)-**34** (0.3 g, 24% yield), ^{1}H NMR (400 MHz, $CDCl_3$) δ 6.83 (dd, *J*=8.5, 11.8 Hz, 1H), 6.62 (dd, *J*=2.9, 6.6 Hz, 1H), 6.53 (td, *J*=3.3, 8.5 Hz, 1H), 6.02 (d, *J*=52.5 Hz, 1H), 4.42 (br s, 2H), 4.22 (dd, *J*=0.7, 15.5 Hz, 1H), 3.97 (d, *J*=15.5 Hz, 1H), 3.56 (br s, 2H), 1.60 (t, *J*=2.0 Hz, 3H); LC-MS m/z 242 $[M+H]^+$.

(5*R*,6*S*)-5-(5-Amino-2-fluorophenyl)-6-fluoro-5-methyl-5,6-dihydro-2*H*-1,4-oxazin-3-amine ((5*R*,6*S*)-34). Starting from (5*R*,6*S*)-**31** (0.27 g) and following the same procedure as for (5*R*,6*R*)-**34** the corresponding (5*R*,6*S*)-**34** was obtained (0.040 g, 15% yield) ^{1}H NMR (360 MHz, $CDCl_3$) δ 7.22 (dd, *J*=3.1, 6.8 Hz, 1H), 6.81 (dd, *J*=8.4, 11.7 Hz, 1H), 6.45-6.54 (m, 1H), 6.05 (dd, *J*=1.5, 51.9 Hz, 1H), 4.70 (br s, 2H), 4.25 (d, *J*=15.5 Hz, 1H), 4.11 (d, *J*=15.5 Hz, 1H), 3.56 (br s, 2H), 1.48-1.53 (m, 3H).

(5*R*,6*S*)-5-(5-Amino-2-fluorophenyl)-6-fluoro-5-methyl-6-(trifluoromethyl)-5,6-dihydro-2*H*-1,4-oxazin-3-amine ((5*R*,6*S*)-35). Starting from (5*R*,6*S*)-**32** (2.0 g, 5.36 mmol) and following the same procedure as for (5*R*,6*R*)-**34** the corresponding (5*R*,6*S*)-**35** was obtained (1.3

g, 78% yield). ^{1}H NMR (360 MHz, $CDCl_3$) δ 6.80 (dd, *J*=8.6, 12.6 Hz, 1H), 6.64 (dd, *J*=2.2, 6.6 Hz, 1H), 6.59 (td, *J*=3.0, 8.2 Hz, 1H), 4.36-4.49 (m, 2H), 4.31 (br s, 2H), 3.51 (br s, 2H), 1.73-1.84 (m, 3H); $[a]^{20}_D$ = +95.8 (*c* = 0.3 in MeOH).

(5*R*,6*R*)-5-(5-Amino-2-fluorophenyl)-6-fluoro-5-methyl-6-(trifluoromethyl)-5,6-dihydro-2*H*-1,4-oxazin-3-amine ((5*R*,6*R*)-35). Starting from (5*R*,6*R*)-**32** (1.1 g, 2.95 mmol) and following the same procedure as for (5*R*,6*R*)-**34** the corresponding (5*R*,6*R*)-**35** was obtained (0.75 g, 82% yield). ^{1}H NMR (360 MHz, $CDCl_3$) δ 6.73-6.85 (m, 2H), 6.58 (td, *J*=3.2, 8.6 Hz, 1H), 4.49 (d, *J*=15.7 Hz, 1H), 4.42 (d, *J*=15.7 Hz, 1H), 4.31 (br s, 2H), 3.51 (br s, 2H), 1.77 (s, 3H);); LC-MS m/z 310 $[M+H]^+$.

(5*R*,6*R*)-5-(5-Amino-2-fluorophenyl)-5-methyl-6-(trifluoromethyl)-5,6-dihydro-2*H*-1,4-oxazin-3-amine ((5*R*,6*R*)-36). Starting from (5*R*,6*R*)-**33** (3.4 g, 9.57 mmol) and following the same procedure as for (*5R,6R*)-**34** the corresponding (5*R*,6*R*)-**36** was obtained (2.5 g, 90% yield). ^{1}H NMR (360 MHz, $CDCl_3$) δ 7.20 (dd, *J*=2.9, 6.6 Hz, 1H), 6.80 (dd, *J*=8.6, 11.9 Hz, 1H), 6.54 (td, *J*=3.6, 8.6 Hz, 1H), 4.61 (q, *J*=8.4 Hz, 1H), 4.27 (br s, 2H), 4.20 (s, 2H), 3.56 (br s, 2H), 1.64 (s, 3H); LC-MS m/z 292 $[M+H]^+$; $[a]^{20}_D$ = -94.9 (*c* = 0.42 in MeOH).

(5*R*,6*S*)-5-(5-Amino-2-fluorophenyl)-5-methyl-6-(trifluoromethyl)-5,6-dihydro-2*H*-1,4-oxazin-3-amine ((5*R*,6*S*)-36). Starting from (5*R*,6*S*)-**33** (0.3 g, 0.84 mmol) and following the same procedure as for (5*R*,6*R*)-**34** the corresponding (5*R*,6*S*)-**36** was obtained (0.10 g, 41% yield). LC-MS m/z 292 $[M+H]^+$.

Methyl 2-(5-bromo-2-fluorophenyl)-2-oxoacetate (37). Thionyl chloride (37 mL, 510 mmol) was added dropwise to a stirred solution of (2)-(5-bromo-2-fluoro-phenyl)-2-oxo-acetic acid (42 g, 170 mmol) in MeOH (456 mL) at 0 °C. The mixture was refluxed for 18 h. The solvents were evaporated *in vacuo* and the residue was partitioned between sat. aq. Na_2CO_3 and DCM. The

organic layer was separated, dried ($MgSO_4$), filtered and concentrated *in vacuo* to yield **37** (30 g, 68% yield) as a yellow oil.

Isopropyl 2-(5-bromo-2-fluoro-phenyl)-2-[(S)-tert-butylsulfinyl]imino-acetate (*S*-38). Titanium(IV) isopropoxide (51.6 mL, 172 mmol) was added to a stirred mixture of **37** (30 g, 115 mmol] and (*S*)-2-methyl-2-propanesulfinamide (16.7 g, 138 mmol) in *n*-heptane (1000 mL). The mixture was stirred at 80 ºC for 24 h. The mixture was partly concentrated *in vacuo,* then diluted with EtOAc. The mixture was cooled to rt and water was added. The resulting mixture was filtered through a pad of celite and rinsed with EtOAc and water. The organic layer was separated, dried (MgSO4), filtered and concentrated in vacuo. The residue was purified by flash column chromatography (silica; EtOAc/heptane 0/100 to 50/50). The desired fractions were collected and concentrated *in vacuo* to yield intermediate *S*-**38** (40 g, 89% yield). ^{1}H NMR (400 MHz, $CDCl_3$) δ 7.92 (dd, *J*=2.1, 6.2 Hz, 1H), 7.59 (ddd, *J*=2.5, 4.3, 8.7 Hz, 1H), 7.03 (dd, *J*=8.8, 10.6 Hz, 1H), 5.29 (spt, *J*=6.2 Hz, 1H), 1.39 (d, *J*=6.2 Hz, 3H), 1.38 (d, *J*=6.2 Hz, 3H), 1.36 (s, 9H); LC-MS m/z 392 $[M+H]^+$.

Isopropyl (2*R*)-2-(5-bromo-2-fluorophenyl)-2-[[(*S*)-*tert*-butylsulfinyl]amino]-2-cyclopropyl-acetate (2*R*-39). A solution of cyclopropylmagnesium bromide (174 mL, 0.5 M, 87 mmol) was added dropwise over 45 min to a stirred solution of 24.4 g (62 mmol) iminoester *S*-**38** in DCM (388 mL) at -78ºC. The reaction mixture was stirred at -78ºC for 30 min. Sat. aq. NH_4Cl was added and the reaction mixture was warmed to rt. The mixture was extracted with DCM and washed with water. The organic layer was separated and dried with MgSO4, filtered and concentrated *in vacuo* to give intermediate 2*R*-**39** (26.4 g 97% yield). ^{1}H NMR (400 MHz, $CDCl_3$) δ 8.01 (dd, *J*=2.5, 6.5 Hz, 1H), 7.48 (ddd, *J*=2.3, 4.5, 8.7 Hz, 1H), 6.94 (dd, *J*=8.7, 10.3 Hz, 1H), 5.13 (spt, *J*=6.3 Hz, 1H), 4.97 (br s, 1H), 1.48 (tt, *J*=5.3, 8.2 Hz, 1H), 1.22 (d, *J*=6.2 Hz,

3H), 1.20 (s, 9H), 1.18 (d, *J*=6.0 Hz, 3H), 0.78-0.88 (m, 1H), 0.60-0.70 (m, 1H), 0.38-0.54 (m, 2H); LC-MS m/z 434 $[M+H]^+$.

(2*R*)-2-Amino-2-(5-bromo-2-fluorophenyl)-2-cyclopropyl-acetic acid hydrochloride (2*R*-40). Intermediate 2*R*-**39** (21 g, 48 mmol) was dissolved in MeOH (96 mL) and then 1 N NaOH (96 mL, 96 mmol) was added. The reaction mixture was refluxed for 4 h and then it was allowed to reach rt. The mixture was partitioned between water and EtOAc. The aqueous layer was separated, acidified with 1 N HCl and extracted with DCM. The combined organic extracts were dried over MgSO4, filtered and the solvent was evaporated *in vacuo* to yield the corresponding carboxylic acid as a white solid (15.5 g, 82% yield). This material was dissolved in dioxane (100 mL) and then HCl (4 N in dioxane, 29.6 mL, 118 mmol) was added dropwise. The resulting solution was stirred at rt for 1 h and the solvent was removed *in vacuo*. The residue was suspended in DIPE, filtered and dried *in vacuo* to give amino acid 2*R*-**40** (HCl salt) as a white solid (10 g, 88% yield). ^{1}H NMR (360 MHz, DMSO-d_6) δ 14.33 (br s, 1H), 8.86 (br s, 3H), 7.98 (dd, *J*=2.4, 6.8 Hz, 1H), 7.74 (ddd, *J*=2.6, 4.4, 8.8 Hz, 1H), 7.35 (dd, *J*=9.0, 10.8 Hz, 1H), 1.70-1.82 (m, 1H), 0.56-0.92 (m, 4H);); LC-MS m/z 286 $[M-H]^-$; $[a]^{20}_D$ = -65.4 (*c* = 0.63 in MeOH).

(3*R*)-3-(5-Bromo-2-fluorophenyl)-3-cyclopropyl-morpholine-2,5-dione (3*R*-41). Amino acid 2*R*-**40** (40 g, 123 mmol) was dissolved in THF (370 mL) and then 1 N NaOH (256 mL, 256 mmol) was added. The reaction mixture was cooled down to 0 ºC and then a solution of 2-chloroacetyl chloride (24.5 mL, 308 mmol) in THF (50 mL) was added dropwise over 1 h at 15 °C while aq. NaOH was simultaneously added (to maintain the pH around 10-11). After the addition was finished, 12 N HCl was added carefully to the mixture until pH 2. The reaction mixture was concentrated *in vacuo* and the resulting precipitate was washed with DIPE and dried *in vacuo*. The resulting solid was dissolved in DMF (1 L) and then $NaHCO_3$ (19.8 g, 236 mmol)

was added. The reaction mixture was stirred at 80 °C for 6 h. The reaction mixture was partially concentrated in a rotary evaporator and filtered through a pad of celite to remove the salts. The solvent was removed *in vacuo* to give morpholine dione 3*R*-**41** as a colourless oil (39 g, 99% yield). ^{1}H NMR (360 MHz, DMSO-d_6) δ 8.74 (br s, 1H), 7.92 (dd, *J*=2.6, 6.9 Hz, 1H), 7.70 (ddd, *J*=2.6, 4.8, 8.8 Hz, 1H), 7.32 (dd, *J*=8.8, 11.0 Hz, 1H), 5.12 (d, *J*=16.8 Hz, 1H), 4.84 (d, *J*=16.8 Hz, 1H), 1.62-1.72 (m, 1H), 0.84-0.97 (m, 1H), 0.58-0.73 (m, 2H), 0.41-0.52 (m, 1H); LC-MS m/z 328 $[M+H]^+$; $[a]^{20}_D$ = +107.5 (*c* = 0.62 in DMF).

(5*R*)-5-(5-Bromo-2-fluorophenyl)-5-cyclopropyl-6-fluoro-morpholin-3-one (5*R*-42). Starting from 3*R*-**41** (7.2 g, 21.94 mmol) and following the same procedure as for 5*R*-**23** the corresponding hemiacetal was obtained as 3:2 mixture of diastereoisomers, and further converted to 5*R*-**42** in 92% yield (6.0 g, 3:2 mixture of 6*S*/6*R* isomers). *Hemiacetal:* ^{1}H NMR (600 MHz, DMSO-d_6) δ 8.22 (s, 0.4H), 8.10 (s, 0.6H), 7.61 (dd, *J*=2.6, 7.0 Hz, 0.6H), 7.53-7.58 (m, 1H), 7.50 (ddd, *J*=2.5, 4.1, 8.7 Hz, 0.4H), 7.12-7.22 (m, 1H), 6.90 (d, *J*=4.7 Hz, 0.4H), 5.44 (dd, *J*=1.2, 4.5 Hz, 0.4H), 5.38 (d, *J*=5.0 Hz, 0.6H), 4.09 (d, *J*=16.4 Hz, 0.4H), 4.07 (d, *J*=16.6 Hz, 0.6H), 3.98 (d, *J*=16.6 Hz, 0.6H), 3.96 (d, *J*=16.4 Hz, 0.4H), 1.52-1.65 (m, 1H), 0.43-0.59 (m, 1H), 0.14-0.43 (m, 3H) (1H exchanged); LC-MS m/z 330 $[M+H]^+$. 5*R*-**42**: ^{1}H NMR (400 MHz, $CDCl_3$) δ 7.94 (br s, 0.4H), 7.51 (dd, *J*=2.5, 7.0 Hz, 0.4H), 7.39-7.48 (m, 1.6H), 7.20 (br s, 0.6H), 6.94-7.04 (m, 1H), 6.30 (dd, *J*=1.5, 51.0 Hz, 0.6H), 6.15 (d, *J*=49.9 Hz, 0.4H), 4.42 (d, *J*=16.7 Hz, 0.4H), 4.33 (d, *J*=17.2 Hz, 0.6H), 4.28 (d, *J*=16.7 Hz, 0.4H), 4.14 (d, *J*=17.2 Hz, 0.6H), 1.58-1.68 (m, 1H), 0.22-0.74 (m, 4H);); LC-MS m/z 332 $[M+H]^+$. This material was used as a diasteromeric mixture in the following step.

(5*R*)-5-(5-Bromo-2-fluorophenyl)-5-cyclopropyl-6-fluoromorpholine-3-thione (5*R*-43). Starting from 5*R*-**42** (3.0 g, 9 mmol) and following the same procedure as for 5*R*-**28** the

corresponding thioamide 5*R*-**43** was obtained (2.8 g, 89% yield) as a mixture of diastereoisomers, which was used as such for the next reaction step.

(5*R*,6*R*)-5-(5-Bromo-2-fluorophenyl)-5-cyclopropyl-6-fluoro-2,6-dihydro-1,4-oxazin-3-amine ((5*R*,6*R*)-44). Starting from 5*R*-**43** (2.8 g) and following the same procedure as for (5*R*,6*R*)-**31** the corresponding both diastereomers (5*R*,6*R*)-**44** (0.98 g, 37% yield) and (5*R*,6*S*)-**44** (1.16 g, 44% yield) were obtained. (5*R*,6*R*)-**44**: ^{1}H NMR (360 MHz, $CDCl_3$) δ 7.29-7.39 (m, 2H), 6.94 (dd, *J*=8.8, 11.7 Hz, 1H), 6.14 (d, *J*=52.0 Hz, 1H), 4.37 (br s, 2H), 4.20 (d, *J*=15.4 Hz, 1H), 3.95 (d, *J*=15.4 Hz, 1H), 1.59 (dq, *J*=4.9, 8.6 Hz, 1H), 0.39-0.59 (m, 2H), 0.29-0.38 (m, 1H), 0.14-0.24 (m, 1H); LC-MS m/z 331 $[M+H]^+$. (5*R*,6*S*)-**44**: ^{1}H NMR (360 MHz, $CDCl_3$) δ 7.94 (dd, *J*=2.6, 6.95 Hz, 1H), 7.35 (ddd, *J*=2.9, 4.2, 8.6 Hz, 1H), 6.93 (dd, *J*=8.6, 11.5 Hz, 1H), 6.18 (dd, *J*=2.2, 51.2 Hz, 1H), 4.29 (br s, 2H), 4.23 (d, *J*=15.4 Hz, 1H), 4.09 (d, *J*=15.4 Hz, 1H), 1.45 (dtt, *J*=2.6, 5.4, 8.1 Hz, 1H), 0.37-0.50 (m, 1H), 0.13-0.33 (m, 3H);); LC-MS m/z 331 $[M+H]^+$.

(5*R*,6*R*)-5-(5-Amino-2-fluorophenyl)-5-cyclopropyl-6-fluoro-2,6-dihydro-1,4-oxazin-3-amine ((5*R*,6*R*)-45). Starting from (5*R*,6*R*)-**44** (1.7 g, 5.1 mmol) and following the same procedure as for (5*R*,6*R*)-**34** the corresponding (5*R*,6*R*)-**45** was obtained (0.81 g, 59% yield). ^{1}H NMR (400 MHz, $CDCl_3$) δ 6.83 (dd, *J*=9.0, 11.8 Hz, 1H), 6.48-6.56 (m, 2H), 6.18 (d, *J*=52.7 Hz, 1H), 4.17 (dd, *J*=1.1, 15.4 Hz, 1H), 3.92 (d, *J*=15.3 Hz, 1H), 3.53 (br s, 2H), 1.60 (dq, *J*=5.0, 8.4 Hz, 1H), 0.39-0.54 (m, 2H), 0.31-0.39 (m, 1H), 0.16-0.25 (m, 1H) (2H exchanged); LC-MS m/z 268 $[M+H]^+$.

***rac*-2-Amino-2-(4-bromopyridin-2-yl)propanenitrile (*rac*-47a).** Starting from 1-(4-bromo-2-pyridinyl)-ethanone **46a** (18 g, 90 mmol) and following the same procedure as for **14a** the corresponding aminonitrile *rac*-**47a** was obtained as a white solid (11 g, 54% yield).

***rac*-2-Amino-2-(2-chloropyridin-4-yl)propanenitrile** (*rac*-**47b**). Starting from 4-acetyl-2-chloropyridine **46b** (18 g, 90 mmol) and following the same procedure as for **14a** the corresponding aminonitrile *rac*-**47b** was obtained (11.4 g, 98% yield) as a yellow solid. LC-MS m/z 182 $[M+H]^+$.

***rac*-2-(4-Bromopyridin-2-yl)alaninamide (*rac*-48a).** Nitrile *rac*-**47a** (23 g, 101.7 mmol) was dissolved in a solution of 48% HBr in acetic acid (200 mL) and the mixture was refluxed for 12 h. After cooling to rt, EtOAc (40 mL) was added and the precipitate was filtered off and washed with EtOAc (100 mL), then dried to give *rac*-**48a** as an off-white solid (25 g, 61% yield).

***rac*-2-Amino-2-(2-chloro-4-pyridyl)propanamide (*rac*-48b).** Intermediate *rac*-**47b** (6 g, 33.04 mmol) was dissolved in HCl (1 M in AcOH, 165 mL) and HBr (33% in AcOH, 25 mL) and the mixture was stirred at 75 °C for 3 h. After cooling to rt, EtOAc (250 mL) was added and the precipitate was filtered off, washed with EtOAc (100 mL) and dried *in vacuo* to give *rac*-**48b** (9.7 g, 81% yield). LC-MS m/z 198 $[M-H]^-$.

***rac*-2-(4-Bromopyridin-2-yl)alanine (*rac*-49a).** 1 N NaOH (412 mL, 412 mmol) was added to a solution of *rac*-**48a** (33.4 g, 82.4 mmol) in THF (1 L) at rt. The resulting mixture was stirred at 65 ºC for 16 h. Then, the reaction mixture was half concentrated, then cooled with an ice bath and brought to pH 7 with 1 N HCl while stirring. A white precipitate formed, which was filtered, washed with diethyl ether, and dried *in vacuo* to provide *rac*-**49a** (13.2 g, 65% yield). ^{1}H NMR (360 MHz, DMSO-d_6) δ 8.39 (d, *J*=5.5 Hz, 1H), 7.91 (d, *J*=1.5 Hz, 1H), 7.81 (br s, 3H), 7.60 (dd, *J*=1.8, 5.1 Hz, 1H), 1.64 (s, 3H). LC-MS m/z 245 $[M+H]^+$.

***rac*-2-Amino-2-(2-chloropyridin-4-yl)propanoic acid (*rac*-49b).** Intermediate *rac*-**48b** (9.7 g, 26.84 mmol) was dissolved in NaOH (1 M in water, 134 mL) and the mixture was stirred at rt for 60 h. The reaction mixture was concentrated to half volume *in vacuo* and then cooled on an

ice bath. The pH of the solution was adjusted to pH = 7 by addition of HCl (1 N in water) and a white solid precipitated. The precipitate was filtered off, washed with Et_2O and dried *in vacuo* to give intermediate *rac*-**49b** (5.48 g, quant. yield) as a white solid. ^{1}H NMR (360 MHz, DMSO-d_6) δ 8.38 (d, *J*=5.1 Hz, 1H), 7.92 (br s, 3H), 7.59 (d, *J*=1.5 Hz, 1H), 7.50 (dd, *J*=1.5, 5.5 Hz, 1H), 1.63 (s, 3H); LC-MS m/z 199 $[M-H]^-$.

***rac*-{[2-Amino-2-(4-bromopyridin-2-yl)propanoyl]oxy}acetic acid trifluoroacetate salt (*rac*-51a).** Amino acid *rac*-**49a** (16.0 g, 65.3 mmol) and Cs_2CO_3 (63.8 g, 195.9 mmol) in dry DMF (500 mL) were stirred for 30 min. Then *tert*-butyl chloroacetate (9.33 mL, 65.3 mmol) was added, and the resulting mixture was stirred at rt for 3 h. Then, ice and DCM were added and the organic layer was separated. The aqueous layer was extracted with DCM. The combined organic layers were dried ($MgSO_4$), filtered and evaporated to dryness providing *rac*-**50a** as an orange oil (note: a high vacuum of 1-3 mbar is needed to remove a low volatile impurity). Ester *rac*-**50a** was dissolved in TFA (234 mL) and stirred at rt for 30 min. Then, the solvent was thoroughly evaporated providing a brown oil, which was treated with diethyl ether and stirred for about 10 min to get white solid which was filtered, washed with diethyl ether and dried *in vacuo* at 50 °C to give the TFA salt of *rac*-**51a** (8.95 g, 29 % yield over two steps). ^{1}H NMR (360 MHz, DMSO-d_6) δ 9.12 (br s, 4H), 8.56 (d, *J*=5.1 Hz, 1H), 8.10 (d, *J*=1.5 Hz, 1H), 7.84 (dd, *J*=1.6, 5.3 Hz, 1H), 4.65-4.87 (m, 2H), 1.95 (s, 3H). LC-MS m/z 303 $[M+H]^+$.

***rac*-{[2-Amino-2-(2-chloropyridin-4-yl)propanoyl]oxy}acetic acid trifluoroacetate salt (*rac*-51b).** Starting from *rac*-**49b** (5.29 g, 26.36 mmol) and following the same procedure as for *rac*-**51a** the corresponding acid *rac*-**51b** was obtained as a trifluoroacetate salt (6.12 g, 96%). ^{1}H NMR (360 MHz, DMSO-d_6) δ 9.50 (br s, 4H), 8.58 (d, *J*=5.4 Hz, 1H), 7.79 (d, *J*=1.5 Hz, 1H), 7.65 (dd, *J*=1.5, 5.4 Hz, 1H), 4.73-4.85 (m, 2H), 1.94 (s, 3H); LC-MS m/z 257 $[M-H]^-$.

***rac*-3-(4-Bromopyridin-2-yl)-3-methylmorpholine-2,5-dione (*rac*-52a).** Amino acid (TFA salt) *rac*-**51a** (12.3 g, 29.5 mmol) was suspended in DCM (764 mL) and 2-chloro-1-methylpyridinium iodide (8.3 g, 32.5 mmol) was added, followed by DIPEA (25.3 mL, 88.6 mmol). The reaction mixture was subsequently refluxed for 4 h. Then, the reaction mixture was concentrated *in vacuo* and purified by column chromatography (silica: Heptane/EtOAc 100/0 to 20/80). Evaporation of the product fractions provided 4.6 g *rac*-**52a** containing about 30% of impurity bearing a chloro instead of bromo on the pyridine 4-position (55% yield).^{1}H NMR (360 MHz, DMSO-d_6) δ 9.18 (br s, 1H), 8.44 (d, *J*=5.1 Hz, 1H), 7.79 (d, *J*=1.5 Hz, 1H), 7.73 (dd, *J*=1.6, 5.3 Hz, 1H), 4.62 (s, 2H), 1.74 (s, 3H); LC-MS m/z 285 $[M+H]^+$.

***rac*-3-(2-Chloropyridin-4-yl)-3-methylmorpholine-2,5-dione (*rac*-52b).** Starting from *rac*-**51b** (5.29 g, 26.36 mmol) and following the same procedure as for *rac*-**52a** the corresponding acid *rac*-**52b** was obtained as white crystals (1.10 g, 19%). ^{1}H NMR (360 MHz, DMSO-d_6) δ 9.43 (br s, 1H), 8.51 (d, *J*=5.4 Hz, 1H), 7.41-7.43 (m, 1H), 7.39 (dd, *J*=1.6, 5.4 Hz, 1H), 4.69 (s, 2H), 1.71 (s, 3H); LC-MS m/z 241 $[M+H]^+$; m. p. = 213.5 ºC.

***rac*-(5*R**,6*R**)-5-(4-Bromo-2-pyridyl)-6-fluoro-5-methyl-morpholin-3-one (*rac*-(5*R**,6*R**)-53a).** Starting from *rac*-**52a** (4.3 g, 5.2 mmol) and following the same procedure as for 5*R*-**23** the corresponding *rac*-(5*R**,6*R**)-**53a** was obtained as a single diastereomer (3.55 g, 81%). ^{1}H NMR (400 MHz, $CDCl_3$) δ 8.42 (dd, *J*=0.5, 5.3 Hz, 1H), 7.67 (dd, *J*=0.5, 1.8 Hz, 1H), 7.42 (dd, *J*=1.8, 5.0 Hz, 1H), 7.32 (br s, 1H), 6.06 (d, *J*=51.7 Hz, 1H), 4.38 (d, *J*=17.2 Hz, 1H), 4.19 (d, *J*=17.2 Hz, 1H), 1.68 (d, *J*=1.8 Hz, 3H); LC-MS m/z 289 $[M+H]^+$; m. p. = 193.1 ºC.

***r*ac-(5*R**,6*R**)-5-(2-Chloro-4-pyridyl)-6-fluoro-5-methyl-morpholin-3-one**

(*rac*-(5*R,6*R**)-53b).** Starting from *rac*-**52b** (1.42 g, 5.90 mmol) and following the same procedure as for 5*R*-**23** the corresponding *rac*-(5*R**,6*R**)-**53b** was obtained as a transparent oil (985 mg, 69%, 65:35 mixture of diastereoisomers). ^{1}H NMR (360 MHz, $CDCl_3$) δ 8.46 (d, *J*=5.5 Hz, 0.35H), 8.46 (d, *J*=5.5 Hz, 0.65H), 7.64 (br s, 0.65H), 7.60 (br s, 0.35H), 7.39-7.44 (m, 0.35H), 7.32-7.36 (m, 0.65H), 7.28-7.32 (m, 0.35H), 7.22 (dd, *J*=1.3, 5.3 Hz, 0.65H), 5.65 (d, *J*=50.1 Hz, 0.65H), 5.51 (d, *J*=49.0 Hz, 0.35H), 4.45 (d, *J*=16.7 Hz, 0.35H), 4.37 (d, *J*=16.8 Hz, 0.65H), 4.34 (d, *J*=16.7 Hz, 0.35H), 4.22 (d, *J*=16.8 Hz, 0.65H), 1.78 (d, *J*=1.5 Hz, 1.05H), 1.70 (d, *J*=1.5 Hz, 1.95H); LC-MS m/z 245 $[M+H]^+$.

***rac*-(5*R**,6*R**)-5-(4-Bromopyridin-2-yl)-6-fluoro-5-methylmorpholine-3-thione (*rac*-(5*R**,6*R**)-54a).** Starting from *rac*-(5*R**,6*R**)-**53a** (3.50 g, 12.11 mmol) and following the same procedure as for 5*R*-**28** the corresponding *rac*-(5*R**,6*R**)-**54a** was obtained as white crystals (2.00 g, 54%). ^{1}H NMR (360 MHz, $CDCl_3$) δ 8.43 (br d, *J*=5.1 Hz, 2H), 7.51 (d, *J*=1.8 Hz, 1H), 7.45 (dd, *J*=1.8, 5.1 Hz, 1H), 6.04 (dd, *J*=1.5, 51.6 Hz, 1H), 4.74 (d, *J*=18.7 Hz, 1H), 4.62 (d, *J*=18.7 Hz, 1H), 1.73 (d, *J*=1.8 Hz, 3H); LC-MS m/z 305 $[M+H]^+$.

***rac*-(5*R**,6*R**)-5-(2-Chloropyridin-4-yl)-6-fluoro-5-methylmorpholine-3-thione (*rac*-54b).** Starting from *rac*-(5*R**,6*R**)-**53b** (0.769 g, 1.53 mmol) and following the same procedure as for 5*R*-**28** the corresponding *rac*-(5*R**,6*R**)-**54b** was obtained as a transparent oil (445 mg, 54%, 60:40 mixture of diastereoisomers). LC-MS m/z 259 $[M-H]^-$.

***rac*-(5*R**,6*R**)-5-(4-Bromopyridin-2-yl)-6-fluoro-5-methyl-5,6-dihydro-2*H*-1,4-oxazin-3-amine (*rac*-(5*R**,6*R**)-55a).** Starting from *rac*-(5*R**,6*R**)-**54a** (2.00 g, 6.55 mmol) and following the same procedure as for 5*R*-**31** the corresponding *rac*-(5*R**,6*R**)-**55a** was obtained as white crystals (1.61 g, 85%). ^{1}H NMR (360 MHz, DMSO-d_6) δ 8.45 (d, *J*=5.1 Hz, 1H), 7.53-

7.60 (m, 2H), 6.22 (br s, 2H), 5.97 (d, *J*=53.8 Hz, 1H), 4.03 (q, *J*=16.0 Hz, 2H), 1.39 (d, *J*=1.8 Hz, 3H); LC-MS m/z 288 $[M+H]^+$; m. p. = 125.1 ºC.

***rac*-(5*R**,6*R**)-5-(2-Chloropyridin-4-yl)-6-fluoro-5-methylmorpholine-3-amine (*rac*-55b).** Starting from *rac*-(5*R**,6*R**)-**54b** (0.445 g, 1.53 mmol) and following the same procedure as for 5*R*-**31** the corresponding amidine *rac*-(5*R**,6*R**)-**55b** was obtained as a white solid (300 mg, 72%). ^{1}H NMR (400 MHz, DMSO-d_6) δ 8.36 (d, *J*=5.3 Hz, 1H), 7.45 (d, *J*=1.5 Hz, 1H), 7.42 (dd, *J*=1.5, 5.3 Hz, 1H), 6.06 (br s, 2H), 5.88 (d, *J*=52.2 Hz, 1H), 4.06 (d, *J*=16.0 Hz, 1H), 3.97 (d, *J*=16.0 Hz, 1H), 1.40 (d, *J*=1.8 Hz, 3H); LC-MS m/z 245 $[M+H]^+$; m. p. = 174.1 ºC. **Note:** the other diastereoisomer was discarded without NMR analysis.

***rac*-(5*R**,6*R**)-5-(4-Aminopyridin-2-yl)-6-fluoro-5-methyl-5,6-dihydro-2*H*-1,4-oxazin-3-amine (*rac*-(5*R**,6*R**)-56a).** Starting from *rac*-(5*R**,6*R**)-**55a** (1.10 g, 3.82 mmol) and following the same procedure as for 5*R*-**34** the corresponding *rac*-(5*R**,6*R**)-**56a** was obtained as white crystals (0.54 g, 64% yield). LC-MS m/z 225 $[M+H]^+$.

***rac*-(5*R**,6*R**)-5-(2-Aminopyridin-4-yl)-6-fluoro-5-methyl-5,6-dihydro-2*H*-1,4-oxazin-3-amine (*rac*-(5*R**,6*R**)-56b).** Starting from *rac*-(5*R**,6*R**)-**55b** (0.300 g, 1.23 mmol) and following the same procedure as for 5*R*-**34** the corresponding aniline *rac*-(5*R**,6*R**)-**56b** was obtained as a transparent oil (200 mg, 72%). LC-MS m/z 225 $[M+H]^+$.

AUTHOR INFORMATION

Corresponding Authors

*e-mail: frombout@its.jnj.com, phone: +3214608216; atrabanc@its.jnj.com, phone: +34925245750

Author Contributions

The manuscript was written through contributions of all authors. All authors have given approval to the final version of the manuscript.

ACKNOWLEDGMENT

The authors thank the analytical departments in Beerse and Toledo for helping with compound characterization and purification. They thank Michel Carpentier for performing the chemical stability experiments on (2*R*,3*R*)-**7a**. They also thank Geert Pille and Sigrid Stockbroekx for the physicochemical measurements. Finally they thank Proteros GMBH for BACE1 crystal growth, soaking and structure determination of 3*R*-**6a**.

ABBREVIATIONS

$AUC_{0\text{-last}}$, area under the curve until last time point sampled; Aβ, amyloid beta; BACE1, beta-site amyloid precursor protein cleaving enzyme 1; BINAP, 2,2'-bis(diphenylphosphino)-1,1'-binaphthyl; C_{max}, maximum plasma concentration; CSF, cerebrospinal fluid; DAST, diethylaminosulfur trifluoride; dLM, dog liver microsomes; DMEDA, N,N′-dimethylethylenediamine; DMTMM, 4-(4,6-dimethoxy-1,3,5-triazin-2-yl)-4-methylmorpholinium chloride; f_u, free (unbound) fraction; HATU, (1-[bis(dimethylamino)methylene]-1*H*-1,2,3-triazolo[4,5-*b*]pyridinium 3-oxid hexafluorophosphate); hLM, human liver microsomes; HPβCD, (2-Hydroxypropyl)-beta-cyclodextrin [128446-35-5]; K_p, brain-to-plasma ratio; n. d., not determined; mLM, mouse liver microsomes; P_{app}, apparent permeability; p. o., per os (= oral); rLM, rat liver microsomes; SBEβCD, sulfobutylether β-cyclodextrin sodium salt [182410-00-0]; s. c., subcutaneous; $T_{½}$, half-life; TBAT, tetrabutylammonium difluorotriphenylsilicate; T_{max}, time at which maximum plasma concentration is reached; WT, wild type.

ASSOCIATED CONTENT

Supporting Information. Crystal structure experimental data. Selection set for pK_a calculations. Correlation of calculated and experimental pK_a. QM calculations on conformation of diastereomers of **7a**. Chemical stability assessment of (2*R*,3*R*)-**7a**.

REFERENCES

(1) Hebert, L. E.; Weuve, J.; Scherr, P. A.; Evans, D. A. Alzheimer disease in the United States (2010-2050) estimated using the 2010 census. *Neurology* **2013**, *80*, 1778-1783.

(2) *Dementia*; Fact Sheet 362, 2015. World Health Organization Web site. http://www.who.int/mediacentre/factsheets/fs362/en/ (accessed August 10, 2015).

(3) Braak, H.; Braak, E. Neuropathological stageing of Alzheimer-related changes. *Acta Neuropathol.* **1991**, *82*, 239-259.

(4) Karran, E.; Mercken, M.; De Strooper, B. The amyloid cascade hypothesis for Alzheimer's disease: an appraisal for the development of therapeutics. *Nat. Rev. Drug Discovery* **2011**, *10*, 698-712.

(5) Thinakaran, G.; Koo, E. H. Amyloid precursor protein trafficking, processing, and function. *J. Biol. Chem.* **2008**, *283*, 29615-29619.

(6) Mawuenyega, K. G.; Sigurdson W.; Ovod V.; Munsell, L.; Kasten, T.; Morris, J. C.; Yarasheski K. E.; Bateman, R. J. Decreased clearance of CNS beta-amyloid in Alzheimer's disease. *Science* **2010**, *330*, 1774.

(7) Greenwald, J.; Riek, R. Biology of amyloid: structure, function, and regulation. *Structure* **2010**, *18*, 1244-1260.

(8) De Strooper, B.; Vassar, R.; Golde, T. The secretases: enzymes with therapeutic potential in Alzheimer disease. *Nat. Rev. Neurol.* **2010**, *6*, 99-107.

(9) Vassar, R.; Bennett, B. D.; Babu-Khan, S.; Kahn, S.; Mendiaz, E. A.; Denis, P.; Teplow, D. B.; Ross, S.; Amarante, P.; Loeloff, R.; Luo, Y.; Fisher, S.; Fuller, J.; Edenson, S.; Lile, J.; Jarosinski, M. A.; Biere, A. L.; Curran, E.; Burgess, T.; Louis, J. C.; Collins, F.; Treanor, J.; Rogers, G.; Citron, M. Beta-secretase cleavage of Alzheimer's amyloid precursor protein by the transmembrane aspartic protease BACE. *Science* **1999**, *286*, 735-741.

(10) Ghosh, A. K.; Osswald, H. L. BACE1 (beta-secretase) inhibitors for the treatment of Alzheimer's disease. *Chem. Soc. Rev.* **2014**, *43*, 6765-6813.

(11) Butini, S.; Brogi, S.; Novellino, E.; Campiani, G.; Ghosh, A. K.; Brindisi, M.; Gemma, S. The structural evolution of beta-secretase inhibitors: a focus on the development of small-molecule inhibitors. *Curr. Top. Med. Chem.* **2013**, *13*, 1787-1807.

(12) Edwards, P. D.; Albert, J. S.; Sylvester, M.; Aharony, D.; Andisik, D.; Callaghan, O.; Campbell, J. B.; Carr, R. A.; Chessari, G.; Congreve, M.; Frederickson, M.; Folmer, R. H.; Geschwindner, S.; Koether, G.; Kolmodin, K.; Krumrine, J.; Mauger, R. C.; Murray, C. W.; Olsson, L. L.; Patel, S.; Spear, N.; Tian, G. Application of fragment-based lead generation to the discovery of novel, cyclic amidine beta-secretase inhibitors with nanomolar potency, cellular activity, and high ligand efficiency. *J. Med. Chem.* **2007**, *50*, 5912-5925.

(13) Baxter, E. W.; Conway, K. A.; Kennis, L.; Bischoff, F.; Mercken, M. H.; De Winter, H. L.; Reynolds, C. H.; Tounge, B. A.; Luo, C.; Scott, M. K.; Huang, Y.; Braeken, M.; Pieters, S. M. A.; Berthelot, D. J. C.; Masure, S.; Bruinzeel, W. D.; Jordan, A. D.; Parker, M. H.; Boyd, R. E.; Qu, J.; Alexander, R. S.; Brenneman, D. E.; Reitz, A. B. 2-amino-3,4-dihydroquinazolines as

inhibitors of BACE-1 (beta-site APP cleaving enzyme): Use of structure based design to convert a micromolar hit into a nanomolar lead. *J. Med. Chem.* **2007**, *50*, 4261-4264.

(14) Rankovic, Z. CNS drug design: balancing physicochemical properties for optimal brain exposure. *J. Med. Chem.* **2015**, *58*, 2584-2608.

(15) Oehlrich, D.; Prokopcova, H.; Gijsen, H. J. The evolution of amidine-based brain penetrant BACE1 inhibitors. *Bioorg. Med. Chem. Lett.* **2014**, *24*, 2033-2045.

(16) Cumming, J. N.; Scott, J. D.; Li, Sarah W.; Cartwright, M.; Chen, X.; Cox, K.; Forman, M.; Gilbert, E. J.; Hodgson, R.; Hyde, L.; Jin, Y.; Kazakevich, I.;Kuvelkar, R.; Liang, X.; Mei, H.; Misiaszek, J.; Orth, P.; Stone, J.; Strickland, C.; Voigt, J. H.; Wang, H.; Werner, B.; Wong, J.; Parker, E. M.; Greenlee, W, J.; Kennedy, M. E.; Stamford, A. W. Discovery of MK-8931: A BACE inhibitor in Phase 3 clinical development for Alzheimer's disease From Abstracts of Papers, 249th ACS National Meeting & Exposition, Denver, CO, United States, March 22-26, 2015 (2015), MEDI-246.

(17) Hilpert, H.; Guba, W.; Woltering, T. J.; Wostl, W.; Pinard, E.; Mauser, H.; Mayweg, A. V.; Rogers-Evans, M.; Humm, R.; Krummenacher, D.; Muser, T.; Schnider, C.; Jacobsen, H.; Ozmen, L.; Bergadano, A.; Banner, D. W.; Hochstrasser, R.; Kuglstatter, A.; David-Pierson, P.; Fischer, H.; Polara, A.; Narquizian, R. β-Secretase (BACE1) inhibitors with high in vivo efficacy suitable for clinical evaluation in Alzheimer's disease. *J. Med. Chem.* **2013**, *56*, 3980-3995.

(18) May, P. C.; Willis, B. A.; Lowe, S. L.; Dean, R. A.; Monk, S. A.; Cocke, P. J.; Audia, J. E.; Boggs, L. N.; Borders, A. R.; Brier, R. A.; Calligaro, D. O.; Day, T. A.; Ereshefsky, L.; Erickso, J. A.; Gevorkyan, H.; Gonzales, C. R.; James, D. E.; Jhee, S. S.; Komjathy, S. F.; Li, L.; Lindstrom, T. D.; Mathe, B. M.; Martenyi, F.; Sheehan, S. M.; Stout, S. L.; Timm, D. E.;

Vaught, G. M.; Watson, B. M.; Winneroski, L. L.; Yang, Z.; Mergott, D. J. The potent BACE1 inhibitor LY2886721 elicits robust central Aβ pharmacodynamic responses in mice, dogs, and humans. *J. Neurosci.* **2015**, *35*, 1199-1210.

(19) Woltering, T. J.; Wostl, W.; Hilpert, H.; Rogers-Evans, M.; Pinard, E.; Mayweg, A.; Gobel, M.; Banner, D. W.; Benz, J.; Travagli, M.; Pollastrini, M.; Marconi, G.; Gabellieri, E.; Guba, W.; Mauser, H.; Andreini, M.; Jacobsen, H.; Power, E.; Narquizian, R. BACE1 inhibitors: a head group scan on a series of amides. *Bioorg. Med. Chem. Lett.* **2013,** *23*, 4239-4243.

(20) Ginman, T.; Viklund, J.; Malmstrom, J.; Blid, J.; Emond, R.; Forsblom, R.; Johansson, A.; Kers, A.; Lake, F.; Sehgelmeble, F.; Sterky, K. J.; Bergh, M.; Lindgren, A.; Johansson, P.; Jeppsson, F.; Falting, J.; Gravenfors, Y.; Rahm, F. Core refinement toward permeable beta-secretase (BACE-1) inhibitors with low hERG activity. *J. Med. Chem.* **2013**, *56*, 4181-4205.

(21) Tresadern, G.; Delgado, F.; Delgado, O.; Gijsen, H.; Macdonald, G. J.; Moechars, D.; Rombouts, F.; Alexander, R.; Spurlino, J.; Van Gool, M.; Vega, J. A.; Trabanco, A. A. Rational design and synthesis of aminopiperazinones as beta-secretase (BACE) inhibitors. *Bioorg. Med. Chem. Lett.* **2011**, *21*, 7255-7260.

(22) Delgado, O.; Monteagudo, A.; Van Gool, M.; Trabanco, A. A.; Fustero, S. A practical entry to beta-aryl-beta-alkyl amino alcohols: application to the synthesis of a potent BACE1 inhibitor. *Org. Biomol. Chem.* **2012**, *10*, 6758-6766.

(23) Cosner, C. C.; Markiewicz, J. T.; Bourbon, P.; Mariani, C. J.; Wiest, O.; Rujoi, M.; Rosenbaum, A. I.; Huang, A. Y.; Maxfield, F. R.; Helquist, P. Investigation of N-aryl-3-alkylidenepyrrolinones as potential Niemann-Pick type C disease therapeutics. *J. Med. Chem.* **2009**, *52*, 6494-6498.

(24) Viklund, J.; Kolmodin, K.; Nordvall, G.; Swahn, B. M.; Svensson, M.; Gravenfors, Y.; Rahm, F. Creation of novel cores for β-Secretase (BACE-1) inhibitors: a multiparameter lead generation strategy. *ACS Med. Chem. Lett.* **2014**, *5*, 440-445.

(25) Values calculated with ACD Labs software v10. pKa. Advanced chemistry development Inc. 110 Yonge Street, 14th Floor, Toronto, Ontario, Canada, M5C 1T4. http://www.acdlabs.com/home/ (accessed August 10, 2015).

(26) Wager, T. T.; Chandrasekaran, R. Y.; Hou, X.; Troutman, M. D.; Verhoest, P. R.; Villalobos, A.; Will, Y. Defining desirable central nervous system drug space through the alignment of molecular properties, in vitro ADME, and safety attributes. *ACS Chem. Neurosci.* **2010**, *1*, 420-434.

(27) Groups at Novartis and Roche have recently patented morpholines with different substitution patterns: (a) Badiger, S.; Chebrolu, M.; Frederiksen, M.; Holzer, P.; Hurth, K.; Lueoend, R. M.; Machauer, R.; Moebitz, H.; Neumann, U.; Ramos, R.; Rueeger, H.; Tintelnot-Blomley, M.; Veenstra, S. J.; Voegtle, M. Oxazine derivatives and their use as BACE inhibitors for the treatment of neurological disorders. WO2011009943, 2011; (b) Badiger, S.; Chebrolu, M.; Hurth, K.; Jacquier, S,; Lueoend, R. M.; Machauer, R.; Rueeger, H.; Tintelnot-Blomley, M.; Veenstra, S. J.; Voegtle, M. Novel heterocyclic derivatives and their use in the treatment of neurological disorders. WO2012095469, 2012; (c) Badiger, S.; Chebrolu, M.; Frederiksen, M.; Holzer, P.; Hurth, K.; Li, L.; Liu, H.; Lueoend, R. M.; Machauer, R.; Moebitz, H.; Neumann, U.; Ramos, R.; Rueeger, H.; Schaefer, M.; Tintelnot-Blomley, M.; Veenstra, S. J.; Voegtle, M., Xiong, X. Oxazine derivatives and their use in the treatment of neurological disorders. WO2012006953, 2012. (d) Andreini, M.; Banner, D.; Guba, W.; Hilpert, H.; Mauser, H.; Mayweg, A. V.; Narquizian, R.; Power, E.; Rogers-Evans, M.; Travagli, M.; Valacchi, M.;

Woltering, T.; Wostl, W. 3-Amino-5-phenyl-5,6-dihydro-2H-[1,4]oxazine derivatives, WO2011020806, 2011; (e) Andreini, M.; Gabellieri, E.; Narquizian, R.; Travagli, M.; Wostl, W. 1,4 Oxazines as BACE1 and/or BACE2 inhibitors. WO2012104263, 2012; (f) Andreini, M.; Gabellieri, E.; Guba, W.; Hilpert, H.; Mauser, H.; Mayweg, A. V.; Narquizian, R.; Power, E.; Travagli, M.; Woltering, T.; Wostl, W. 1,4 Oxazines as BACE1 and/or BACE2 inhibitors. WO2012098064, 2012.

(28) Liao, C.; Nicklaus, M. C. Comparison of nine programs predicting pK_a values of pharmaceutical substances. *J. Chem. Inf. Mod.* **2009**, *49*, 2801-2812.

(29) Two tautomeric forms were considered in the calculation with ACD. One with endocyclic double bond, and one with exoxyclic double bond. Performance of ACD on the training set was worse using an endocyclic double bonded NH tautomer (see SI). However the endocyclic form is better for the final morpholine examples but still not as good as ADMET Predictor and introduces uncertainty of choosing the most appropriate tautomer.

(30) Xu, Y; Li, M. J.; Greenblatt, H.; Chen, W.; Paz, A.; Dym, O.; Peleg, Y.; Chen, T.; Shen, X.; He, J.; Jiang, H.; Silman, I.; Sussman, J. L. Flexibility of the flap in the active site of BACE1 as revealed by crystal structures and molecular dynamics simulations. *Acta Cryst.* **2012**, *D68*, 13-25.

(31) Please note the oxazine ring numbering reverses in the final compounds compared to the previous intermediates.

(32) Tvaroska, I.; Carver, J. P. Ab-initio molecular-orbital calculation on carbohydrate model compounds .1. The anomeric effect in fluoro and chloro derivatives of tetrahydropyran. *J. Phys. Chem.* **1994**, *98*, 6452-6458.

(33) Lee, S. S.; Greig, I. R.; Vocadlo, D. J.; McCarter, J. D.; Patrick, B. O.; Withers, S. G. Structural, mechanistic, and computational analysis of the effects of anomeric fluorines on anomeric fluoride departure in 5-fluoroxylosyl fluorides. *J. Am. Chem. Soc.* **2011**, *133*, 15826-15829.

(34) Borghys, H.; Jacobs, T.; Van Broeck, B.; Dillen, L.; Dhuyvetter, D.; Gijsen, H.; Mercken, M. Comparison of two different methods for measurement of amyloid-beta peptides in cerebrospinal fluid after BACE1 inhibition in a dog model. *J. Alzheimer's Dis.* **2014**, *38*, 39-48.

(35) Van Broeck, B., Chen, J.-M., Tréton, G., Desmidt, M., Hopf, C., Ramsden, N., Karran, E., Mercken, M. and Rowley, A. Chronic treatment with a novel γ-secretase modulator, JNJ-40418677, inhibits amyloid plaque formation in a mouse model of Alzheimer's disease. *Br. J. Pharmacol.* **2011**, *163*, 375-389.

(36) Sirius Analytical Ltd., Forest Row Business Park, Station Road, Forest Row, East Sussex. RH18 5DW. http://www.sirius-analytical.com/ (accessed June 23, 2015).

(37) Zhu, Z.; McKittrick, B.; Sun, Z.-Y.; Ye, Y. C.; Voigt, J. H.; Strickland, C.; Smith, E. M.; Stamford, A.; Greenlee, W. J.; Mazzola, R. D., Jr.; Caldwell, J.; Cumming, J. N.; Wang, L.; Wu, Y.; Iserloh, U.; Liu, X.; Huang, Y.; Li, G.; Pan, J.; Misiaszek, J. A.; Guo, T.; Le, T. X. H.; Saionz, K. W.; Babu, S. D.; Hunter, R. C.; Morris, M. L.; Gu, H.; Qian, G.; Tadesse, D.; Lai, G.; Duo, J.; Qu, C.; Shao, Y. Preparation of imidazolidin-2-imines and their analogs as aspartyl protease inhibitors for treating various diseases. WO2008103351A2, 2008.

TABLE OF CONTENTS GRAPHIC

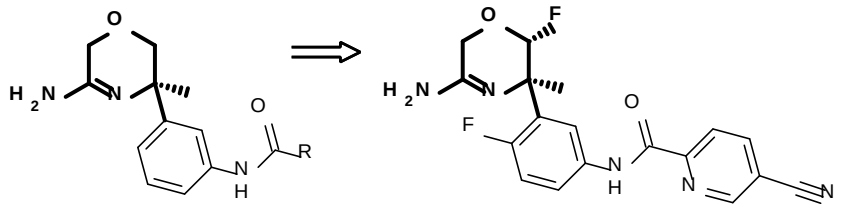

pK$_a$ 9.6
non-brain penetrant

pK$_a$ 7.8
brain penetrant

(2*R*,3*R*)-**7d**
BACE1 IC$_{50}$ 7.6 nM
hAβ42 cell IC$_{50}$ 8.1 nM
Aβ dog EC$_{50}$ 20 ng/mL

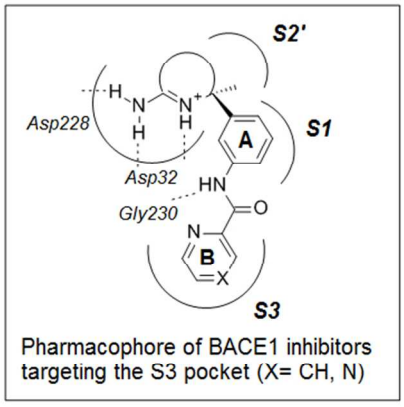

Pharmacophore of BACE1 inhibitors targeting the S3 pocket (X= CH, N)

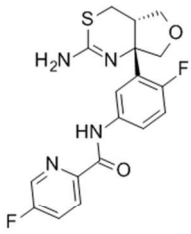

1 (LY-2886721, Eli Lilly)
BACE1 IC_{50} 15.5 nM
hAβ42 cell IC_{50} 6.6 nM

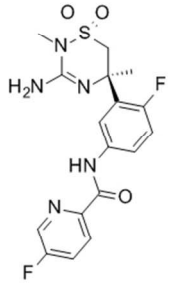

2 (MK-8931, Merck)
BACE1 IC_{50} 3.2 nM
hAβ42 cell IC_{50} 1.3 nM

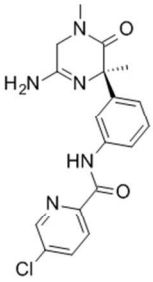

3 (Janssen)
BACE1 IC_{50} 324 nM
hAβ42 cell IC_{50} 36 nM

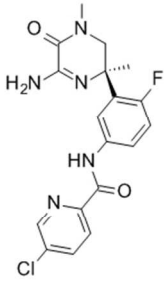

4 (Janssen)
BACE1 IC_{50} 23 nM
hAβ42 cell IC_{50} 28 nM

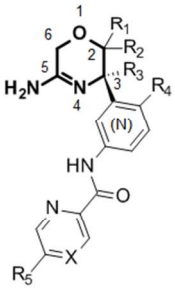

5, *This paper*

Chart 1.
237x214mm (96 x 96 DPI)

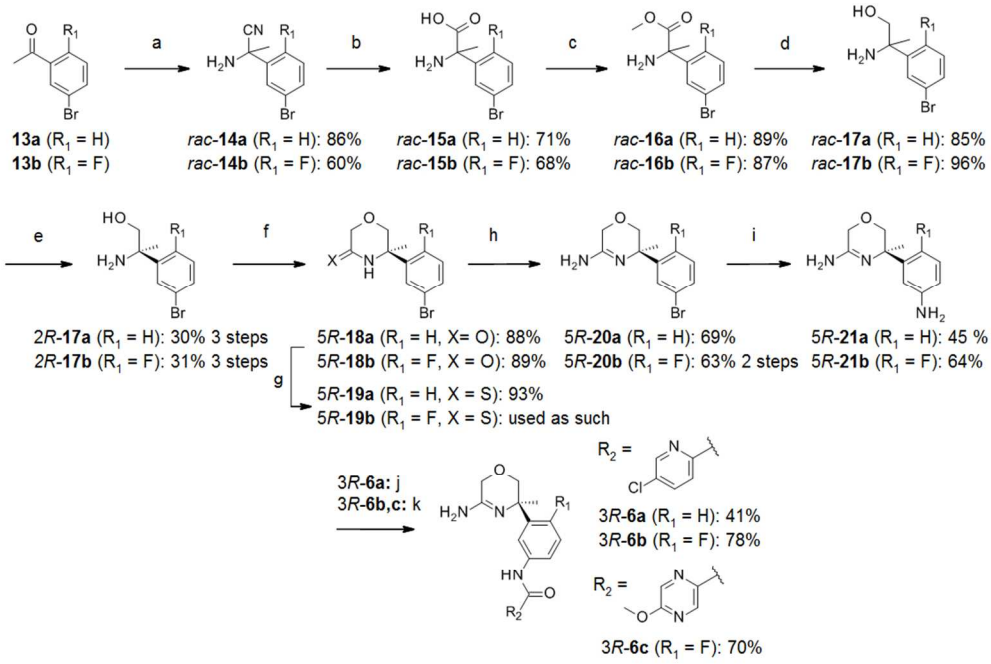

Scheme 1.
300x198mm (96 x 96 DPI)

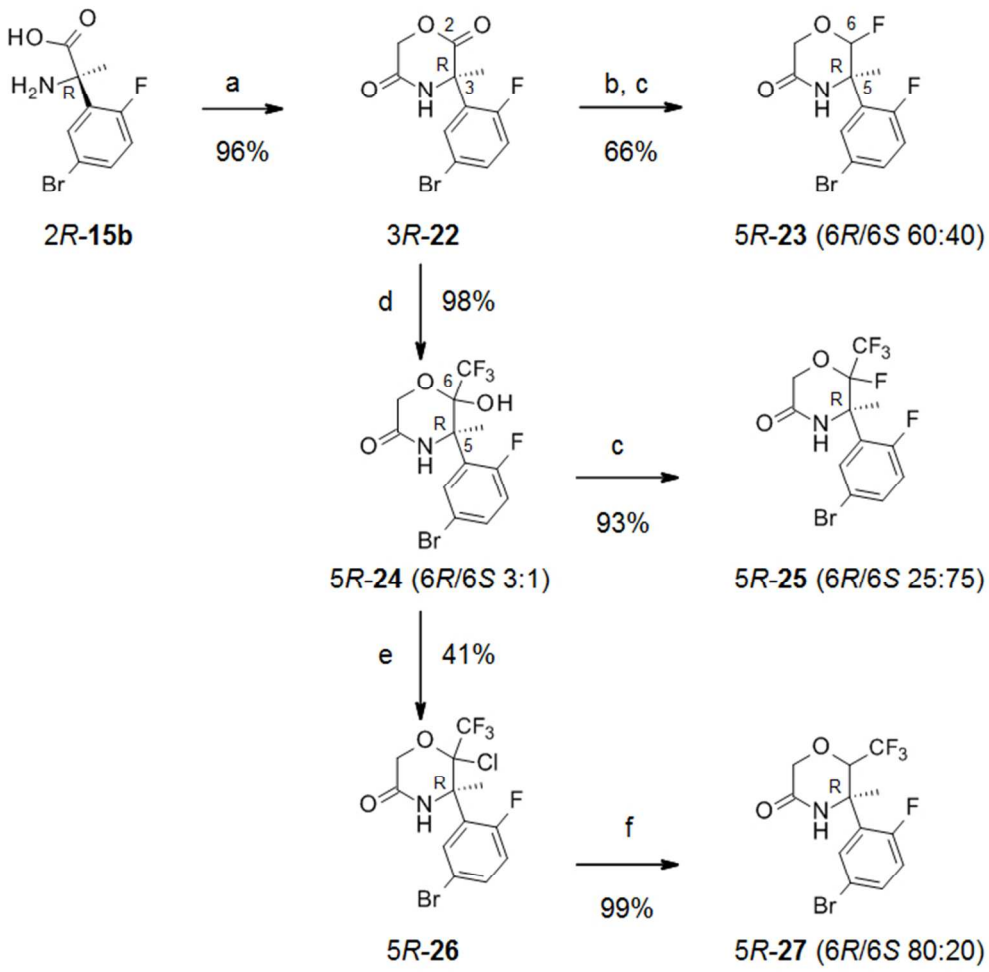

Scheme 2.
195x190mm (96 x 96 DPI)

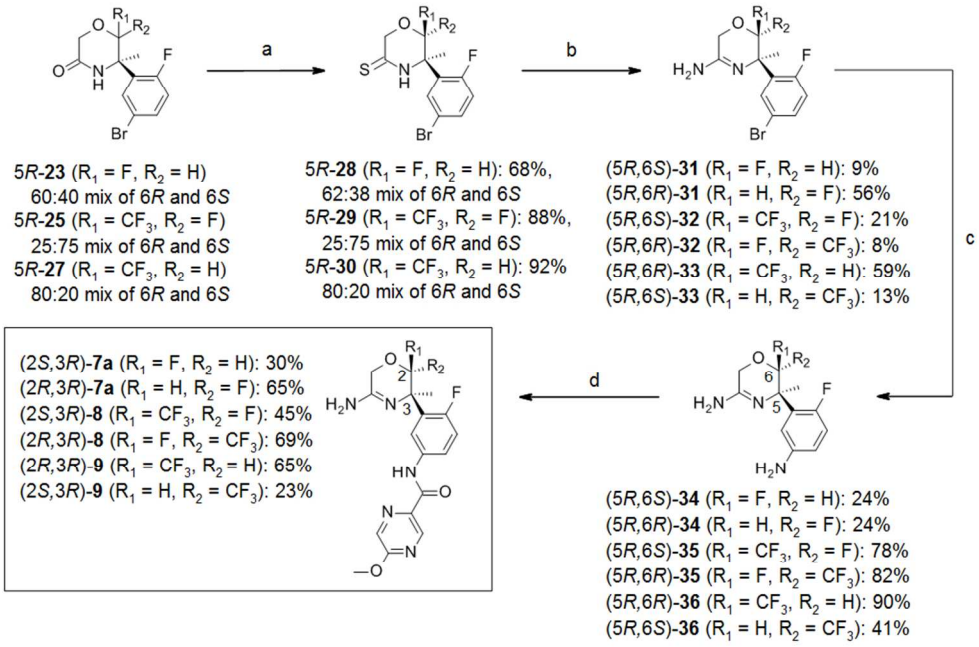

Scheme 3.
276x184mm (96 x 96 DPI)

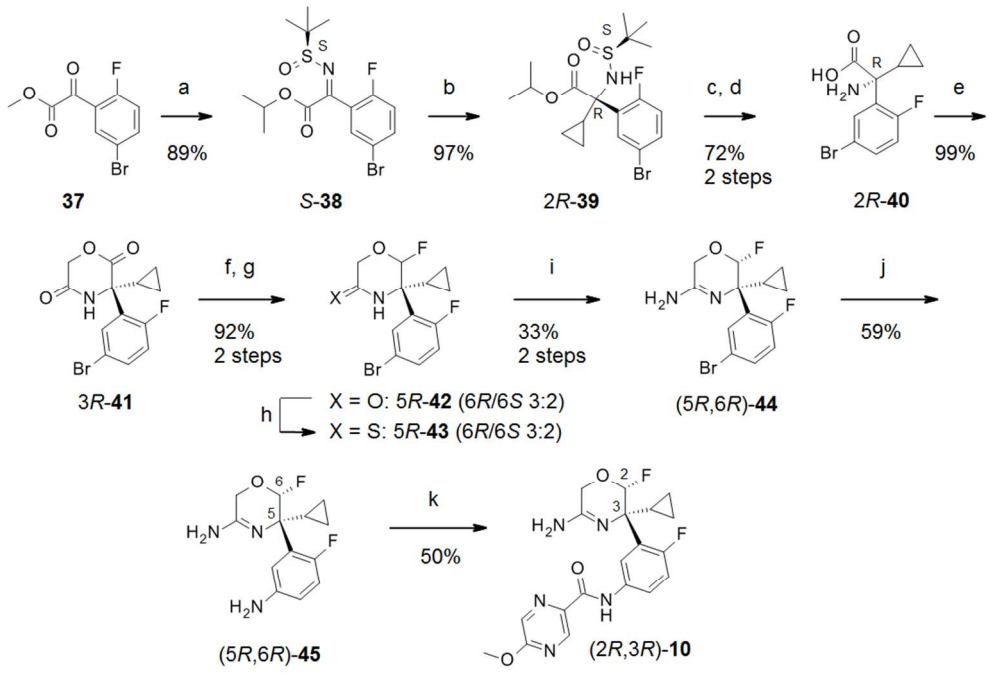

Scheme 4.
302x205mm (96 x 96 DPI)

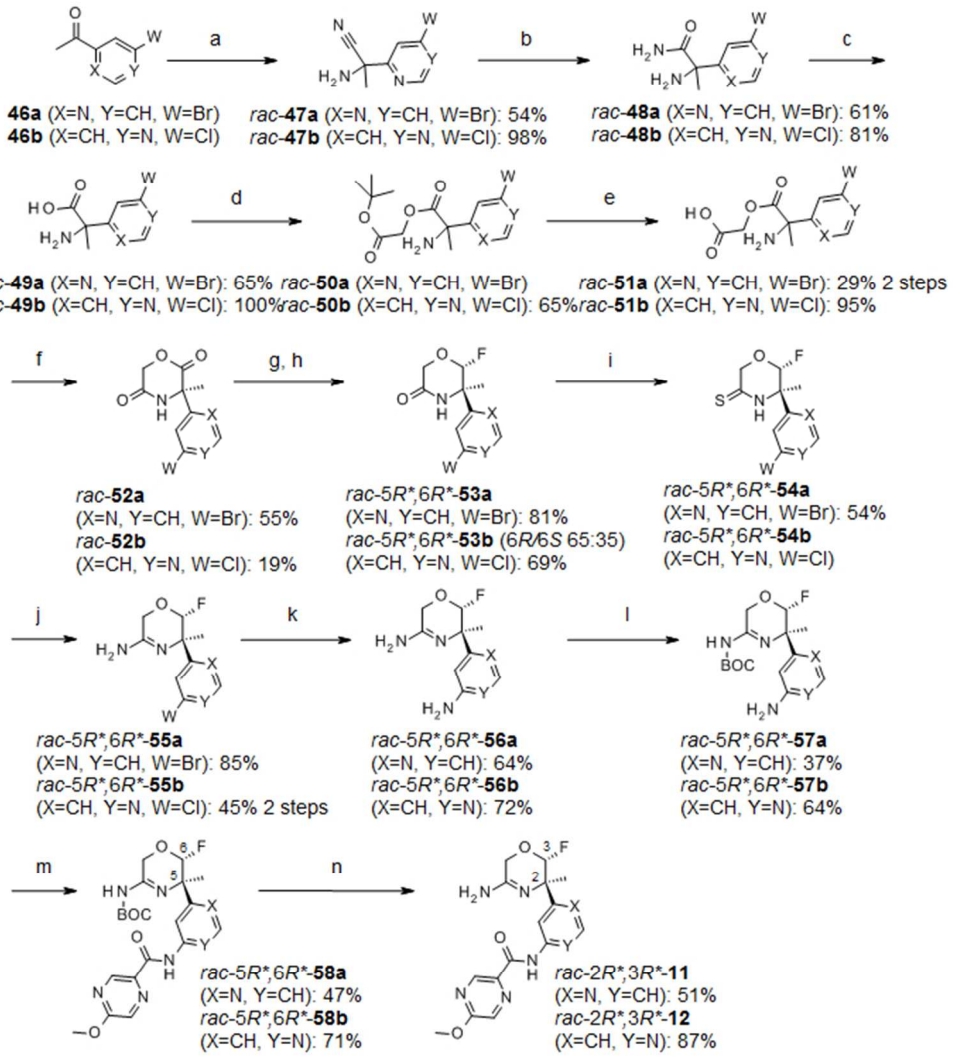

Scheme 5.
187x202mm (96 x 96 DPI)

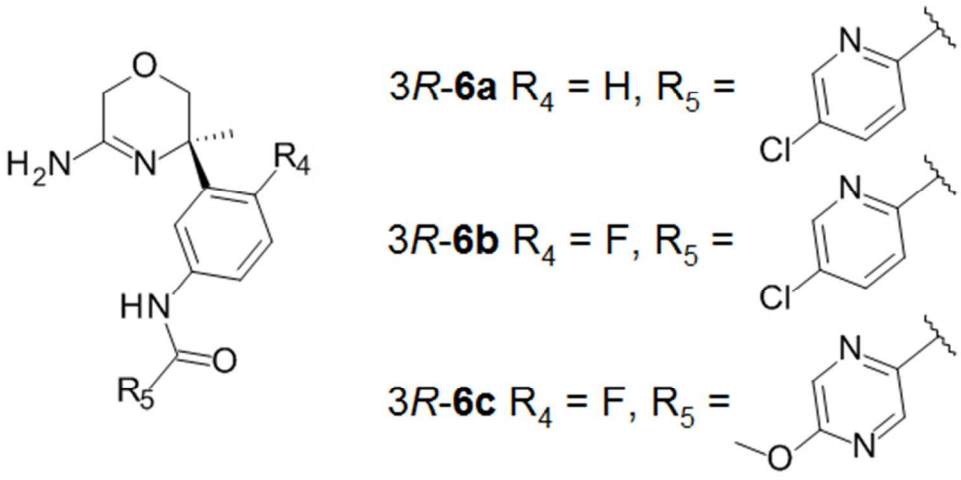

Table 1.
154x76mm (96 x 96 DPI)

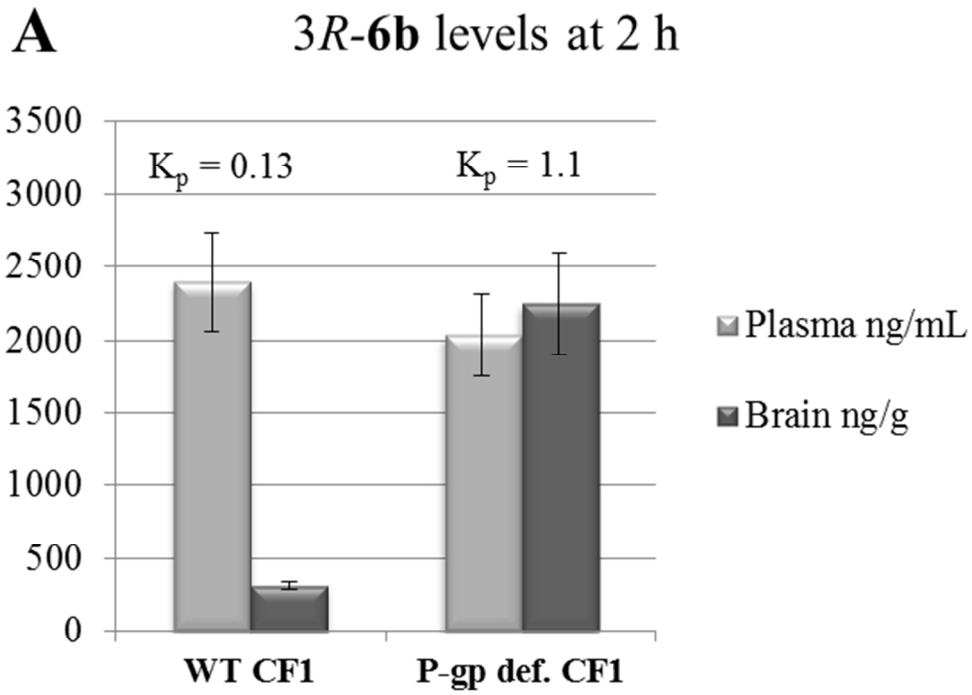

Table 2. A
110x83mm (150 x 150 DPI)

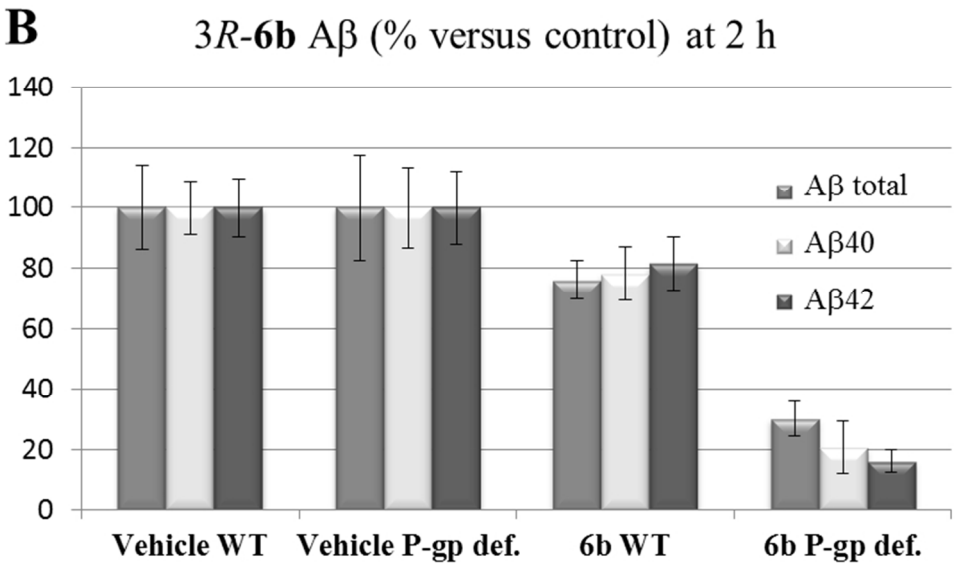

Table 2. B
136x83mm (150 x 150 DPI)

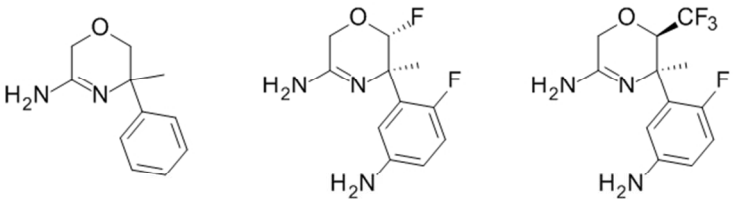

pKa Experiment	**9.8**	**8.1**	**8.0**
pKa calculated ACD[a]	**6.4**	**3.8**	**4.6**
pKa calculated ACD[b]	**10.4**	**9.7**	**9.9**
pKa calculated with AP	**9.6**	**7.3**	**6.7**

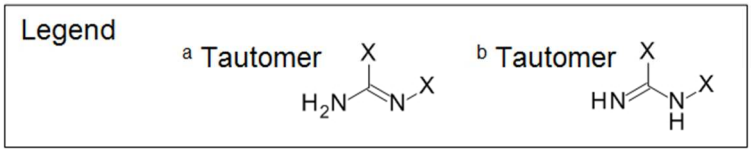

Scheme 6.
224x148mm (96 x 96 DPI)

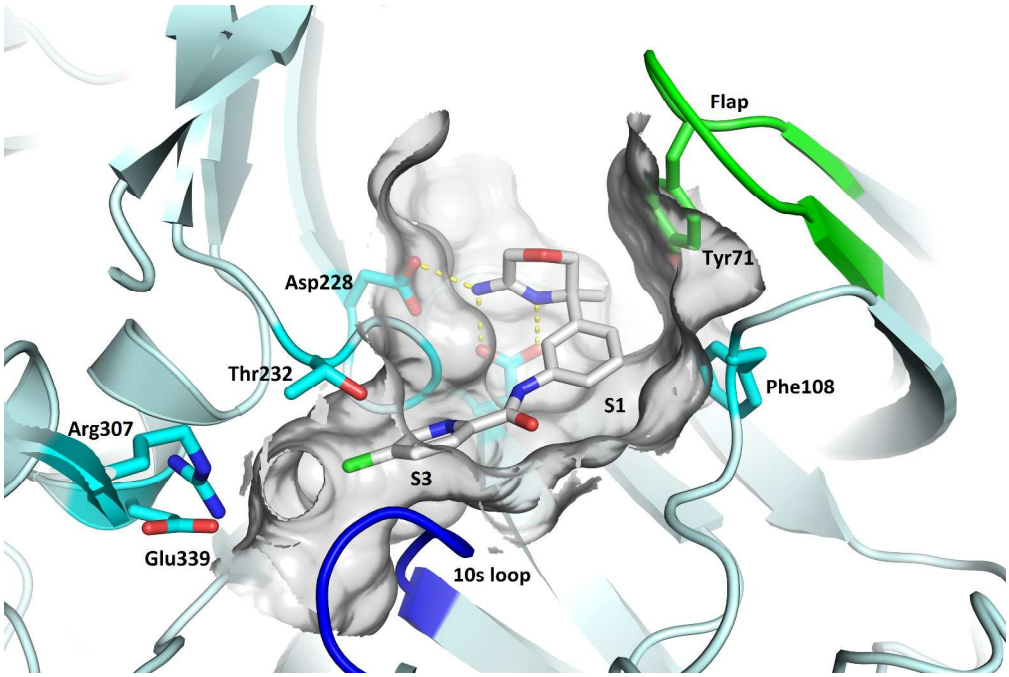

952x635mm (96 x 96 DPI)

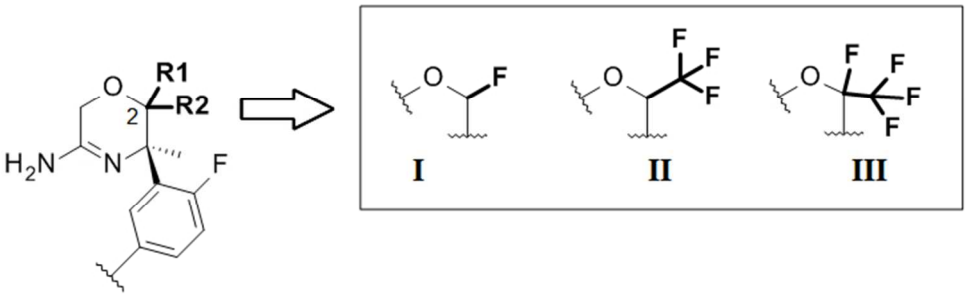

Chart 2.
199x63mm (96 x 96 DPI)

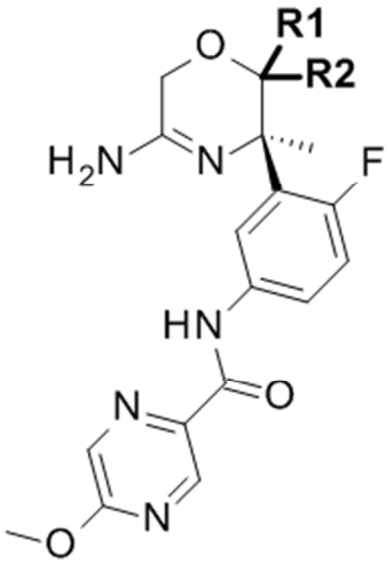

Table 3. Top graphic
55x77mm (96 x 96 DPI)

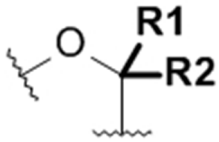

Table 3. Graph in column 1
33x24mm (96 x 96 DPI)

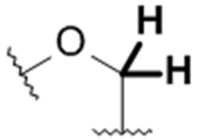

Table 3. Graph in column 2
29x22mm (96 x 96 DPI)

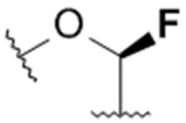

Table 3. Graph in column 3
29x20mm (96 x 96 DPI)

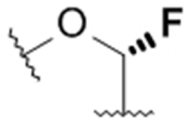

Table 3. Graph in column 4
29x20mm (96 x 96 DPI)

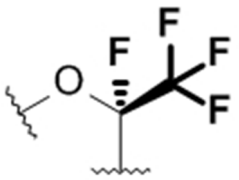

Table 3. Graph in column 5
35x27mm (96 x 96 DPI)

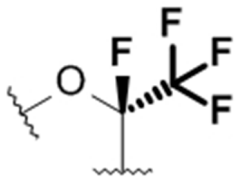

Table 3. Graph in column 6
34x26mm (96 x 96 DPI)

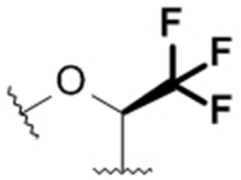

Table 3. Graph in column 7
35x27mm (96 x 96 DPI)

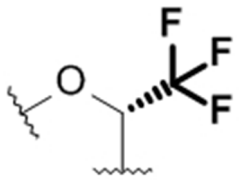

Table 3. Graph in column 8
35x27mm (96 x 96 DPI)

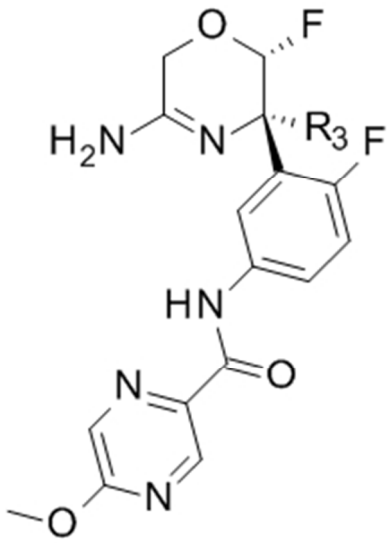

Table 4. Top graph
54x75mm (96 x 96 DPI)

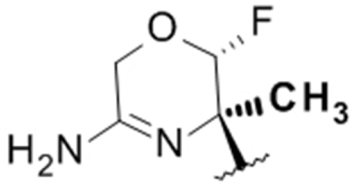

Table 4. Graph in column 2
52x28mm (96 x 96 DPI)

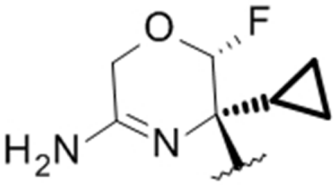

Table 4. Graph in column 3
48x28mm (96 x 96 DPI)

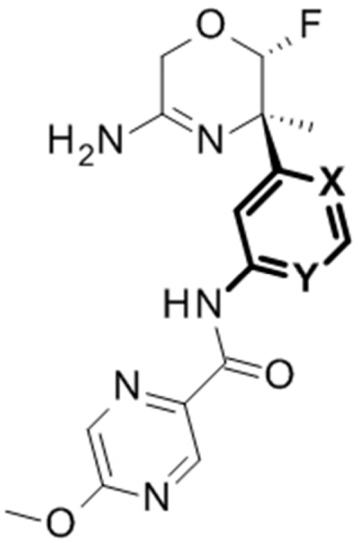

Table 5. Top graph
49x74mm (96 x 96 DPI)

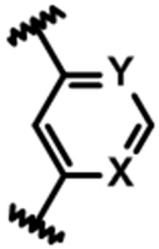

Table 5. Graph in column 1
24x37mm (96 x 96 DPI)

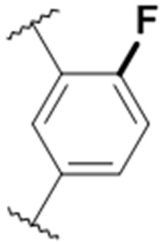

Table 5. Graph in column 2
26x36mm (96 x 96 DPI)

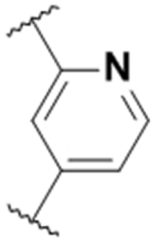

Table 5. Graph in column 3
25x36mm (96 x 96 DPI)

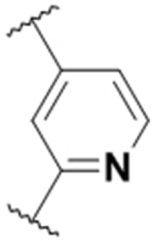

Table 5. Graph in column 4
25x36mm (96 x 96 DPI)

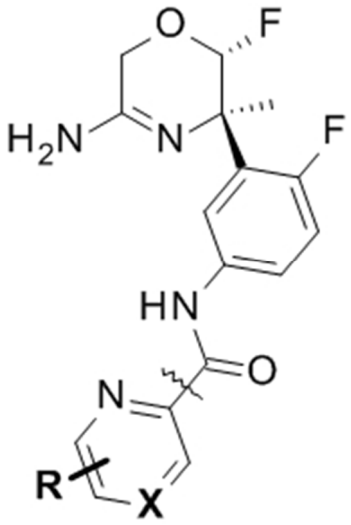

Table 6. Top graph
48x72mm (96 x 96 DPI)

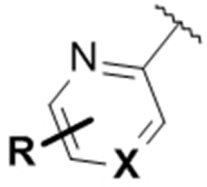

Table 6. Graph in column 1
30x34mm (96 x 96 DPI)

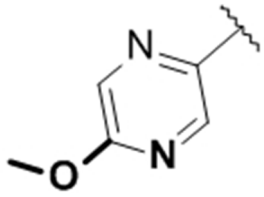

Table 5. Graph in column 2
40x30mm (96 x 96 DPI)

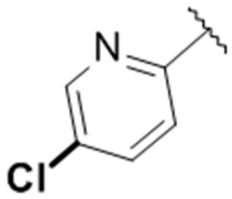

Table 5. Graph in column 3
35x31mm (96 x 96 DPI)

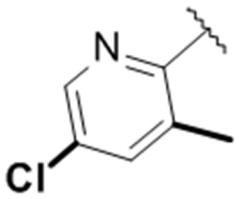

Table 5. Graph in column 4
35x31mm (96 x 96 DPI)

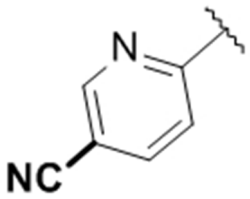

Table 6. Graph for column 5
38x30mm (96 x 96 DPI)

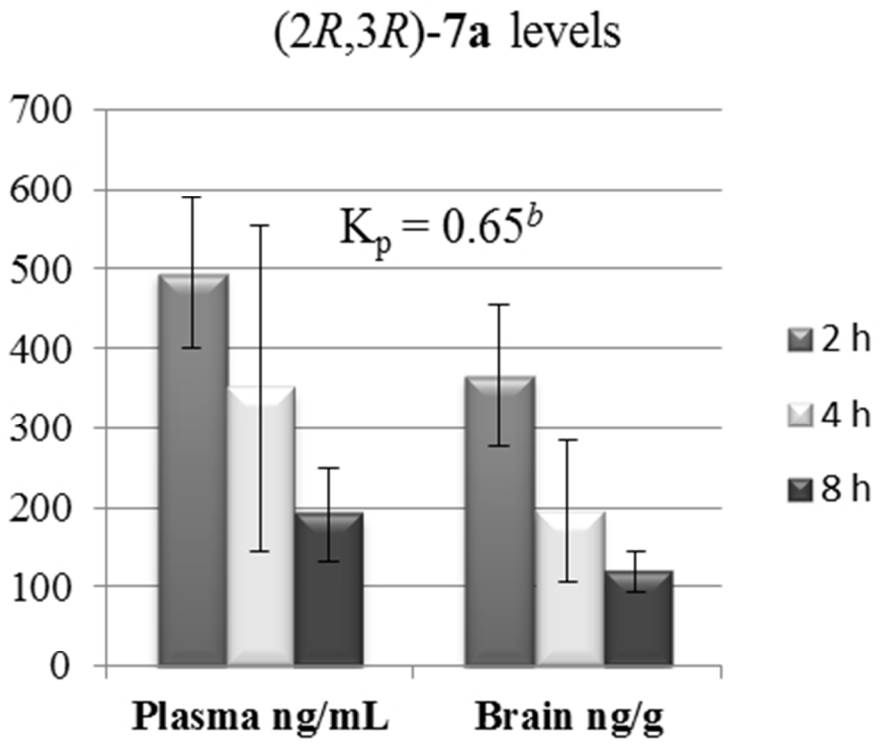

Table 7. A
78x67mm (150 x 150 DPI)

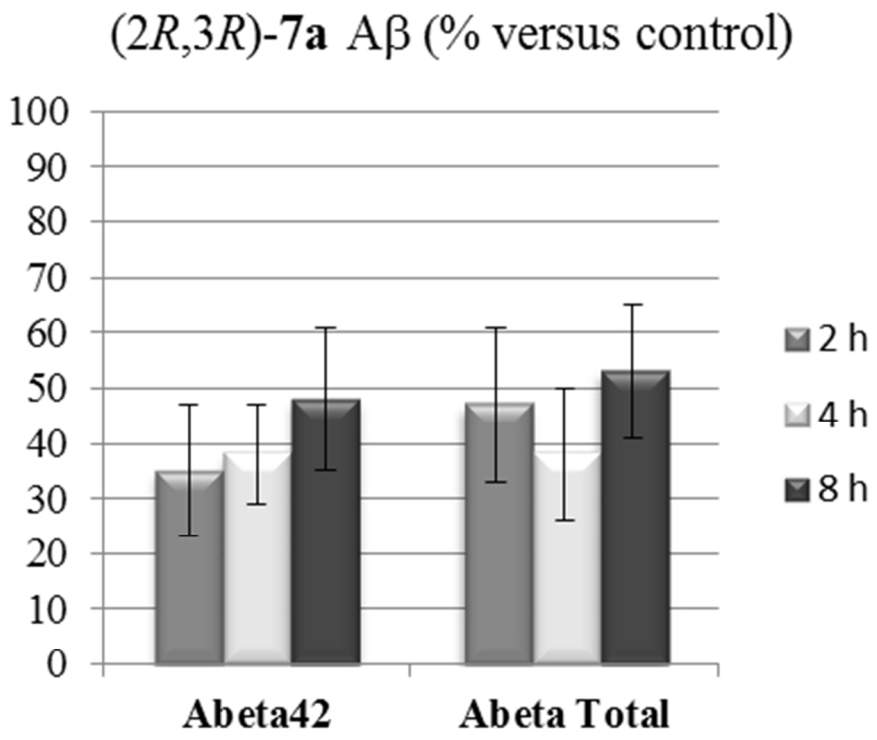

Table 7. B
78x67mm (150 x 150 DPI)

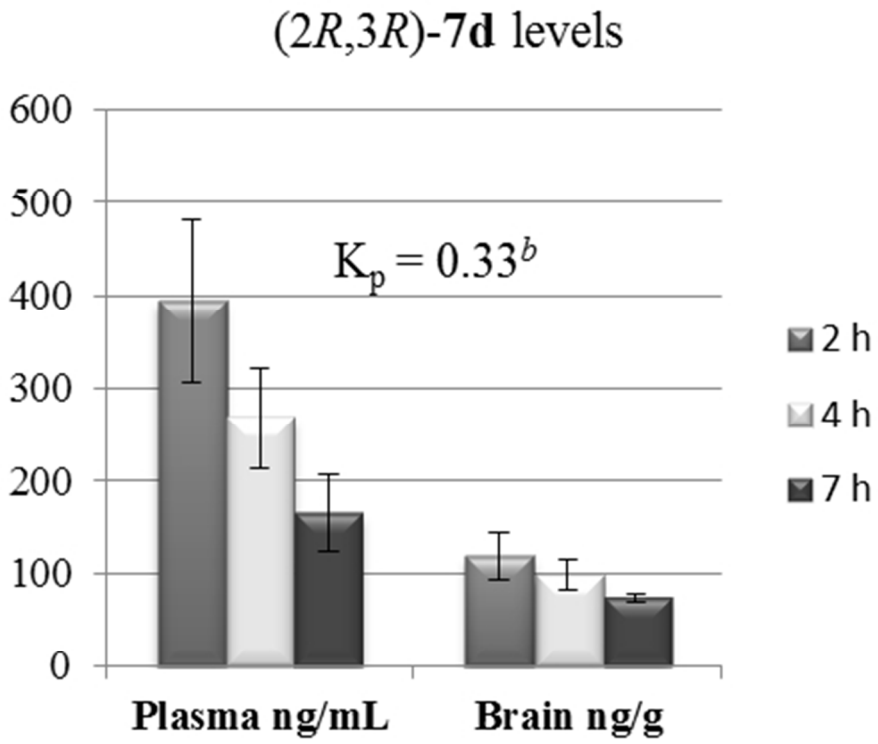

Table 7. C
78x67mm (150 x 150 DPI)

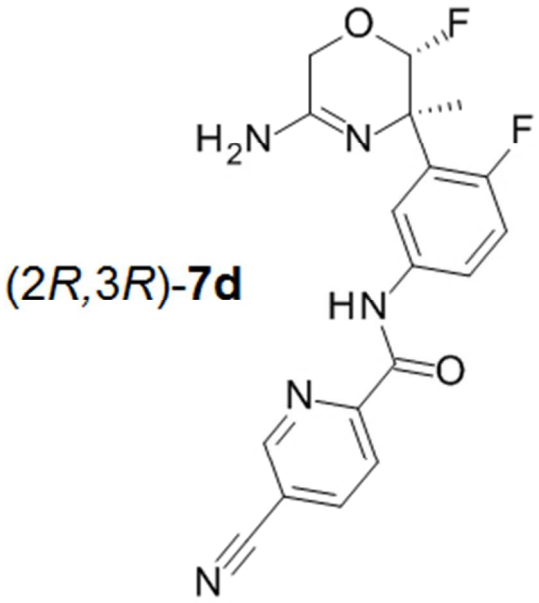

73x83mm (96 x 96 DPI)

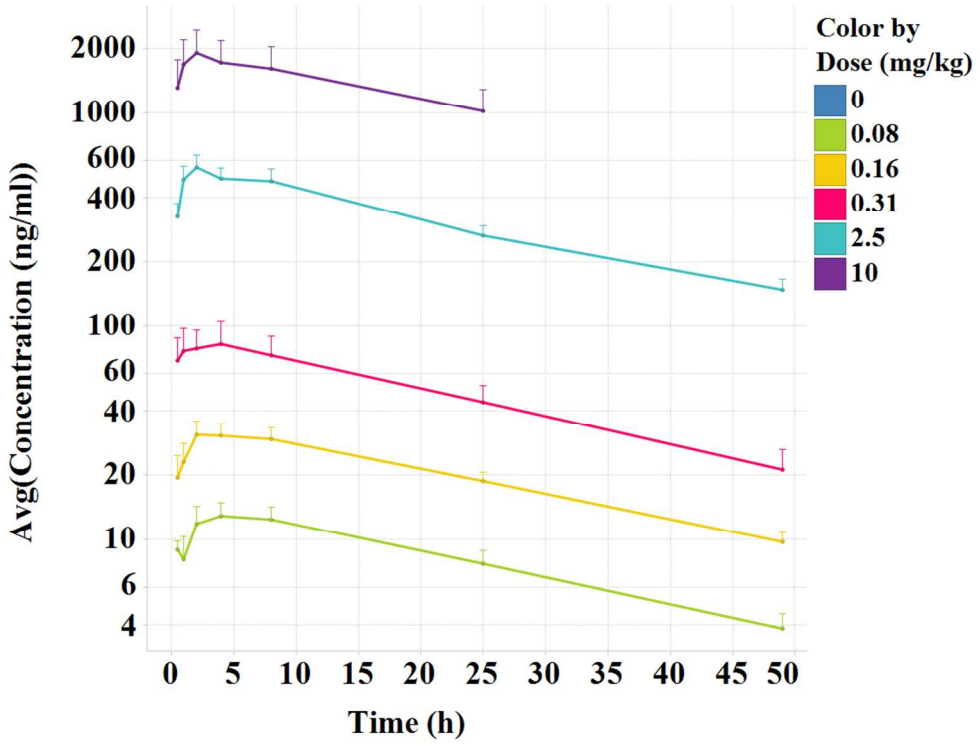

305x227mm (96 x 96 DPI)

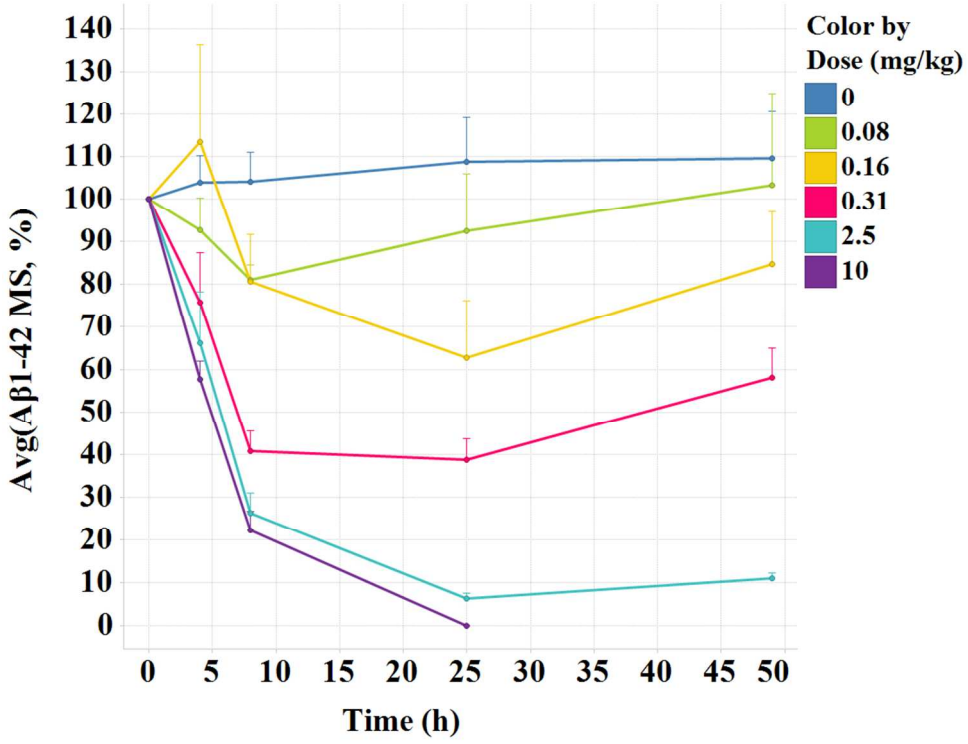

305x227mm (96 x 96 DPI)

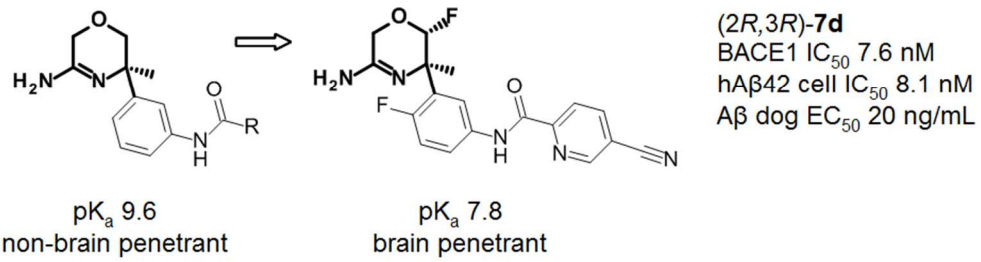

TOC graph
249x67mm (96 x 96 DPI)